

# Fidelity approach to quantum phase transitions

Shi-Jian Gu\*

*Department of Physics and Institute of Theoretical Physics,  
The Chinese University of Hong Kong, Hong Kong, China*

(Dated: November 19, 2008)

We review briefly the quantum fidelity approach to quantum phase transitions in a pedagogical manner. We try to relate all established but scattered results on the leading term of the fidelity into a systematic theoretical framework, which might provide an alternative paradigm for understanding quantum critical phenomena. The definition of the fidelity and the scaling behavior of its leading term, as well as their explicit applications to the one-dimensional transverse-field Ising model and the Lipkin-Meshkov-Glick model, are introduced at the graduate-student level. In addition, we survey also other types of fidelity approach, such as the fidelity per site, reduced fidelity, thermal-state fidelity, operator fidelity, etc; as well as relevant works on the fidelity approach to quantum phase transitions occurring in various many-body systems.

PACS numbers: 03.67.-a, 64.60.-i, 05.30.Pr, 75.10.Jm

## Contents

<b>I. Introduction</b>	1	<b>E. Density-functional fidelity</b>	23
A. Overview: quantum phase transitions	1	<b>VI. Fidelity in strongly correlation systems</b>	24
B. Brief historical retrospect	2	A. Pure-state fidelity	24
C. About the review	4	1. One-dimensional spin systems	24
<b>II. Quantum fidelity: a measure of similarity between states</b>	4	2. One-dimensional fermionic systems	27
A. Pure state and mixed state fidelity	4	3. The fidelity in topological quantum phase transitions	29
B. Quantum state overlap and adiabatic evolution	5	B. Mixed-state fidelity	32
<b>III. Fidelity and quantum phase transitions</b>	7	1. Reduced fidelity in quantum phase transitions	32
A. Quantum phase transitions: fidelity perspective	7	2. Thermal state fidelity in strongly correlated systems	33
B. Example: the one-dimensional transverse-field Ising model	8	<b>VII. Numerical methods for the ground-state fidelity</b>	34
<b>IV. Fidelity susceptibility, scaling and universality class</b>	11	A. Exact diagonalization	34
A. The leading term of the fidelity and dynamic structure factor	11	B. Density matrix renormalization group	36
B. Scaling analysis and universality class	15	<b>VIII. Summary and outlook</b>	38
C. Example A: the one-dimensional transverse-field Ising model	16	<b>Acknowledgments</b>	38
D. Example B: the Lipkin-Meshkov-Glick model	17	<b>References</b>	38
E. Higher order of the fidelity	19	<b>I. INTRODUCTION</b>	
<b>V. Fidelity per site, mixed state fidelity, and related</b>	20	<b>A. Overview: quantum phase transitions</b>	
A. Fidelity per site	20		
B. Reduced fidelity	21		
C. Fidelity between thermal states	22		
D. Operator fidelity	22		

Quantum phase transitions [1] of a quantum many-body system are characterized by the change in the ground-state properties caused by modifications in the interactions among the system's constituents. Contrary to thermal phase transitions where the temperature plays a crucial role, quantum phase transitions are completely driven by quantum fluctuations and are incarnated via the non-analytic behavior of the ground-state properties as the system's Hamiltonian  $H(\lambda)$  varies across a transition point  $\lambda_c$ .

---

\*Electronic address: sjgu@phy.cuhk.edu.hk

From the point view of eigenenergy, quantum phase transitions are caused by the reconstruction of the Hamiltonian's energy spectra, especially of the low-lying excitation spectra [2]. More precisely, the low-energy spectra can be reconstructed in two qualitatively different ways around the critical point  $\lambda_c$ , and hence the physical quantities show different behaviors. The first one is the ground-state level-crossing in which the first derivative of the ground-state energy with respect to  $\lambda$  is usually discontinuous at the transition point. Such a transition is called the first-order phase transition. The second one corresponds roughly to all other cases in the absence of the ground-state level-crossing. It is usually a continuous phase transition.

Traditionally, continuous phase transitions can be characterized by the Landau-Ginzburg-Wilson spontaneous symmetry-breaking theory where the correlation function of local order parameters plays a crucial role. Nevertheless, some systems cannot be described in this framework built on the local order parameter. This might be due to the absence of preexistent symmetry in the Hamiltonian, such as systems undergoing topological phase transitions [3] and Beresinskii-Kosterlitz-Thouless phase transitions [4, 5].

## B. Brief historical retrospect

In recent years, ambitions on quantum computer and other quantum information devices have driven many people to develop quantum information theory [6]. Though a practicable quantum computer seems still a dream, progresses in quantum information theory have developed other related fields forward. A noticeable one is the relation between quantum entanglement and quantum phase transitions [7, 8, 9, 10, 11, 12, 13, 14, 15, 16, 17, 18, 19]. Since the entanglement is regarded as a purely quantum correlation and is absent in classical systems, people think that the entanglement should play an important role in quantum phase transitions. Though a unified theory on the role of entanglement in quantum phase transitions is still unavailable, some definitive conclusions have been commonly accepted [20].

Another attractive approach is the quantum fidelity [21, 22, 23, 24, 25, 26, 27, 28, 29, 30, 31, 32, 33, 34], a concept also emerging in quantum information theory. The fidelity measures the similarity between two states, while quantum phase transitions are intuitively accompanied by an abrupt change in the structure of the ground-state wavefunction, this primary observation motivates people to explore the role of fidelity in quantum phase transitions [35, 36]. Since the fidelity is purely a quantum information concept, where no *a priori* knowledge of any order parameter and changes of symmetry of the system is assumed, it would be a great advantage if one can use it to characterize the quantum phase transitions. Many works have been done along this stream [35, 36, 37, 38, 39, 40, 41, 42, 43, 44, 45, 46, 47, 48, 49,

50, 51, 52, 53, 54, 55, 56, 57, 58, 59, 60, 61, 62, 63, 64, 65, 66, 67, 68, 69, 70, 71, 72, 73, 74, 75, 76, 77, 78, 79, 80, 81, 82, 83, 84, 85, 86, 87, 88, 89, 90, 91, 92, 93, 94, 95, 96, 97, 98, 99, 100, 101, 102, 103, 104, 105].

The motivation of the fidelity approach to quantum phase transitions can be traced back to the work of Quan *et al* [35] in determining two ground-state phases of the one-dimensional transverse-field Ising model by the Loschmidt echo. The Loschmidt echo [119] has been introduced to describe the hypersensitivity of the time evolution to perturbations experienced by the environmental system. They found the quantum critical behavior of the environmental system strongly affects its capability of enhancing the decay of Loschmidt echo. Since the Loschmidt echo is defined as the overlap between two time-dependent states corresponding to two points separated slightly by a target spin with Ising interaction, its decay around the critical point represents a large distance between two states. Subsequently, Zanardi and Paunković [36] proposed out that a static fidelity might be a good indicator for quantum phase transitions with examples of the one-dimensional transverse-field XY model and the Dicke model. Similar idea was also proposed by Zhou and Barjaktarevic [37]. Motivated by these works, the fidelity approach to quantum phase transitions was quickly applied to free fermionic systems [38] and graphs [39], matrix-product states [40], and the Bose-Hubbard model [41]. An attempt to understand quantum phase transitions from the thermal fidelity was also made [42]. At that time, the successes of the fidelity in these studies [35, 36, 37, 38, 39, 40, 41, 42] gave peoples a deep impression that the fidelity is able to characterize any quantum phase transition, including those cannot be described in the framework of Landau-Ginzburg-Wilson theory, such as the Beresinskii-Kosterlitz-Thouless transitions and topological transitions. Two groups addressed the role of the leading term of the fidelity in the quantum critical phenomena. Zanardi *et al* introduced, based on the differential-geometry approach, the Riemannian metric tensor [44] inherited from the parameter space to denote the leading term in the fidelity, and argued that the singularity of this metric corresponds to quantum phase transitions. While You *et al* introduced another concept, the so-called fidelity susceptibility (FS) [43], and established a general relation between the leading term of the fidelity and the structure factor (correlation functions) of the driving term in the Hamiltonian. Both of them obtained also that, if one extend the fidelity to thermal states, the leading term of the fidelity between two neighboring thermal states is simply the specific heat. In the following, we will use "fidelity susceptibility" to name the leading term of the fidelity because it not only denotes mathematically the fluctuation of the driving term, such as the specific heat derived from the internal energy, but also is closer to the picture of condensed matter physics, i.e. the response of the fidelity to driving parameter. From then on, the field of the fidelity approach to quantum (or thermal) phase

transitions can be divided roughly into two streams. The first stream still focuses on the fidelity itself, for which the distance between two points in the parameter space is still important, while the second stream pays particular attention to the leading term of the fidelity.

Along the first stream, a connection between the fidelity, scaling and renormalization was introduced by Zhou [45, 46], in which the fidelity between two reduced states of a part of the system described by a reduced-density matrix was proposed. Zhou *et al* [59] tried to understand the fidelity from a geometric perspective. In works of Zhou and his colleagues, the fidelity is averaged over the system size, and is named as fidelity per site. They found that the fidelity per site is a very useful tool for various interacting systems. Interestingly, the fidelity per site, as an analog of the free energy per site, can be computed in the context of tensor network algorithms [58, 146, 147].

While along the second stream, several questions appeared at that time. 1) Since the leading term of the fidelity is a combination of correlation functions, which seems a tool widely used only in the Landau-Ginzburg-Wilson theory, is the fidelity still able to describe the Beresinskii-Kosterlitz-Thouless and topological phase transitions? 2) What is the scaling behavior of the fidelity and its relation to the universality class? 3) How about the thermal phase transitions and those quantum phase transitions induced by the continuous ground-state level-crossing where the perturbation method is not applicable. Most subsequent works are more or less related to these questions, though some topics are still controversial.

Based on the general relation between the leading term of the fidelity and correlation functions of the driving term [43], Venuti and Zanardi [47] applied the traditional scaling transformation, and obtained an interesting scaling relation between the dynamic exponent, the dimension of the system, and the size exponents of the fidelity. A similar scaling relation was also obtained numerically by Gu *et al* [49] in their studies on the one-dimensional asymmetric Hubbard model. Both relations imply that the fidelity susceptibility might not have singular behavior in some cases, such the Beresinskii-Kosterlitz-Thouless transition occurring in the asymmetric Hubbard model at half-filling [49].

On the other hand, Yang [52] tried to understand the singular behavior of the fidelity susceptibility from the ground-state energy density and pointed out that the fidelity susceptibility might not be able to detect the high-order phase transitions. A little surprising is that their example, i.e. the effective model of the one-dimensional XXZ chain, which undergoes a Beresinskii-Kosterlitz-Thouless transition of infinite order at the isotropic point, shows singular behavior in the fidelity susceptibility. Similar analysis on the Luttinger Liquid model with a wave functional approach was also done by Fjrestad [60]. The further investigations on spin-1 XXZ chain with uniaxial anisotropy by Yang *et al* [53, 70] sup-

ported partially their previous conclusion and the scaling relation obtained by Venuti and Zanardi [47].

Later, Chen *et al* [61] addressed the feasibility of the fidelity susceptibility in quantum phase transitions of various order by the perturbation theory, and concluded that the fidelity susceptibility cannot describe the phase transition of infinite order. This conclusion conflicts with both Yang's works on the one-dimensional XXZ model [52] and the subsequent studies on the one-dimensional Hubbard model [63], but supports previous conclusion obtained by You *et al* [43]. Therefore, the issue on fidelity in describing high-order phase transitions seems still controversial.

Recently it was realized that the fidelity susceptibility can be either intensive, extensive, or superextensive, then the critical exponents of the rescaled fidelity susceptibility at both sides of the critical point can be different [78]. In addition to the fidelity susceptibility, the sub-leading term of the fidelity might appear when parameters are changed along a critical manifold [76].

It became a branch of the story when Hamma *et al* [65] firstly touched the feasibility of the fidelity in topological phase transitions. They found that though the fidelity shows an obvious drop around the critical point of a topological transition, it cannot tell the type of transition. Almost one year later, three groups revisited the role of fidelity in the topological transitions. Zhou *et al* [66] studied the fidelity in the Kitaev honeycomb model and found that fidelity has shows singular behavior at the critical point. Yang *et al* [67] studied the fidelity susceptibility in the same model and obtained various critical exponents, they also witnessed a kind of long-range correlation in the ground state of Kitaev honeycomb model. While Abasto *et al* [68] studied the fidelity in the deformed Kitaev toric model and obtained a form of fidelity between thermal states. The three groups drew a similar conclusion that the fidelity can describe the topological phase transitions occurring in the both models.

A noteworthy advance in the fidelity approach is the success of using the state overlap to detect quantum critical point by a nuclear-magnetic-resonance quantum simulator [71]. It was observed that the different types of quantum phase transitions in the transverse-field Ising model can be witnessed in experiments. Such an advance is remarkable. It makes the fidelity approach to quantum phase transitions no longer purely theoretical.

On the other hand, the global-state fidelity cannot characterize those quantum phase transitions induced by continuous level-crossing due to its collapse at each crossing point. Kwok *et al* [72] firstly tackled this type of phase transition with the strategy of the reduced fidelity, which actually was introduced in previous works [45, 55]. Meanwhile, Ma *et al* [73] also studied the critical behavior of the reduced fidelity in the Lipkin-Meshkov-Glick model. The reduced fidelity was latter applied to the one-dimensional transverse-field Ising [81, 88] and XY models [90], the dimerized Heisenberg chain [82], and the one-dimensional extended Hubbard model [88].

Despite of the absence of the thermal phase transition in the one-dimensional XY model, the thermal-state fidelity was firstly used to study the crossover occurring in the low-temperature critical region [42]. Interestingly, the leading term of the thermal-state fidelity was later found to be just the specific heat [43, 44]. The thermal-state fidelity was also applied to the BCS superconductivity and the Stoner-Hubbard model with the mean-field approach [56]. Moreover, Quan and Cucchietti [75] tried to find the advantages and disadvantages of the fidelity approach to the thermal phase transitions.

Finally, though we focus on the fidelity between the static ground state only, we would like to mention that the Loschmidt echo has also been widely applied to study the quantum phase transitions [93, 94, 95, 96, 97, 98, 99, 100, 101, 102, 103, 104, 105]. In studies of the Loschmidt echo, one needs to consider the dynamic behavior of the fidelity of a target object, for instance, a spin coupled with all other spins in the Ising chain. Then the decoherence property should be taken into account. These issues are beyond the scope of this review.

### C. About the review

The main purpose of this review is to gather these distributed works into a unified paradigm, then provides interested readers, especially beginners, a systematic framework of the fidelity approach to quantum phase transitions. Some practical and numerical methods, such as the exact diagonalization and density matrix renormalization group, are introduced too. We try to keep the treatment as simple as the subject allows, showing most calculations in explicit detail. Since the field is still quickly developing, such a review is far from completeness. We hope that the article can offer some introductory essays first, then to arouse more wonderful ideas.

The article is organized as follows. In Section II, we give a brief overview on the fidelity measure and its properties in an adiabatic evolution exemplified by a 1/2 spin subjected to an external field. In Section III, we introduce in considerable detail the general relations between the fidelity and quantum phase transitions, and try to illustrate the role of fidelity in quantum phase transitions by the one-dimensional transverse-field Ising model. In Section IV, we focus on the leading term of the fidelity, i.e. the fidelity susceptibility, and discuss its general properties around the critical point. We also use the one-dimensional transverse-field Ising model and the Lipkin-Meshkov-Glick model as examples for the fidelity susceptibility in describing the universality class. In Section V, we review other types of fidelity in the quantum phase transition, such as the fidelity per site, partial-state fidelity, thermal-state fidelity, operator fidelity, and density-functional fidelity. In Section VI, we give a survey on the fidelity approach to quantum phase transitions in various strongly correlated system. In Section VII, we show how to calculate the fidelity and fidelity suscepti-

bility via some numerical methods. An outlook and a summary will be presented in the concluding section.

## II. QUANTUM FIDELITY: A MEASURE OF SIMILARITY BETWEEN STATES

In this section, we introduce briefly the concept of quantum fidelity and discuss its properties in a simple quantum-state adiabatic evolution of a 1/2 spin subjected to an external field.

### A. Pure state and mixed state fidelity

In quantum physics, an overlap between two quantum states usually denotes the transition amplitude from one state to the another [21, 22, 23, 24]. While from the point view of information theory, the overlap can measure the similarity (closeness) between two states [25, 26, 27]. That is the overlap gives unity if two states are exactly the same, while zero if they are orthogonal. Such an interpretation has a special meaning in quantum information theory [6] since physicists in the field (for examples, Ref [106, 107, 108]) hope that a quantum state can be transferred over a long distance without loss of any information. The overlap between the input and output states becomes a useful measure of the loss of information during the transportation. The overlap is used to define the fidelity in quantum information theory.

To be precise, if we define the overlap between two pure states as

$$f(\Psi', \Psi) = \langle \Psi' | \Psi \rangle, \quad (1)$$

the fidelity is simply the modulus of the overlap, i.e.

$$F(\Psi', \Psi) = |\langle \Psi' | \Psi \rangle| \quad (2)$$

where  $|\Psi\rangle, |\Psi'\rangle$  are the input and output states respectively, and both of them are normalized. The fidelity has a geometric meaning as well. Since a pure state in quantum mechanics mathematically is a vector in the Hilbert space, then according to Linear algebra, an inner product of two vectors  $\mathbf{a}, \mathbf{b}$  is

$$\mathbf{a} \cdot \mathbf{b} = ab \cos(\theta) \quad (3)$$

where  $a(b)$  is the magnitude of  $\mathbf{a}(\mathbf{b})$ , and  $\theta$  is the angle between them. In quantum mechanics, wave functions are usually normalized, and the fidelity represents the angle distance between two states.

The fidelity has the following expected properties (*axioms*) [26]

$$0 \leq F(\Psi', \Psi) \leq 1, \quad (4)$$

$$F(\Psi', \Psi) = F(\Psi, \Psi'), \quad (5)$$

$$F(U\Psi', U\Psi) = F(\Psi', \Psi), \quad (6)$$

$$F(\Psi_1 \otimes \Psi_2, \Psi'_1 \otimes \Psi'_2) = F(\Psi'_1, \Psi_1)F(\Psi'_2, \Psi_2), \quad (7)$$

where  $U$  denotes a unitary transformation and  $\Psi_{1(2)}$  is the state of one subsystem. For pure states, the global phase difference may affect the overlap, but not the fidelity.

**Example:**

The quantum state of a single spin can be expressed in the basis  $\{|\uparrow\rangle, |\downarrow\rangle\}$ . For two normalized states of the spin, say

$$\begin{aligned} |\Psi(\theta)\rangle &= \cos\theta|\uparrow\rangle + \sin\theta|\downarrow\rangle, \\ |\Psi(\theta')\rangle &= \cos\theta'|\uparrow\rangle + \sin\theta'|\downarrow\rangle, \end{aligned}$$

the fidelity between them is

$$F(\Psi(\theta'), \Psi(\theta)) = |\cos(\theta - \theta')|.$$

The quantum fidelity between two mixed states  $(\rho, \rho')$  is defined as [21]

$$F(\rho, \rho') = \text{tr} \sqrt{\rho^{1/2} \rho' \rho^{1/2}}. \quad (8)$$

Here  $\rho(\rho')$  is semi-positive defined and normalized, i.e.  $\text{tr}\rho = \text{tr}\rho' = 1$ . The definition satisfies the expected properties of the fidelity, i.e. Eqs. (4-7).

It is not easy to evaluate the fidelity between two arbitrary mixed states. Nevertheless, there are some special useful cases:

- 1) If both states are pure  $F(\rho, \rho') = |\langle\Psi'|\Psi\rangle|$ ,
- 2) If one of state is pure, i.e.  $\rho = |\Psi\rangle\langle\Psi|$ , then  $F(\rho, \rho') = \sqrt{\langle\Psi|\rho'|\Psi\rangle}$ , which is simply the square root of the expectation value of  $\rho'$  [27],
- 3) If both of states are diagonal in the same basis, such as the thermal equilibrium state, the fidelity (or classical fidelity) can be calculated as

$$F(\rho, \rho') = \sum_j \sqrt{\rho_{jj} \rho'_{jj}}. \quad (9)$$

**Example:**

If a spin is coupled to environment, it can be described by a reduced-density matrix. For two reduced-density matrices

$$\rho = \begin{pmatrix} a & 0 \\ 0 & b \end{pmatrix}, \quad \rho' = \begin{pmatrix} c & 0 \\ 0 & d \end{pmatrix}$$

the fidelity can be calculated as

$$F(\rho, \rho') = \sqrt{ac} + \sqrt{bd}.$$

Though the fidelity itself is not a metric, it can be used to define a metric on the set of quantum state, i.e.

$$\theta_B(\rho, \rho') = \cos^{-1}[F(\rho, \rho')], \quad (10)$$

$$D_B(\rho, \rho') = \sqrt{2 - 2F(\rho, \rho')}, \quad (11)$$

$$S_B(\rho, \rho') = \sqrt{1 - [F(\rho, \rho')]^2}, \quad (12)$$

called commonly as Bures angle, Bures distance [29], and sine distance [30], respectively.

Besides the above well-accepted definitions, there are some alternative definitions of the fidelity. For example, Chen *et al* [31] proposed

$$\begin{aligned} |F(\rho, \rho')|^2 &= \\ \frac{1-r}{2} + \frac{1+r}{2} &\left[ \text{tr}(\rho\rho') + \sqrt{1 - \text{tr}(\rho^2)}\sqrt{1 - \text{tr}(\rho'^2)} \right], \end{aligned} \quad (13)$$

where  $r = 1/(d-1)$  with  $d$  being the dimension of the system. This definition has a hyperbolic geometric interpretation, and is reduced to Eq. 8 in the special case of  $d = 2$ . The definition [Eq. (13)] was recently simplified to [33]

$$|F(\rho, \rho')|^2 = \text{tr}(\rho\rho') + \sqrt{1 - \text{tr}(\rho^2)}\sqrt{1 - \text{tr}(\rho'^2)}. \quad (14)$$

Obviously, one of advantages of the above definitions is that the fidelity can be easily evaluated for arbitrary mixed states. Nevertheless, it seems that for two density matrices of two sets of mutually independent events, Eq. (14) gives a nonzero value. Therefore, another definition of the fidelity was proposed [34], i.e.

$$F(\rho, \rho') = \frac{|\text{tr}(\rho\rho')|}{\sqrt{\text{tr}(\rho^2)\text{tr}(\rho'^2)}}. \quad (15)$$

The fidelity has been widely used in many fields. In quantum information science, the fidelity between quantum states have been proved useful resources in approaching a number of fundamental problems such as quantifying entanglement [111, 112, 113]. There are also many interesting works on the fidelity in adiabatic processes. For example, the adiabatic fidelity was used to describe atom-to-molecule conversion [114, 115] in atomic systems and the time evolution in a Bose-Einstein condensate [116, 117, 118]. Physicists working on quantum chaos [119, 120, 121] use quantum fidelity (Loschmidt echo) to measure the hypersensitivity to small perturbations of quantum dynamics. In the latter case, the fidelity usually depends on the time. Interested readers can find more details about the Loschmidt echo in a recent review article by Gorin *et al* [32]. In the fidelity approach to quantum phase transitions, which will be introduced in this review, the fidelity depends on the adiabatic parameter (or driving parameter) of the Hamiltonian, and is usually static.

## B. Quantum state overlap and adiabatic evolution

To well understand the fidelity in the ground-state state evolution, in this subsection, we take a 1/2 spin sub-

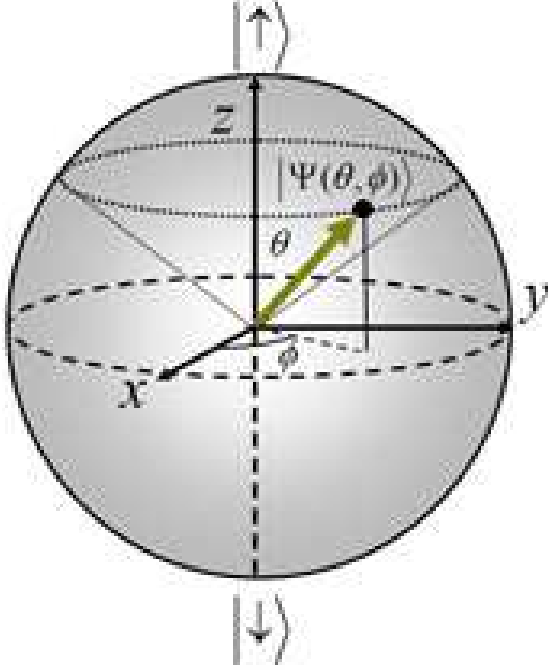


FIG. 1: (Color online) A single 1/2 spin state defined on a Bloch sphere.

jected an external magnetic field as a warm-up example. The Hamiltonian of a free spin under an arbitrary field  $\mathbf{B}(B \sin \theta \cos \phi, B \sin \theta \sin \phi, B \cos \theta)$  with magnitude  $B$  is

$$H = -\mathbf{B} \cdot \boldsymbol{\sigma}, \quad (16)$$

where  $\boldsymbol{\sigma} = (\sigma^x, \sigma^y, \sigma^z)$  are the Pauli matrices. In  $\sigma^z$  basis  $|\uparrow\rangle, |\downarrow\rangle$ , Pauli matrices take the form

$$\sigma^x = \begin{pmatrix} 0 & 1 \\ 1 & 0 \end{pmatrix}, \sigma^y = \begin{pmatrix} 0 & -i \\ i & 0 \end{pmatrix}, \sigma^z = \begin{pmatrix} 1 & 0 \\ 0 & -1 \end{pmatrix}. \quad (17)$$

Then the Hamiltonian (16) matrix can be rewritten as

$$H = -B \begin{pmatrix} \cos \theta & e^{-i\phi} \sin \theta \\ e^{i\phi} \sin \theta & -\cos \theta \end{pmatrix}. \quad (18)$$

The Hamiltonian can be easily diagonalized and the spin's ground state, with eigenenergy  $E_0 = -B$ , is

$$|\Psi(\theta, \phi)\rangle = \cos \frac{\theta}{2} |\uparrow\rangle + e^{i\phi} \sin \frac{\theta}{2} |\downarrow\rangle. \quad (19)$$

Here  $\theta$  and  $\phi$  define a point on the unit three-dimensional Bloch sphere to which the spin points to (see Fig. 1). The state can be multiplied by an arbitrary global phase. Obviously,  $\theta$  and  $\phi$  can be regarded as adiabatic parameters. *For simplicity and without loss of generality, we fixed  $\theta$  first.* Then the overlap between two states corresponding to two points on the ring of a given  $\theta$  is

$$\begin{aligned} f(\theta, \phi; \theta, \phi') &= \langle \Psi(\theta, \phi) | \Psi(\theta, \phi') \rangle \\ &= \cos^2 \frac{\theta}{2} + e^{i(\phi - \phi')} \sin^2 \frac{\theta}{2}. \end{aligned} \quad (20)$$

There are two parts in the overlap. The real part denotes the difference in the geometrical structure, while the imaginary one corresponds to the overall phase difference.

Though the overlap shows also the similarity between two states, it does not show the response of the state at a given point to the adiabatic parameter  $\phi$ . For this purpose, we expand the overlap around a given  $\phi$  as

$$\begin{aligned} f(\theta, \phi; \theta, \phi + \delta\phi) &= \langle \Psi(\theta, \phi) | \Psi(\theta, \phi) \rangle + \delta\phi \left\langle \Psi(\theta, \phi) \left| \frac{\partial}{\partial \phi} \Psi(\theta, \phi) \right. \right\rangle \\ &\quad + \frac{(\delta\phi)^2}{2} \left\langle \Psi(\theta, \phi) \left| \frac{\partial^2}{\partial \phi^2} \Psi(\theta, \phi) \right. \right\rangle + \dots, \end{aligned} \quad (21)$$

where

$$\left\langle \Psi(\theta, \phi) \left| \frac{\partial}{\partial \phi} \Psi(\theta, \phi) \right. \right\rangle = i \sin^2 \frac{\theta}{2}, \quad (22)$$

$$\left\langle \Psi(\theta, \phi) \left| \frac{\partial^2}{\partial \phi^2} \Psi(\theta, \phi) \right. \right\rangle = -\sin^2 \frac{\theta}{2}. \quad (23)$$

The linear term is the Berry adiabatic connection, which contribute a Pancharatnam-Berry phase [122, 123] to the spin as the magnetic field rotates adiabatically around cone direction (the dotted circle in Fig. 1), i.e.

$$\begin{aligned} \gamma(\theta, \phi) &= -i \int_0^\phi \left\langle \Psi(\theta, \phi') \left| \frac{\partial}{\partial \phi'} \Psi(\theta, \phi') \right. \right\rangle d\phi', \\ &= -\phi \sin^2 \frac{\theta}{2}. \end{aligned} \quad (24)$$

The phase equals to the solid angle of the cone if the spin rotates one periodicity. The Berry connection must be a purely imaginary number because of

$$\left\langle \Psi(\theta, \phi) \left| \frac{\partial}{\partial \phi} \Psi(\theta, \phi) \right. \right\rangle + \left\langle \frac{\partial}{\partial \phi} \Psi(\theta, \phi) \left| \Psi(\theta, \phi) \right. \right\rangle = 0. \quad (25)$$

The global phase can be rectified by a gauge transformation  $e^{-i\gamma(\theta, \phi)}$ , which can compensate the geometric phase  $\gamma(\theta, \phi)$  accumulated during the adiabatic evolution. The new state becomes

$$|\Psi(\theta, \phi)\rangle = e^{-i\gamma(\theta, \phi)} \left( \cos \frac{\theta}{2} |\uparrow\rangle + e^{i\phi} \sin \frac{\theta}{2} |\downarrow\rangle \right). \quad (26)$$

Then the overlap between two geometrically similar states becomes

$$\begin{aligned} f(\theta, \phi; \theta, \phi + \delta\phi) &= \exp \left[ i\delta\phi \sin^2 \frac{\theta}{2} \right] \\ &\quad \times \left( \cos^2 \frac{\theta}{2} + e^{-i\delta\phi} \sin^2 \frac{\theta}{2} \right) \\ &= 1 - \frac{(\delta\phi)^2}{2} \sin^2 \frac{\theta}{2} \cos^2 \frac{\theta}{2} + \dots \end{aligned} \quad (27)$$

The most relevant term is then the second derivative of the overlap. Moreover, the gauge transformation not only eliminates the Berry adiabatic connection, but also modifies the second order term. After the phase rectification, the second-order term is reduced to a minimum. On the other hand, the phase rectification denotes mathematically a rotation in the complex plane, which makes the overlap be a purely geometric quantity.

If we take the modulus of the overlap, it becomes the fidelity

$$\begin{aligned} |f|^2 &= \left( 1 + i\delta\phi \sin^2 \frac{\theta}{2} - \frac{(\delta\phi)^2}{2} \sin^2 \frac{\theta}{2} + \dots \right)^2 \\ &= 1 - (\delta\phi)^2 \sin^2 \frac{\theta}{2} \cos^2 \frac{\theta}{2} + \dots \end{aligned} \quad (28)$$

Then the fidelity, if we express it in a series form, becomes

$$F = |f| = 1 - \frac{(\delta\phi)^2}{2} \sin^2 \frac{\theta}{2} \cos^2 \frac{\theta}{2} + \dots \quad (29)$$

Therefore, the leading response of the fidelity to the adiabatic parameter is its second derivative. This is quite natural because the fidelity can not be large than its upper limit 1, it must be an even function of the perturbation of the adiabatic parameter. The leading term is called fidelity susceptibility in some literatures because it is physically a kind of structure of the driving term,

$$\begin{aligned} \chi_F &= \sin^2 \frac{\theta}{2} \cos^2 \frac{\theta}{2} \\ &= \frac{1}{4} \sin^2 \theta. \end{aligned} \quad (30)$$

Though the phase rectification can change the Berry adiabatic connection and the second derivative of the overlap, the fidelity susceptibility does not change. This phenomenon is due to the simple reason a gauge transformation cannot affect the modulus of the overlap.

On the other hand, when we study quantum phase transitions occurring in a quantum-many body system, the ground-state wavefunction is usually defined in the real space, then the imaginary part of the overlap does not appear. If the adiabatic parameter is defined on the flat manifold, the linear correction is zero. The second term is the most important. It denotes the leading response of the wave function to the adiabatic parameter. Though for the present case it is simply a constant due to the rotational symmetry of  $\phi$ , it might become singular for a many-body system in the thermodynamic limit.

Now we consider another case of fixing both  $\theta$  and  $\phi$ , and changing the magnitude of the external field. If  $B > 0$ , the ground state is

$$|\Psi(\theta, \phi)\rangle = \cos \frac{\theta}{2} |\uparrow\rangle + e^{i\phi} \sin \frac{\theta}{2} |\downarrow\rangle, \quad (31)$$

with eigenenergy  $-B$ , while if  $B < 0$ , the ground state becomes

$$|\Psi(\theta, \phi)\rangle = e^{i\phi} \sin \frac{\theta}{2} |\uparrow\rangle - \cos \frac{\theta}{2} |\downarrow\rangle, \quad (32)$$

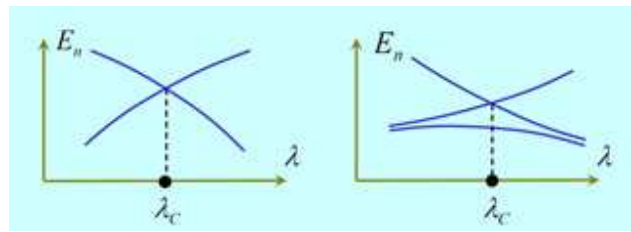


FIG. 2: (Color online) A sketch of a ground-state level crossing (LEFT) and the first-excited state level-crossing (RIGHT) as the system's driving parameter varies.

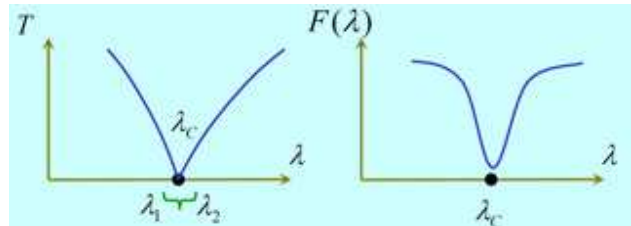


FIG. 3: (Color online) A sketch of a quantum phase transition occurred at  $\lambda_c$  (LEFT) and corresponding expected behavior of the fidelity  $F = \langle \Psi_0(\lambda_1) | \Psi_0(\lambda_2) \rangle$  as a function of  $\lambda = (\lambda_1 + \lambda_2)/2$  for a fixed  $\delta\lambda = \lambda_2 - \lambda_1$  (RIGHT).

with eigenenergy  $B$ . A ground-state level-crossing occurs at the point  $B = 0$ . Then the fidelity shows a very sharp drop at  $B = 0$  due to the level-crossing between two orthogonal states. While if we expand the fidelity in term of  $B$ , one may find that either the fidelity susceptibility or the Berry adiabatic connection is zero except for  $B = 0$ . The point is a singular for both of the fidelity susceptibility and the Berry adiabatic connection. In many studies on the Pancharatnam-Berry phase, this level-crossing point is regarded as a monopole in the parameter space.

### III. FIDELITY AND QUANTUM PHASE TRANSITIONS

The fidelity and its leading term introduced in the last section is illustrative. In this section, we try to establish a bridge between quantum phase transitions and the fidelity in considerable detail through the one-dimensional transverse-field Ising model.

#### A. Quantum phase transitions: fidelity perspective

Without loss of generality, the Hamiltonian of a general quantum many-body system, which might undergo a quantum phase transition in parameter space, can be

written as

$$H(\lambda) = H_0 + \lambda H_I, \quad (33)$$

where  $H_I$  is the driving Hamiltonian and  $\lambda$  denotes its strength. According to quantum mechanics, the system satisfies the Schrödinger equation

$$H(\lambda)|\Psi_n(\lambda)\rangle = E_n|\Psi_n(\lambda)\rangle, \quad n = 0, 1, \dots, \quad (34)$$

where  $E_n$  is the eigenenergy and set to an increasing order  $E_0 < E_1 \leq E_2 \dots$ , and  $|\Psi_n(\lambda)\rangle$  defines a set of orthogonal complete bases in the Hilbert space, i.e.

$$\sum_n |\Psi_n(\lambda)\rangle \langle \Psi_n(\lambda)| = I. \quad (35)$$

As the driving parameter  $\lambda$  varies, the energy spectra are changed correspondingly. The quantum phase transition occurs as the ground-state energy undergoes a significant change at a certain point. Precisely, its first- or higher-order derivative with respect to the driving parameter becomes discontinuous at the transition point. There are two distinct ways. The first one is the energy level-crossing occurring in the ground state (left plot of Fig. 2). The second is that the level-crossing occurs only in the low-lying excitations [2], and the ground state keeps nondegenerate (right plot of Fig. 2). For both cases, the structures of the ground-state wavefunction become qualitatively different across the transition point. That is, if we compare two ground states on both sides of the transition point, their distance is very large; while if we compare two ground states in the same phase, their distance is relatively small. Therefore, if we calculate the fidelity between two ground states, i.e., the fidelity of  $\Psi_0(\lambda_1)$  and  $\Psi_0(\lambda_2)$  at two slightly separated points  $\lambda_{1(2)}$  with fixed  $\delta = \lambda_1 - \lambda_2$ , it should manifest a minimum at the transition point, as shown in Fig. 3. Such a fascinating perspective for quantum phase transitions was first observed in the one-dimensional transverse-field Ising model [35, 36].

Obviously, the fidelity between two ground states does not bear any apparent information about the difference in order properties between two phases. Instead, it is a pure geometric quantity of quantum states. In its approach to quantum phase transitions, one of obvious advantage is that *no priori* knowledge of order parameter and symmetry-breaking is required. For example, if a quantum phase transition is induced by the ground-state level crossing, then the two crossing states at the transition point are orthogonal, then the overlap between them is zero; while the fidelity almost equals to one in other region away from the crossing point. Therefore, it is believed that the fidelity can describe quantum phase transitions in its own way.

### B. Example: the one-dimensional transverse-field Ising model

The one-dimensional transverse-field Ising model [125, 126, 127] is one of the simplest models which can be

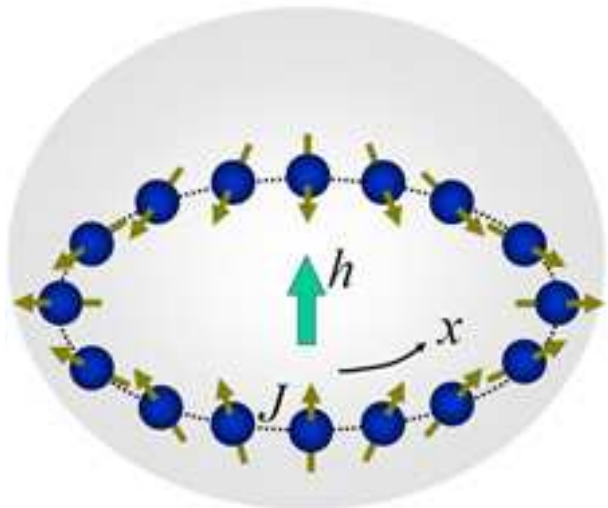


FIG. 4: (Color online) A sketch of the one-dimensional transverse-field Ising model with periodic boundary conditions. Two arbitrary neighboring spins interact with each other by the Ising interaction  $\sigma_j^x \sigma_{j+1}^x$  (dotted line). All spins are subject to an external field  $h$  along  $z$  direction.

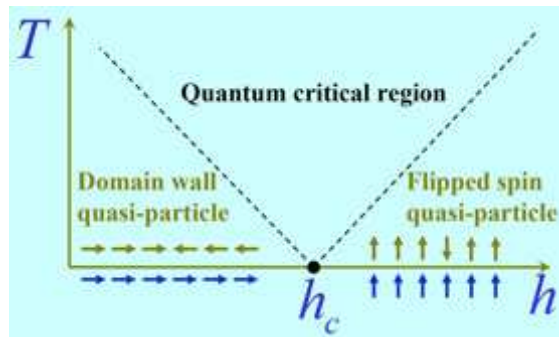


FIG. 5: (Color online) A schematic ground-state phase diagram of the one-dimensional transverse-field Ising model. At the left hand side of  $h_c$ , the ground state is in a ferromagnetic long-range order phase whose low-lying excitations are flipped spin quasi-particle. While at the right hand side of  $h_c$ , the ground state is a fully polarized phase whose low-lying excitations are domain wall quasi-particles.

solved exactly [128, 129] in the field of condensed matter physics. Due to its simplicity and clear physical pictures, the model is often used as a starting model to test new physical ideas and approaches, among which the fidelity does not make an exception. The following procedure is standard, and the final expression of fidelity is obtained by Zanardi and Paunković [36].

The Hamiltonian of the one-dimensional transverse-

field Ising model with periodic boundary conditions reads

$$H = -\sum_{j=1}^N (\sigma_j^x \sigma_{j+1}^x + h \sigma_j^z), \quad (36)$$

$$\sigma_1^x = \sigma_{N+1}^x, \quad (37)$$

where  $h$  is the transverse field and  $N$  is the number of spins. As inferred from the model's name, the Hamiltonian describes a chain of spins with the nearest-neighbor Ising interaction along  $x$ -direction, and all spins are subject to a transverse magnetic field  $h$  along the  $z$ -direction (Fig. 4).

The Hamiltonian is invariant under translational operation. Moreover, unlike usual spin systems, the  $z$ -component of total spins in this model, i.e.

$$\sigma^z = \sum_{j=1}^N \sigma_j^z, \quad (38)$$

is not conserved. Instead, if we introduce

$$\sigma^+ = \frac{1}{2}(\sigma^x + i\sigma^y), \quad \sigma^- = \frac{1}{2}(\sigma^x - i\sigma^y), \quad (39)$$

$$\sigma^+ = \begin{pmatrix} 0 & 1 \\ 0 & 0 \end{pmatrix}, \quad \sigma^- = \begin{pmatrix} 0 & 0 \\ 1 & 0 \end{pmatrix}, \quad (40)$$

and

$$\sigma^- |\uparrow\rangle = |\downarrow\rangle, \quad \sigma^+ |\downarrow\rangle = |\uparrow\rangle, \quad (41)$$

the Hamiltonian (36) can be transformed into

$$H = -\sum_{j=1}^N [(\sigma_j^+ \sigma_{j+1}^- + \sigma_j^- \sigma_{j+1}^+) + (\sigma_j^+ \sigma_{j+1}^+ + \sigma_j^- \sigma_{j+1}^-) + h \sigma_j^z], \quad (42)$$

then we can see that the off-diagonal terms in the Hamiltonian (42) either exchange the state of a pair of anti-parallel spins, or flip two upward spins to downward or vice versa. So they do not change the parity of the system. This property defines a classification of subspaces based on the parity operators, i.e.

$$P = \prod_{j=1}^N \sigma_j^z, \quad (43)$$

and the Hamiltonian cannot change the parity of the state, i.e.

$$[H, P] = 0. \quad (44)$$

Therefore, we have two subspaces corresponding to parity  $P = \pm 1$  respectively.

The ground state of the one-dimensional transverse-field Ising model can be understood from its two limiting cases. If  $h = 0$ , the Hamiltonian becomes the classical

one-dimensional Ising model. Defining the eigenstates of  $\sigma^x$  as

$$|\rightarrow\rangle = \frac{1}{\sqrt{2}}(|\uparrow\rangle + |\downarrow\rangle), \quad |\leftarrow\rangle = \frac{1}{\sqrt{2}}(|\uparrow\rangle - |\downarrow\rangle), \quad (45)$$

the doubly degenerate ground states of the Hamiltonian take the form

$$|\Psi_1\rangle = |\rightarrow\rightarrow\rightarrow\cdots\rangle, \quad (46)$$

$$|\Psi_2\rangle = |\leftarrow\leftarrow\leftarrow\cdots\rangle, \quad (47)$$

which are of ferromagnetic order. The ground-state properties change as the external field  $h$  turns on. Because of

$$\sigma^z |\rightarrow\rangle = |\leftarrow\rangle, \quad \sigma^z |\leftarrow\rangle = |\rightarrow\rangle, \quad (48)$$

the magnetic field mixes  $|\Psi_1\rangle$  and  $|\Psi_2\rangle$  and the ground state becomes non-degenerate for a finite system. Despite of this, the ground-state property does not change qualitatively. The ground state still manifests the ferromagnetic long-range order. Precisely, the correlation function

$$\langle \Psi_0 | \sigma_j^x \sigma_{j+r}^x | \Psi_0 \rangle - \langle \Psi_0 | \sigma_j^x | \Psi_0 \rangle \langle \Psi_0 | \sigma_{j+r}^x | \Psi_0 \rangle, \quad (49)$$

does not vanish even if  $r \rightarrow \infty$ . The correlation function, therefore, can be used as an order parameter to describe the phase in the small  $h$  region. While if  $h \rightarrow \infty$ , the Ising interaction is neglectable, all spins are fully polarized along  $z$ -direction. The ground state is non-degenerate and takes the form

$$|\Psi_0\rangle = |\uparrow\uparrow\uparrow\cdots\uparrow\uparrow\rangle. \quad (50)$$

In this limit, the correlation function Eq. (49) does not show long-range behavior. Therefore, a quantum phase transition between an ordered phase to a disordered phase is expected to occur as  $h$  changes from zero to infinite. A schematic ground-state phase diagram of the model is shown in Fig. 5.

In order to discuss the fidelity in the ground state, we now diagonalize the Hamiltonian in detail. We need three transformations, i.e., the Jordan-Wigner transformation [130], Fourier transformation, and Bogoliubov transformation.

*The Jordan-Wigner transformation:* The Jordan-Wigner transformation maps  $1/2$  spins to spinless fermions, that is

$$\sigma_n^+ = \exp \left[ i\pi \sum_{j=1}^{n-1} c_j^\dagger c_j \right] c_n = \prod_{j=1}^{n-1} \sigma_j^z c_n, \quad (51)$$

$$\sigma_n^- = \exp \left[ -i\pi \sum_{j=1}^{n-1} c_j^\dagger c_j \right] c_n^\dagger = \prod_{j=1}^{n-1} \sigma_j^z c_n^\dagger, \quad (52)$$

$$\sigma_n^z = 1 - 2c_n^\dagger c_n, \quad (53)$$

where  $c_n^\dagger$  and  $c_n$  are fermionic operators and satisfy the anticommutation relations

$$\{c_n^\dagger, c_m\} = \delta_{nm}, \quad (54)$$

$$\{c_n, c_m\} = \{c_n^\dagger, c_m^\dagger\} = 0. \quad (55)$$

After the Jordan-Wigner transformation, the Hamiltonian becomes

$$\begin{aligned} H = & - \sum_{j=1}^{N-1} \left[ (c_j^\dagger c_{j+1} + c_{j+1}^\dagger c_j) + (c_j^\dagger c_{j+1}^\dagger + c_{j+1} c_j) \right] \\ & + (c_1^\dagger c_N + c_N^\dagger c_1) \exp \left[ i\pi \sum_{j=1}^N c_j^\dagger c_j \right] \\ & + (c_N^\dagger c_1^\dagger + c_1 c_N) \exp \left[ i\pi \sum_{j=1}^N c_j^\dagger c_j \right] \\ & - \sum_{j=1}^N h (1 - 2c_j^\dagger c_j). \end{aligned} \quad (56)$$

The exponential factor

$$P = \exp \left[ i\pi \sum_{j=1}^N c_j^\dagger c_j \right],$$

is nothing but the parity of the system which is a constant, i.e. for periodic boundary conditions  $P = -1$  and antiperiodic boundary conditions  $P = 1$ . The Hamiltonian can be simplified as

$$\begin{aligned} H = & - \sum_{j=1}^N \left[ (c_j^\dagger c_{j+1} + c_{j+1}^\dagger c_j) + (c_j^\dagger c_{j+1}^\dagger + c_{j+1} c_j) \right] \\ & - \sum_{j=1}^N h (1 - 2c_j^\dagger c_j). \end{aligned} \quad (57)$$

*Fourier transformation:* Since the Hamiltonian is invariant under translational operation, we can perform standard Fourier transformation. For the present case, the transformations are

$$\begin{aligned} c_j &= \frac{1}{\sqrt{N}} \sum_k e^{-ikj} c_k, \\ c_j^\dagger &= \frac{1}{\sqrt{N}} \sum_k e^{ikj} c_k^\dagger, \end{aligned} \quad (58)$$

where the momentum  $ks$  are chosen under conditions:

$$k = \begin{cases} \frac{(2n+1)\pi}{N} & P = 1 \\ \frac{2n\pi}{N} & P = -1 \end{cases}, \quad (59)$$

with  $n = 0, 1, 2, \dots, N-1$ . Then the Hamiltonian can be transformed into  $k$ -space form,

$$\begin{aligned} H = & - \sum_k \left[ (2 \cos k - 2h) c_k^\dagger c_k + i \sin k (c_{-k}^\dagger c_k^\dagger + c_{-k} c_k) \right] \\ & - Nh. \end{aligned} \quad (60)$$

*Bogoliubov transformation:* Obviously, the quadratic Hamiltonian can be further diagonalized under the famous Bogoliubov transformation:

$$\begin{aligned} c_k &= u_k b_k + i v_k b_{-k}^\dagger, \\ c_k^\dagger &= u_k b_k^\dagger - i v_k b_{-k}, \\ c_{-k} &= u_k b_{-k} - i v_k b_k^\dagger, \\ c_{-k}^\dagger &= u_k b_{-k}^\dagger + i v_k b_k, \end{aligned} \quad (61)$$

where  $b_k$  and  $b_k^\dagger$  are also fermionic operator and satisfy the same anticommutation relation as  $c_k$  and  $c_k^\dagger$ . Because of this, one can find the coefficients in the transformation (61) should satisfy the following condition

$$v_k = -v_{-k}, \quad u_k^2 + v_k^2 = 1. \quad (62)$$

So we can introduce trigonal relation

$$v_k = \sin \theta_k, \quad u_k = \cos \theta_k. \quad (63)$$

Inserting the Bogoliubov transformation into Eq. (60), the coefficients are determined by

$$\begin{aligned} \cos 2\theta_k &= \frac{\cos(k) - h}{\sqrt{1 - 2h \cos(k) + h^2}}, \\ \sin 2\theta_k &= \frac{\sin(k)}{\sqrt{1 - 2h \cos(k) + h^2}}, \end{aligned} \quad (64)$$

such that the Hamiltonian becomes a quasi-free fermion system,

$$H = \sum_k \epsilon(k) (2b_k^\dagger b_k - 1), \quad (65)$$

where

$$\epsilon(k) = \sqrt{1 - 2h \cos(k) + h^2} \quad (66)$$

is the dispersion relation of the quasi particles. The dispersion relation shows that the thermodynamic system is gapless only at  $h = 1$ , and gapped in both phases of  $0 < h < 1$  and  $h > 1$ . Therefore, the quantum phase transition occurs at the point  $h = 1$ .

*The ground state:* The ground state of the model is defined as the vacuum state of  $b_k |\Psi_0\rangle = 0$  where

$$\begin{aligned} b_k &= \cos \theta_k c_k - i \sin \theta_k c_{-k}^\dagger, \\ b_{-k} &= \cos \theta_k c_{-k} + i \sin \theta_k c_k^\dagger. \end{aligned} \quad (67)$$

Since the condition

$$b_k \begin{pmatrix} a|0\rangle_k |0\rangle_{-k} + b|1\rangle_k |0\rangle_{-k} \\ + c|0\rangle_k |1\rangle_{-k} + d|1\rangle_k |1\rangle_{-k} \end{pmatrix} = 0 \quad (68)$$

gives

$$a = \cos \theta_k, \quad b = 0, \quad c = 0, \quad d = i \sin \theta_k, \quad (69)$$

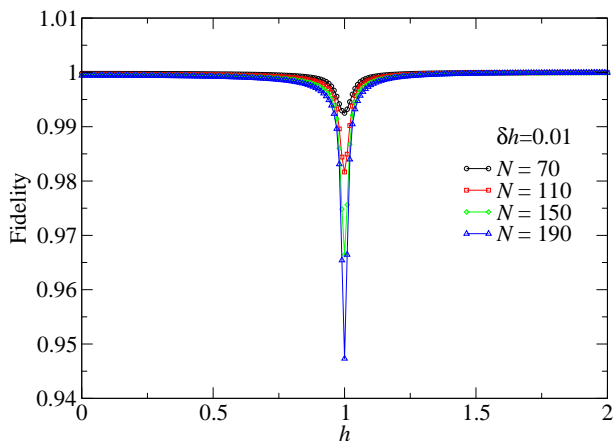


FIG. 6: (Color online) The fidelity of the one-dimensional

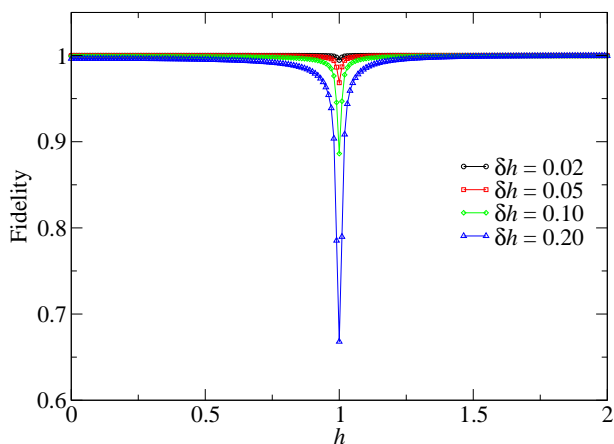


FIG. 7: (Color online) The fidelity of the one-dimensional transverse-field Ising model for various  $\delta h$ . Here  $N = 290$ .

the ground state takes the form

$$|\Psi_0(h)\rangle = \prod_{k>0} (\cos \theta_k |0\rangle_k |0\rangle_{-k} + i \sin \theta_k |1\rangle_k |1\rangle_{-k}). \quad (70)$$

The low-lying excitation can be obtained by applying  $b_k^\dagger$  to the ground state. In the ferromagnetic phase, the excitation is visualized as a quasi-particle of a flipped spin; and as a domain wall quasi-particle in the fully polarized phase (Fig. 5).

*Fidelity:* Once the ground state is obtained explicitly, the fidelity between  $h$  and  $h'$  can be calculated as [130]

$$F(h, h') = |\langle \Psi_0(h') | \Psi_0(h) \rangle| = \prod_{k>0} \cos(\theta_k - \theta'_k). \quad (71)$$

As is always emphasized, the fidelity is purely a geometrical quantity since it is an inner product between two vectors. Eq. (71) refresh our mind on this point because the expression is just an angle between two vectors. It is also consistent with the fourth fidelity axiom of Eq. (7)

because the ground-state wavefunction (70) is already a product state.

Fig. 6 shows the ground-state fidelity of the transverse-field Ising model as a function of  $h$  with parameter difference  $\delta h = 0.01$ . The numerical results of a smaller sample, say 20 sites, have also been compared with exact numerical computations and the agreement is essentially perfect (see Table II of section VII). As expected, the quantum critical region is clearly marked by a sudden drop of the value of fidelity. The behavior can be ascribed to a dramatic change in the structure of the ground state of the system during the quantum phase transition. The drop becomes sharper and sharper as the system size increases. Meanwhile the fidelity in the non-critical region is also reduced though the reduced magnitude is smaller than that at the critical point. This property can be interpreted due to the increasing of number of degree of freedom. Actually, in the thermodynamic limit, the fidelity between two different ground states might be zero, no matter how small the difference in parameter  $\delta h$  is. That is the two ground states are orthogonal to each other. This phenomena has been studied in quantum many-body systems, and is known as *the Anderson orthogonality catastrophe*[124]. Fig. 7 shows the fidelity for a given size system but various  $\delta h$ . The figure is easy to be understood. The larger the distance between two points in the parameter space, the larger the distance between the two corresponding ground states.

#### IV. FIDELITY SUSCEPTIBILITY, SCALING AND UNIVERSALITY CLASS

##### A. The leading term of the fidelity and dynamic structure factor

*The differential form:* A sudden drop of the fidelity caused by the ground-state level-crossing is too obvious to be interesting enough. People are interested in those ground-state wavefunctions which are differentiable in parameter space. Therefore, the overlap between two ground states at  $\lambda$  and  $\lambda + \delta\lambda$  can be defined as

$$f(\lambda, \lambda + \delta\lambda) = \langle \Psi_0(\lambda) | \Psi_0(\lambda + \delta\lambda) \rangle. \quad (72)$$

Performing series expansion, the overlap becomes

$$f(\lambda, \lambda + \delta\lambda) = 1 + \delta\lambda \left\langle \Psi_0(\lambda) \left| \frac{\partial}{\partial \lambda} \Psi_0(\lambda) \right. \right\rangle + \frac{(\delta\lambda)^2}{2} \left\langle \Psi_0(\lambda) \left| \frac{\partial^2}{\partial \lambda^2} \Psi_0(\lambda) \right. \right\rangle + \dots \quad (73)$$

The fidelity, as the absolute value of the overlap, then becomes

$$\begin{aligned}
& |f(\lambda, \lambda + \delta\lambda)|^2 \\
&= 1 + \delta\lambda \left( \left\langle \Psi_0 \left| \frac{\partial}{\partial\lambda} \Psi_0 \right\rangle + \left\langle \frac{\partial}{\partial\lambda} \Psi_0 \left| \Psi_0 \right\rangle \right) \right. \\
&\quad + (\delta\lambda)^2 \left( \left\langle \frac{\partial}{\partial\lambda} \Psi_0 \left| \Psi_0 \right\rangle \left\langle \Psi_0 \left| \frac{\partial}{\partial\lambda} \Psi_0 \right\rangle \right. \right. \\
&\quad \left. \left. + \frac{1}{2} \left\langle \Psi_0 \left| \frac{\partial^2}{\partial\lambda^2} \Psi_0 \right\rangle + \frac{1}{2} \left\langle \frac{\partial^2}{\partial\lambda^2} \Psi_0 \left| \Psi_0 \right\rangle \right) \right) + \dots \quad (75)
\end{aligned}$$

The linear correction must be zero. There are two reasons. The first is due to the normalization condition, i.e.

$$\left\langle \Psi_0 \left| \frac{\partial}{\partial\lambda} \Psi_0 \right\rangle + \left\langle \frac{\partial}{\partial\lambda} \Psi_0 \left| \Psi_0 \right\rangle = \frac{\partial}{\partial\lambda} \langle \Psi_0 | \Psi_0 \rangle = 0. \quad (76)$$

The second is that the  $|f|$  must be small than 1, then the leading term must be an even function of  $\delta\lambda$ . Therefore,

$$F(\lambda, \lambda + \delta\lambda) = 1 - \frac{(\delta\lambda)^2}{2} \chi_F + \dots, \quad (77)$$

where  $\chi_F$  denotes the fidelity susceptibility of the ground state,

$$\begin{aligned}
\chi_F &= \left\langle \frac{\partial}{\partial\lambda} \Psi_0 \left| \frac{\partial}{\partial\lambda} \Psi_0 \right\rangle \right. \\
&\quad \left. - \left\langle \frac{\partial}{\partial\lambda} \Psi_0 \left| \Psi_0 \right\rangle \left\langle \Psi_0 \left| \frac{\partial}{\partial\lambda} \Psi_0 \right\rangle \right. \right). \quad (78)
\end{aligned}$$

This is the differential form the fidelity susceptibility.

On the other hand, if the ground-state wavefunction is defined in the multi-dimensional parameter space, say  $\lambda = \{\lambda_a\}$ ,  $a = 1, 2, \dots, \Lambda$ , the overlap between two states at  $\lambda$  and  $\lambda' = \lambda + \delta\lambda$  is

$$\begin{aligned}
f(\lambda, \lambda + \delta\lambda) &= 1 + \sum_a \delta\lambda_a \left\langle \Psi_0 \left| \frac{\partial}{\partial\lambda_a} \Psi_0 \right\rangle \right. \\
&\quad \left. + \sum_{ab} \frac{\delta\lambda_a \delta\lambda_b}{2} \left\langle \Psi_0 \left| \frac{\partial}{\partial\lambda_a} \frac{\partial}{\partial\lambda_b} \Psi_0 \right\rangle \right. + \dots \quad (79)
\end{aligned}$$

The fidelity susceptibility becomes

$$\begin{aligned}
\chi_F &= \sum_{ab} \frac{\partial\lambda_a}{\partial\lambda} \frac{\partial\lambda_b}{\partial\lambda} \left( \frac{1}{2} \left\langle \frac{\partial}{\partial\lambda_a} \Psi_0 \left| \frac{\partial}{\partial\lambda_b} \Psi_0 \right\rangle \right. \right. \\
&\quad \left. \left. + \frac{1}{2} \left\langle \frac{\partial}{\partial\lambda_b} \Psi_0 \left| \frac{\partial}{\partial\lambda_a} \Psi_0 \right\rangle \right. \right. \quad (80) \\
&\quad \left. \left. - \left\langle \frac{\partial}{\partial\lambda_a} \Psi_0 \left| \Psi_0 \right\rangle \left\langle \Psi_0 \left| \frac{\partial}{\partial\lambda_b} \Psi_0 \right\rangle \right) \right), \quad (81)
\end{aligned}$$

where the vector  $\partial\lambda_a/\partial\lambda$  denotes the direction of the short displacement  $\delta\lambda$  in parameter space. The term in

the parenthesis of Eq. (81) is called quantum metric tensor [109, 110] or the Riemann metric tensor [44]

$$\begin{aligned}
g_{ab} &= \frac{1}{2} \left\langle \frac{\partial}{\partial\lambda_a} \Psi_0 \left| \frac{\partial}{\partial\lambda_b} \Psi_0 \right\rangle + \frac{1}{2} \left\langle \frac{\partial}{\partial\lambda_b} \Psi_0 \left| \frac{\partial}{\partial\lambda_a} \Psi_0 \right\rangle \right. \\
&\quad \left. - \left\langle \frac{\partial}{\partial\lambda_a} \Psi_0 \left| \Psi_0 \right\rangle \left\langle \Psi_0 \left| \frac{\partial}{\partial\lambda_b} \Psi_0 \right\rangle \right. \right). \quad (82)
\end{aligned}$$

The quantum metric tensor is symmetric under exchange of the index  $a$  and  $b$ . It is the real part of a more generalized quantum geometric tensor [109] of the ground state. Precisely, if we defined the projection operator

$$P \equiv I - |\Psi_0\rangle\langle\Psi_0|, \quad (83)$$

which projects out the ground state, the quantum geometric tensor then is defined as

$$T_{ab} = \left\langle \frac{\partial}{\partial\lambda_a} \Psi_0 \left| P \left| \frac{\partial}{\partial\lambda_b} \Psi_0 \right\rangle \right. \right). \quad (84)$$

Therefore,

$$g_{ab} = \text{Re} T_{ab}, \quad (85)$$

and the imaginary part of  $T_{ab}$  defines a 2-form phase,

$$V_{ab} = 2\text{Im} T_{ab}. \quad (86)$$

The 2-form phase  $V_{ab}$  plays a very important role in geometric phase. Its flux gives the Berry phase. While the quantum geometric tensor provides a natural means of measuring distance along the evolution path in parameter space. The distance between two ground states can be expressed in the differential-geometrical form, i.e

$$ds^2 = \sum_{ab} g_{ab} \delta\lambda_a \delta\lambda_b. \quad (87)$$

In addition, if the ground state of the system evolves adiabatically from  $\lambda$  to  $\lambda'$  at a given path  $S$ , the quantum distance  $R_q$  in the parameter space is

$$R_q = \oint_S \sqrt{\sum_{ab} g_{ab} d\lambda_a d\lambda_b}. \quad (88)$$

Therefore, if we do geodesics,

$$\delta R_q = 0. \quad (89)$$

we can in principle find the shortest path connecting the two ground states at  $\lambda$  and  $\lambda'$ .

**Example:**

Take the spin in an external field as an example, its ground state is

$$|\Psi(\theta, \phi)\rangle = \cos \frac{\theta}{2} |\uparrow\rangle + e^{i\phi} \sin \frac{\theta}{2} |\downarrow\rangle.$$

The quantum metric tensor takes the form

$$g = \begin{pmatrix} 1 & \\ & \sin^2 \theta \end{pmatrix}.$$

so

$$ds^2 = d\theta^2 + \sin^2 \theta d\phi^2$$

which is the metric on the sphere of parameters.

*The perturbation form:* We concern mainly on the fidelity in continuous phase transitions. That is, the ground state of the Hamiltonian is nondegenerate for a finite system. Therefore, as the point  $\lambda + \delta\lambda$  closing to  $\lambda$ , the ground-state wavefunction can be obtained, to the first order, as

$$|\Psi_0(\lambda + \delta\lambda)\rangle = |\Psi_0(\lambda)\rangle + \delta\lambda \sum_{n \neq 0} \frac{H_I^{n0}(\lambda) |\Psi_n(\lambda)\rangle}{E_0(\lambda) - E_n(\lambda)}, \quad (90)$$

where

$$H_I^{n0} = \langle \Psi_n(\lambda) | H_I | \Psi_0(\lambda) \rangle \quad (91)$$

is the hopping matrix of the driving Hamiltonian  $H_I$ . Therefore, if we normalized the wavefunction  $|\Psi_0(\lambda + \delta\lambda)\rangle$ , the fidelity becomes, to the leading order,

$$F^2 = 1 - \delta\lambda^2 \sum_{n \neq 0} \frac{|\langle \Psi_n(\lambda) | H_I | \Psi_0(\lambda) \rangle|^2}{[E_n(\lambda) - E_0(\lambda)]^2} + \dots \quad (92)$$

Obviously, the fidelity depends both on  $\lambda$  and  $\delta\lambda$ . The most relevant term is the leading term in Eq. (92), i.e. the second order derivative of the fidelity with respect to  $\delta\lambda$ . The term actually defines the response of the fidelity to a small change in  $\lambda$ . The fidelity susceptibility can be obtained as

$$\chi_F(\lambda) \equiv \lim_{\delta\lambda \rightarrow 0} \frac{-2 \ln F}{\delta\lambda^2} \quad (93)$$

$$= -\frac{\partial^2 F}{\partial(\delta\lambda)^2}. \quad (94)$$

With Eq. (92), it can be rewritten as [43, 44]

$$\chi_F(\lambda) = \sum_{n \neq 0} \frac{|\langle \Psi_n(\lambda) | H_I | \Psi_0(\lambda) \rangle|^2}{[E_n(\lambda) - E_0(\lambda)]^2}. \quad (95)$$

This is the summation form of the fidelity susceptibility. The form establishes a relation between the structure difference of two wavefunctions and low-lying energy spectra.

**Example:**

To understand Eq. (95), we still take the spin in an external field [Eq. (16)] as an example. The driving term in the Hamiltonian at a fix point can be obtained as

$$\frac{\partial H}{\partial \phi} = iB \begin{pmatrix} 0 & e^{-i\phi} \sin \theta \\ -e^{i\phi} \sin \theta & 0 \end{pmatrix}.$$

The excited state is

$$|\Psi_1(\theta, \phi)\rangle = e^{i\phi} \sin \frac{\theta}{2} |\uparrow\rangle - \cos \frac{\theta}{2} |\downarrow\rangle$$

Then the hopping matrix between the ground state and excited state takes the form

$$\left\langle \Psi_1(\theta, \phi) \left| \frac{\partial H}{\partial \phi} \right| \Psi_0(\theta, \phi) \right\rangle = iB e^{i\phi} \sin \theta$$

The energy different between two state is  $2B$ , then the fidelity susceptibility becomes

$$\chi_F = \frac{1}{4} \sin^2 \theta$$

which is the same as Eq. (30).

On the other hand, according the perturbation theory, the second order perturbation to the ground-state energy takes the form

$$E_0^{(2)} = \sum_{n \neq 0} \frac{|\langle \Psi_n(\lambda) | H_I | \Psi_0(\lambda) \rangle|^2}{E_0(\lambda) - E_n(\lambda)}. \quad (96)$$

Obviously, Eq. (95) and Eq. (96) are very similar in their form except for different exponents in both denominators [61]. Therefore, one might expect that the origin of the singularity of the fidelity susceptibility and  $E_0^{(2)}$  are both due to the vanishing of the energy gap though the fidelity susceptibility shows a sharper peak than  $E_0^{(2)}$ . For the finite-order phase transition, however,  $E_0^{(2)}$  can be still a continuous function of the driving parameter, then there is no reason to require that the fidelity susceptibility shows singular behavior in high-order ( $> 2$ ) quantum phase transitions. It was also pointed out later that the fidelity susceptibility might be related to the third energy perturbation [63],

$$\chi_F = \frac{1}{H_I^{00}} \sum_{i,j>0} \frac{H_I^{0i} H_I^{ij} H_I^{j0}}{(E_i - E_0)(E_j - E_0)} - \frac{E_0^{(3)}}{E_0^{(1)}}. \quad (97)$$

Therefore, the fidelity susceptibility might not be able to witness those phase transitions of infinite order [43, 61], such as the Beresinskii-Kosterlitz-Thouless transition.

*The fidelity susceptibility as a kind of fluctuation:* The hopping matrix  $\langle \Psi_n | H_I | \Psi_0 \rangle$  implies dynamics behaviors of

the fidelity susceptibility. Similar to the linear response theory, one can define the *dynamic fidelity susceptibility* as

$$\chi_F(\omega) = \sum_{n \neq 0} \frac{|\langle \Psi_n | H_I | \Psi_0 \rangle|^2}{[E_n - E_0]^2 + \omega^2}. \quad (98)$$

Performing a Fourier transformation, the dynamic fidelity susceptibility becomes

$$\chi_F(\tau) = \sum_{n \neq 0} \frac{\pi |\langle \Psi_n | H_I | \Psi_0 \rangle|^2}{E_n - E_0} e^{-(E_n - E_0)|\tau|}. \quad (99)$$

The energy difference in the denominators can be canceled if one take a derivative with respect to  $\tau$ , the dynamic fidelity susceptibility then is

$$\frac{\partial \chi_F(\tau)}{\partial \tau} = -\pi G_I(\tau) \theta(\tau) + \pi G_I(-\tau) \theta(-\tau).$$

Here  $\theta(\tau)$  is the step function

$$\theta(\tau) = \begin{cases} 1 & \tau > 0 \\ 1/2 & \tau = 0 \\ 0 & \tau < 0 \end{cases} \quad (100)$$

and

$$G_I(\tau) = \langle \Psi_0 | H_I(\tau) H_I(0) | \Psi_0 \rangle - \langle \Psi_0 | H_I | \Psi_0 \rangle^2 \quad (101)$$

$$H_I(\tau) = e^{H(\lambda)\tau} H_I e^{-H(\lambda)\tau}, \quad (102)$$

with  $\tau$  being the imaginary time. Performing an inverse Fourier transformation, we can obtain

$$\chi_F(\omega) = \frac{1}{\omega} \int_0^\infty \sin(\omega\tau) G_I(\tau) d\tau. \quad (103)$$

The fidelity susceptibility then becomes

$$\chi_F = \lim_{\omega \rightarrow 0} \frac{1}{\omega} \int_0^\infty \sin(\omega\tau) G_I(\tau) d\tau. \quad (104)$$

For any finite system, the correlation function  $G_I(\tau)$  decays in the large  $\tau$  limit, the above limit satisfies the Lebesgue's convergent theorem, the fidelity susceptibility, finally, has the form [43]

$$\chi_F = \int_0^\infty \tau G_I(\tau) d\tau. \quad (105)$$

Therefore, the fidelity susceptibility is nothing but a kind of dynamics structure factor of the driving Hamiltonian.

The Eq. (105) is remarkable because it connects the fidelity to dynamical response of the system by the driving Hamiltonian  $H_I$ . In this way, the adiabatic evolution of the ground state and the fidelity susceptibility are expressed in terms of standard quantities in linear response

theory and their physics content is clarified. Traditionally, quantum phase transitions are said to be driven by quantum fluctuations, which originate from the Heisenberg uncertainty relation. In the Hamiltonian (33),

$$[H_0, H_I] \neq 0. \quad (106)$$

The second order perturbation to the ground-state energy

$$E_0^{(2)} = \int [\langle \Psi_0 | H_I(\tau) H_I(0) | \Psi_0 \rangle - \langle \Psi_0 | H_I | \Psi_0 \rangle^2] d\tau \quad (107)$$

is also a kind of fluctuation. Clearly, both  $E_0^{(2)}$  and  $\chi_F$  become zero if  $[H_0, H_I] = 0$ . Therefore, the expression (105) provides a new angle to understand the role of quantum fluctuation in quantum phase transitions.

*The quantum metric tensor:* In case that the Hamiltonian is defined in a high-dimensional parameter space, the fidelity susceptibility becomes a metric tensor. The Hamiltonian in  $\Lambda$ -dimensional parameter space reads,

$$H = \sum_a \lambda_a H_a, \quad a = 1, \dots, \Lambda, \quad (108)$$

where  $\lambda_a$ s are coupling parameters. Clearly

$$H_a = \frac{\partial H}{\partial \lambda_a}. \quad (109)$$

In the parameter space, we can always let the ground state of the system evolves along a certain path, i.e

$$\lambda_a = \lambda_a(\lambda), \quad (110)$$

where  $\lambda$  plays a kind of driving parameter along the evolution line. Therefore, the driving term in the Hamiltonian at a given point  $\lambda$  is

$$H_I = \frac{\partial H}{\partial \lambda} = \sum_a \frac{\partial \lambda_a}{\partial \lambda} H_a. \quad (111)$$

Then the fidelity susceptibility along this line can be calculated as

$$\begin{aligned} \chi_F(\lambda) &= \sum_{n \neq 0} \frac{|\langle \Psi_n(\lambda) | H_I | \Psi_0(\lambda) \rangle|^2}{[E_n(\lambda) - E_0(\lambda)]^2} \\ &= \sum_{ab} \frac{\partial \lambda_a}{\partial \lambda} \frac{\partial \lambda_b}{\partial \lambda} \sum_{n \neq 0} \frac{H_a^{0n} H_b^{n0}}{[E_n(\lambda) - E_0(\lambda)]^2}, \end{aligned} \quad (112)$$

where  $H_{a(b)}^{mn} = \langle \Psi_m(\lambda) | H_{a(b)} | \Psi_n(\lambda) \rangle$ . So the quantum metric tensor takes the form

$$g_{ab} = \sum_n \frac{H_a^{0n} H_b^{n0}}{[E_n(\lambda) - E_0(\lambda)]^2}. \quad (113)$$

This is the perturbative form for the quantum metric tensor.

$$g_{ab} = \int \tau G_{ab}(\tau) d\tau, \quad (114)$$

where  $G_{ab}(\tau)$  is a time-dependent correlation function,

$$G_{ab}(\tau) = \theta(\tau)(\langle \Psi_0 | H_a(\tau) H_b(0) | \Psi_0 \rangle - \langle \Psi_0 | H_a(0) | \Psi_0 \rangle \langle \Psi_0 | H_b(0) | \Psi_0 \rangle). \quad (115)$$

Clearly, Eq. (114) is an extension of Eq. (105). Both of them clarify the physics content of the fidelity approach and the role of quantum fluctuation in the adiabatic evolution.

### B. Scaling analysis and universality class

In physics, if a physical quantity depends linearly on the system size, the quantity is extensive (additive), such as energy; and if it is independent of the system size, it is intensive, such as energy density. If we define  $\Delta$  as the energy gap between the ground state and the lowest excitation with nonzero  $\langle \Psi_n(\lambda) | H_I | \Psi_0(\lambda) \rangle$ , the fidelity susceptibility satisfies the following inequalities

$$\begin{aligned} \chi_F &\leq \frac{1}{\Delta} \sum_{n \neq 0} \frac{|\langle \Psi_n(\lambda) | H_I | \Psi_0(\lambda) \rangle|^2}{[E_n(\lambda) - E_0(\lambda)]} = -\frac{1}{2\Delta} \frac{\partial^2 E(\lambda)}{\partial \lambda^2}, \\ &\leq \frac{1}{\Delta^2} \sum_{n \neq 0} |\langle \Psi_n(\lambda) | H_I | \Psi_0(\lambda) \rangle|^2, \\ &= \frac{1}{\Delta^2} [\langle \Psi_0(\lambda) | H_I^2 | \Psi_0(\lambda) \rangle - \langle \Psi_0(\lambda) | H_I | \Psi_0(\lambda) \rangle^2]. \end{aligned} \quad (116)$$

The inequalities tell us some useful information about the properties of the fidelity susceptibility away from the critical point:

1. If the system is gapped and  $H_I$  behaves like a single particle,  $\chi_F$  is an intensive quantity.
2. If the system is gapped, the fidelity susceptibility share the same (or smaller) dependence on the system size as the second order derivative of the ground state energy.
3. If  $\chi_F$  is a superextensive quantity, the ground state of the system should be gapless.

Therefore, unlike conventional physical quantities, the fidelity susceptibility can either be an extensive quantity, like the energy, or has other type of dependence on the system size. To have an explicit view of the dependence of the fidelity susceptibility on the system size, it is useful to perform scaling transformation, which is firstly carried out by Venuti and Zanardi [47]. Without loss of generality, the interaction Hamiltonian can be written as a summation of local terms, i.e.

$$H_I = \sum_r V(r), \quad (117)$$

and number of site

$$N = L^d, \quad (118)$$

where  $d$  is the real dimension of the system. Then the fidelity susceptibility becomes [43]

$$\frac{\chi_F}{L^d} = \sum_r \int \tau C(r, \tau) d\tau, \quad (119)$$

where

$$C(r, \tau) = \langle \Psi_0(\lambda) | V(r, \tau) V(0, 0) | \Psi_0(\lambda) \rangle - \langle \Psi_0(\lambda) | V(r, 0) | \Psi_0(\lambda) \rangle \langle \Psi_0(\lambda) | V(0, 0) | \Psi_0(\lambda) \rangle. \quad (120)$$

In the vicinity of the critical point, the scaling transformation goes [131, 132]

$$r' = s r, \quad \tau' = s^\zeta \tau, \quad V(r') = s^{-\Delta_V} V(r), \quad (121)$$

where  $s > 1$ ,  $\zeta$  is the dynamic exponent, and  $\Delta_V$  is the scaling dimension of  $V(r)$ , one can find that

$$\frac{\chi'_F}{(L'/s)^d} = \frac{1}{s^{2\zeta - 2\Delta_V}} \sum_{r'} \int \tau' C(r', \tau) d\tau'. \quad (122)$$

Therefore

$$\frac{\chi'_F}{(L')^d} = \frac{1}{s^{d+2\zeta-2\Delta_V}} \frac{\chi_F}{L^d}, \quad (123)$$

which defines the scaling transformation of the fidelity susceptibility. Around the critical point, the correlation length is divergent and the only length scale is the system size itself, the fidelity susceptibility scales like

$$\frac{\chi_F}{L^d} \sim L^{d+2\zeta-2\Delta_V}. \quad (124)$$

The expression is interesting. It establishes a relation between the size dependence of the fidelity susceptibility, the dynamic exponent, and the scaling dimension of the diverging term.

In most cases, we can regard  $\chi_F/L^d$  as an intensive quantity in general quantum phases because the system is usually gapped. Therefore, the singular behavior of the fidelity susceptibility is due to

$$d + 2\zeta > 2\Delta_V \quad (125)$$

at the critical point. If the fidelity susceptibility diverges as

$$\frac{\chi_F}{L^d} \sim \frac{1}{|\lambda - \lambda_c|^\alpha}. \quad (126)$$

the scaling exponents satisfy

$$\alpha = \frac{d + 2\zeta - 2\Delta_V}{\nu}, \quad (127)$$

where  $\nu$  is the critical exponent of the correlation length. A similar relation was also obtained by Gu *et al* [49] in their studies on the one-dimensional asymmetric Hubbard model.

However, Eqs. (124-127) are not universally true in all quantum phase transitions. Considering a general correlation function

$$C(r, \tau) = \frac{1}{r^{2\Delta_V}} f(r\tau^{1/\zeta}) \quad (128)$$

the fidelity susceptibility, in the thermodynamic limit, becomes

$$\frac{\chi_F}{L^d} = \sum_r \int \frac{\tau}{r^{2\Delta_V}} f(r\tau^{1/\zeta}) d\tau, \quad (129)$$

$$\sim \sum_r \frac{1}{r^{2\Delta_V - 2\zeta}} \quad (130)$$

$$\propto \begin{cases} L^{d+2\zeta-2\Delta_V}, & 2\Delta_V - 2\zeta \neq d \\ \ln L, & 2\Delta_V - 2\zeta = d \end{cases}. \quad (131)$$

Such an explicit expression implies that the fidelity susceptibility is not always extensive. Even in a gapped phase, as we can see from the Lipkin-Meshkov-Glick model, it can be intensive. Therefore, if we define the size exponent above (below) the critical point as  $d^+$  ( $d^-$ ), that is the fidelity susceptibility

$$\chi(\lambda) \propto L^{d^\pm}. \quad (132)$$

Hence  $\chi_F/L^{d^\pm}$  is an intensive quantity in corresponding phases. Physically, since the fidelity susceptibility denotes the response of the ground state to the adiabatic parameter and  $d_a^\pm$  is the dimensional dependence of the adiabatic evolution,  $d_a^\pm$  has been called *adiabatic dimension*.

Therefore, the singular part of the fidelity susceptibility as an intensive quantity, around the critical point behaves [49]

$$\frac{\chi_F}{L^{d_a^\pm}} \sim \frac{1}{|\lambda - \lambda_c|^{\alpha^\pm}}, \quad (133)$$

where  $\alpha^\pm$  denote the critical exponents of the fidelity susceptibility above or below the critical point. On the other hand, if the fidelity susceptibility around the critical point shows a peak for a finite system, its maximum point at  $\lambda_{\max}$  scales like

$$\chi(\lambda = \lambda_{\max}) \propto L^{d_a^c}, \quad (134)$$

where  $d_a^c$  denotes the critical adiabatic dimension, and can be either analyzed from Eq. (124) or obtained from numerical scaling analysis. The following function can include the above two asymptotic behaviors,

$$\frac{\chi(\lambda, L)}{L^{d_a^\pm}} = \frac{A}{L^{-d_a^c + d_a^\pm} + B(\lambda - \lambda_{\max})^{\alpha^\pm}}, \quad (135)$$

where  $A$  is a constant,  $B$  is a nonzero function of  $\lambda$  around the critical point, and both of them are independent of the system size. According to Eq. (135), the rescaled FS

is a universal function of the rescaled driving parameter  $L^\nu(\lambda - \lambda_{\max})$ , i.e.,

$$\frac{\chi_{F(\lambda)}(\lambda = \lambda_{\max}, L) - \chi_{F(\lambda)}(\lambda, L)}{\chi_{F(\lambda)}(\lambda, L)} = f[L^\nu(\lambda - \lambda_{\max})], \quad (136)$$

where  $\nu$  is the critical exponent of the correlation length. Then we have [49, 78]

$$\alpha^\pm = \frac{d_a^c - d_a^\pm}{\nu}. \quad (137)$$

Therefore, unlike the second derivative of the ground-state energy, the fidelity susceptibility might have different critical exponents at both sides of the critical point. The above procedure is useful to determine the critical exponent from numerical computations, and has been used in some models. Nevertheless, it is still not complete. In some cases, the fidelity susceptibility shows logarithmic divergence around the critical point. Then we have  $\alpha = 0$ , and Eqs. (133-137) should be changed correspondingly. For this case, at one side of the critical point, if  $\chi_F/L^{d_a}$  is intensive, and

$$\frac{\chi(\lambda = \lambda_{\max})}{L^{d_a}} \propto \ln L, \quad (138)$$

around the critical point. The logarithmic divergence implies that

$$1 - \exp[\chi_{F(\lambda)}(\lambda, L) - \chi_{F(\lambda)}(\lambda = \lambda_{\max}, L)] = f[L^\nu(\lambda - \lambda_{\max})], \quad (139)$$

should be a universal function.

Clearly, unlike conventional physical quantity that is either intensive or extensive, the fidelity susceptibility, as analyzed above, manifests distinct scaling behavior. This property might be due to both the relevance of the driving Hamiltonian under the renormalization group transformation and distinct dynamic exponent in different phases.

### C. Example A: the one-dimensional transverse-field Ising model

The one-dimensional transverse-field Ising model gives us a simple example. For the Ising model, the fidelity is

$$F(h, h') = |\langle \Psi_0(h') | \Psi_0(h) \rangle| = \prod_{k>0} \cos(\theta_k - \theta'_k). \quad (140)$$

At the point  $h$ , the fidelity susceptibility can be calculated as

$$\chi_F = \sum_{k>0} \left( \frac{d\theta_k}{d\lambda} \right)^2, \quad (141)$$

where

$$\frac{d\theta_k}{d\lambda} = \frac{1}{2} \frac{\sin k}{1 + h^2 - 2h \cos k}. \quad (142)$$

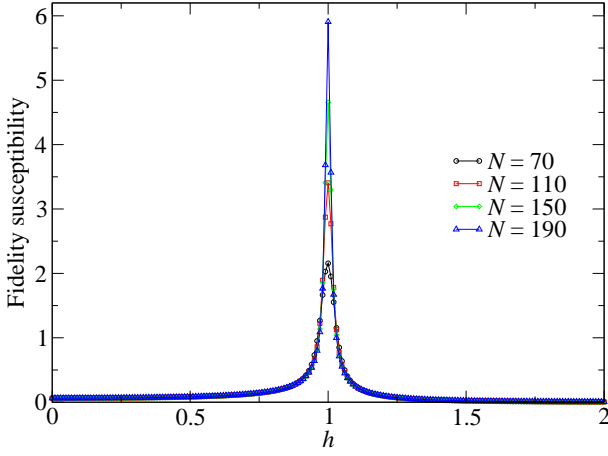


FIG. 8: (Color online) The fidelity susceptibility  $\chi_F/N$  of the one-dimensional transverse-field Ising model for various system sizes.

To find the scaling behavior of the fidelity susceptibility, let us first consider the case of  $h = 1$ , then

$$\chi_F = \frac{1}{16} \sum_k \frac{\sin^2 k}{(1 - \cos k)^2}, \quad (143)$$

$$\simeq \frac{N}{2} \int_{\pi/N}^{\pi(N-1)/N} \frac{1}{k^2} dk, \quad (144)$$

$$\propto N^2. \quad (145)$$

Therefore, we have

$$d_a^c = 2, \quad (146)$$

for the one-dimensional transverse-field Ising model (see Fig. 8). On the other hand, if  $h \neq 1$ , the fidelity susceptibility becomes

$$\chi_F = \frac{N}{2} \int_{\pi/N}^{\pi(N-1)/N} \left( \frac{\sin k}{1 + h^2 - 2h \cos k} \right)^2 dk.$$

Obviously, there is no pole in the denominator of integrand.  $\chi_F$  then is an extensive quantity (see Fig. 8),

$$\frac{\chi_F}{N} = \frac{1}{2} \int_0^1 \left[ \frac{\sin(2\pi x)}{1 + h^2 - 2h \cos(2\pi x)} \right]^2 dx. \quad (147)$$

So the adiabatic dimension for the Ising model is  $d_a^\pm = 1$ . Explicitly, the integration can be evaluated by the residue theorem [74]. Let

$$\begin{aligned} \sin(2\pi x) &= \frac{1}{2i} \left( z - \frac{1}{z} \right), \\ \cos(2\pi x) &= \frac{1}{2} \left( z + \frac{1}{z} \right), \end{aligned}$$

Eq. (147) becomes a contour integration along a unit circle. Then, we can obtain

$$\frac{\chi_F}{N} = \frac{1}{16(1 - h^2)},$$

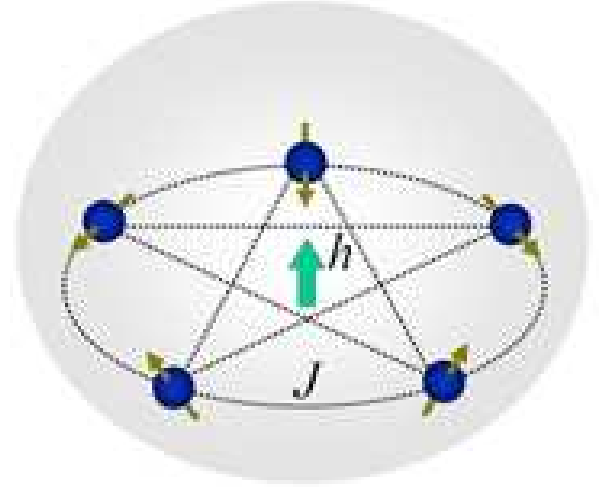


FIG. 9: (Color online) A sketch of the Lipkin-Meshkov-Glick model of 5 spins in which all 5 spins are mutually interact with each other (dotted lines) and subject to an external field  $h$  along  $z$  direction.

for  $h < 1$ , and

$$\frac{\chi_F}{N} = \frac{1}{16h^2(h^2 - 1)}.$$

for  $h > 1$ . At both sides of  $h_c = 1$ , we have

$$\alpha^\pm = 1, \quad (148)$$

as the critical exponents. One can observe that in the both phases of the Ising model, the fidelity susceptibility is an extensive quantity. In addition, taking into account that the exponents correlation length  $\nu = 1$ . The scaling relation  $\alpha^\pm = (d_a^c - d_a^\pm)/\nu$  is satisfied.

#### D. Example B: the Lipkin-Meshkov-Glick model

The one-dimensional transverse-field Ising model is not clear enough to explain the role played by the adiabatic dimension. For this purpose, we now take the Lipkin-Meshkov-Glick model [133, 134, 135] as an example. The Lipkin-Meshkov-Glick model was originally introduced by Lipkin, Meshkov, and Glick [133, 134, 135] to describe a collective motion in nuclei. The model consists of a cluster of mutually interacting spins in a transverse magnetic field  $\lambda$ . Its Hamiltonian reads

$$H = -\frac{1}{N} \sum_{i < j} (\sigma_i^x \sigma_j^x + \gamma \sigma_i^y \sigma_j^y) - \lambda \sum_i \sigma_i^z, \quad (149)$$

$$= -\frac{2}{N} (S_x^2 + \gamma S_y^2) - 2\lambda S_z + \frac{1}{2}(1 + \gamma), \quad (150)$$

where  $S_\kappa = \sum_i \sigma_i^\kappa / 2$  ( $\kappa = x, y, z$ ) are spin 1/2 operators,  $S_\pm = S_x \pm iS_y$ , and  $N$  the number of spins. The prefactor

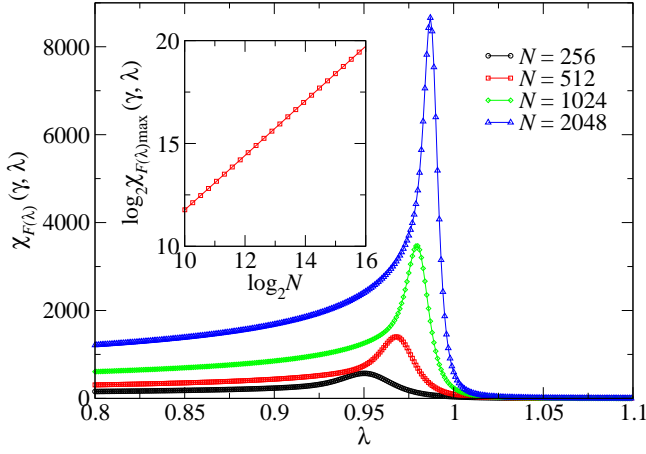


FIG. 10: (Color online) The fidelity susceptibility in the ground state of the Lipkin-Meshkov-Glick model as a function of  $\lambda$  at  $\gamma = 0.5$ . The inset denotes the scaling behavior of the maximum of the fidelity susceptibility, in which the slope of the line represents the size exponent of the fidelity  $\epsilon$

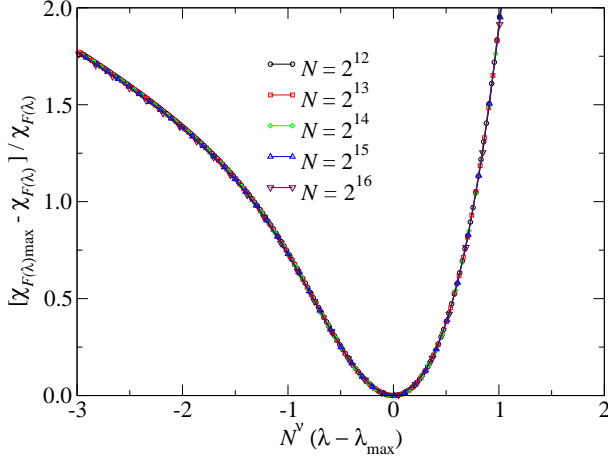


FIG. 11: (Color online) The finite size scaling analysis is performed for the case of power-law divergence at  $\gamma = 0.5$  for system sizes  $N = 2^n$  ( $n = 12, 13, 14, 15, 16$ ). The fidelity susceptibility is considered as a function of system size and driving parameter is a function of  $N^\nu(\lambda - \lambda_{\max})$  only, with the critical exponent  $\nu \simeq 0.665$  (From Ref. [57]).

$1/N$  is to ensure finite energy per spin in the thermodynamic limit  $N \rightarrow \infty$ . In the anisotropic case:  $\gamma \neq 1$ , the Hamiltonian commutes with both the total spin  $S^2$  and the parity  $P = \prod_i \sigma_i^z$ , i.e.

$$[H, S^2] = [H, P] = 0. \quad (151)$$

The symmetries significantly reduce the dimension of Hilbert space. For the present case, the ground state is a ferromagnetic when  $\lambda > 0$ . Then the dimension of the subspace in which the ground state locates is  $N/2$ . This reduces the complexity of the problem, and one can

study numerically a sample up to  $2^{16}$  spins using the standard diagonalization method.

In the thermodynamic limit, the ground state of the system undergoes a second order quantum phase transition at  $\lambda_c = 1$ . If  $\lambda > \lambda_c$ , the system is fully magnetized, while  $0 < \lambda < \lambda_c$  it is a symmetry-broken state. This conclusion was early drawn by the mean-field approaches [136, 137]. The finite-size scaling of this model was studied by the  $1/N$  expansion in the Holstein-Primakoff single boson representation [138] and by the continuous unitary transformations [139, 140]. Recent studies also reveals a rich structure of the spectrum, four regions are distinguished in the parameter space [141]. Besides, peoples also found that entanglement properties [142, 143, 144, 145] and fidelity [57] in the ground state of model can provide us a deep understanding on the quantum phase transition.

The following results based on the fidelity approach done by Kwok *et al* [57]. Fig. 10 show the dependence of the fidelity susceptibility on the driving parameter for various system sizes. As expected, the peak around the critical point becomes sharper and sharper as the system size increases. Numerical analysis show that  $\chi_F(\lambda = \lambda_{\max}) \sim N^{d_a^c}$  with  $d_a^c \simeq 1.33$ . The second observation is that the fidelity susceptibility shows different dependence on the system size in both phases. In the symmetry-breaking phase,  $\chi_F(\lambda) \sim N$ , while in the classical phase,  $\chi_F(\lambda)$  in an intensive quantity. Then adiabatic dimension of the fidelity susceptibility takes  $d^- = 1$  and  $d^+ = 0$  respectively. On the other hand, according to the scaling analysis discussed above, the rescaled fidelity susceptibility

$$\frac{\chi_F(\lambda = \lambda_{\max}, N) - \chi_F(\lambda, N)}{\chi_F(\lambda, N)},$$

should be a function of  $N^\nu(\lambda - \lambda_{\max})$ . Fig. 11 shows this function for various system size. All lines fall onto a single line for  $\nu \simeq 0.665$ , Therefore, the exponents for  $\chi_F(\lambda, N)/N^{d^\pm}$  around the critical point, as an intensive quantity,

$$\alpha^\pm = \begin{cases} 1/2 & \lambda < 1 \\ 2 & \lambda > 1 \end{cases} \quad (152)$$

Therefore, the Lipkin-Meshkov-Glick model shows distinct critical exponents around the critical point. Fortunately, the Lipkin-Meshkov-Glick model is also an exactly solvable model. The exact results then help us the check the numerical results obtained by scaling analysis.

In the region  $\lambda > 1$ , the Lipkin-Meshkov-Glick model can be diagonalized using the Holstein-Primakoff transformation [138]

$$S_z = S - a^\dagger a, \quad (153)$$

$$S_+ = (2S - a^\dagger a)^{1/2} a, \quad (154)$$

where  $a(a^\dagger)$  is bosonic annihilation(creation) operator satisfying  $[a, a^\dagger] = 1$ . In the large  $S(N)$  limit, the Hamil-

TABLE I: Critical exponents  $d_a^c, \nu, d^\pm, \alpha^\pm$  in various quantum phase transitions. The scaling relation  $\alpha^\pm = (d_a^c - d^\pm)/\nu$  so far can be tested explicitly in the first five models. For the Ising model, the Kitaev toric model, and Harper model, we have  $d_a^+ = d_a^-$ , hence  $\alpha^+ = \alpha^-$ ; while for both the Lipkin-Meshkov-Glick model and the Kitaev honeycomb model,  $d_a^\pm$  and  $\alpha^\pm$  are different.

Model	$d_a^c$	$\nu$	$d_a^+$	$\alpha^+$	$d_a^-$	$\alpha^-$
1D Ising model( $h_c = 1$ )[36]	2	1	1	1	1	1
Deformed Kitaev toric model [ $\lambda_c = \frac{1}{2}\ln(\sqrt{2} + 1)$ ][68]	ln	1	1	ln	1	ln
Extended Harper model [ $\lambda = 2\mu$ ][83]	5(or 2)	2.5(or 1)	0	2	0	2
Lipkin-Meshkov-Glick model( $h_c = 1$ )[57]	4/3	2/3	0	2	1	1/2
Kitaev honeycomb model( $J_{z,c} = 1/2$ )[67, 78]	2.50	1	2	1	2+ln	1/2-ln
1D AHM ( $t_c = 0.456$ for $n = 2/3$ )[49]	5.3	2.65	-	-	1	1.6
Luttinger model( $\lambda_c = 1$ of XXZ model)[52]	-	-	-	-	-	1
Luttinger model( $\lambda_c = -1$ of XXZ model)[52]	-	-	-	1	-	-

tonian can be transformed into,

$$H = -\lambda N + [2\lambda - \gamma - 1]a^\dagger a - \frac{1-\gamma}{2}(a^{\dagger 2} + a^2). \quad (155)$$

Obviously, the Hamiltonian is quadratic, and can be diagonalized via the standard Bogoliubov transformation, i.e.

$$\begin{aligned} a^\dagger &= \cosh(\theta)b^\dagger + \sinh(\theta)b, \\ a &= \sinh(\theta)b^\dagger + \cosh(\theta)b. \end{aligned} \quad (156)$$

Here  $b(b^\dagger)$  is bosonic annihilation (creation) operator, and the hyperbolic functions are set to ensure the bosonic commutation relation  $[b, b^\dagger] = 1$ . At the condition

$$\tanh[2\theta(h \geq 1)] = \frac{1-\gamma}{2\lambda - \gamma - 1}, \quad (157)$$

the Hamiltonian becomes a diagonal form

$$H = -\lambda(N+1) + 2\sqrt{(\lambda-1)(\lambda-\gamma)}\left(b^\dagger b + \frac{1}{2}\right). \quad (158)$$

Therefore, the set of eigenstate of the Hamiltonian is simply denoted as  $\{|n\rangle\}$  with

$$E_n = -\lambda(N+1) + 2\sqrt{(\lambda-1)(\lambda-\gamma)}(n+1/2), \quad (159)$$

where  $n$  is the number of quasiparticles. The driving term in the Hamiltonian becomes

$$\begin{aligned} -\sum_i \sigma_z^i &= -2S_z = 2a^\dagger a - 2S, \\ &= -2S + 2[\cosh(\theta)b^\dagger + \sinh(\theta)b] \\ &\quad \times [\sinh(\theta)b^\dagger + \cosh(\theta)b], \end{aligned} \quad (160)$$

in which only  $\sinh(2\theta)b^{\dagger 2}$  is the relevant term acting on the ground state and on projecting excited state. The fidelity susceptibility can be calculated, to the leading order, as

$$\chi_F(\gamma, \lambda) = \frac{(1-\gamma)^2}{32(1-\lambda)^2(\lambda-\gamma)^2}. \quad (161)$$

So the critical  $\alpha^+ = 2$ . In the region  $0 < \lambda < 1$ , the Lipkin-Meshkov-Glick model can be diagonalized similarly. The fidelity susceptibility becomes, to the leading order,

$$\chi_F(\gamma, \lambda) = \frac{N}{4\sqrt{(1-\lambda^2)(1-\gamma)}}. \quad (162)$$

The critical exponent  $\alpha^- = 1/2$ . Therefore, the critical exponents are different on both sides of the critical point. The exact results are the same as those obtained from the numerical data.

As a brief summary of the scaling and universality of the fidelity susceptibility, we collect the critical exponents of the fidelity susceptibility in various quantum phase transitions, and show them in Table. I. From the table, we can see that quantum phase transitions can be classified into two distinct types, depending on whether the adiabatic dimension changes or not during the transition. For the former case, the change in the adiabatic dimension plays naturally a role of order parameter.

## E. Higher order of the fidelity

The fidelity susceptibility denotes only the leading term of the fidelity. In case that the fidelity susceptibility is invalid, it might be useful to look into the higher order term in the fidelity. In this subsection, we present some basic formulism of the fidelity expansion.

The overlap between two wavefunction  $|\Psi_0(\lambda)\rangle$  and  $|\Psi_0(\lambda + \delta\lambda)\rangle$  can be expanded to an arbitrary order, i.e.

$$f(\lambda, \lambda + \delta\lambda) = 1 + \sum_{n=1}^{\infty} \frac{(\delta\lambda)^n}{n!} \left\langle \Psi_0(\lambda) \left| \frac{\partial^n}{\partial \lambda^n} \Psi_0(\lambda) \right. \right\rangle.$$

Therefore, the fidelity becomes

$$\begin{aligned}
F^2 &= 1 + \sum_{n=1}^{\infty} \frac{(\delta\lambda)^n}{n!} \left\langle \Psi_0 \left| \frac{\partial^n}{\partial \lambda^n} \Psi_0 \right\rangle \right. \\
&+ \sum_{n=1}^{\infty} \frac{(\delta\lambda)^n}{n!} \left\langle \frac{\partial^n}{\partial \lambda^n} \Psi_0 \left| \Psi_0 \right\rangle \right. \\
&+ \sum_{m,n=1}^{\infty} \frac{(\delta\lambda)^{m+n}}{m!n!} \left\langle \Psi_0 \left| \frac{\partial^n}{\partial \lambda^n} \Psi_0 \right\rangle \left\langle \frac{\partial^m}{\partial \lambda^m} \Psi_0 \left| \Psi_0 \right\rangle \right.
\end{aligned} \quad (163)$$

Using the relation for a given  $n$

$$\sum_{m=0}^n \frac{n!}{m!(n-m)!} \left\langle \frac{\partial^m}{\partial \lambda^m} \Psi_0 \left| \frac{\partial^{n-m}}{\partial \lambda^{n-m}} \Psi_0 \right\rangle = 0 \quad (164)$$

we can find that

$$F^2 = 1 - \sum_{l=1}^{\infty} (\delta\lambda)^l \chi_F^{(l)} \quad (165)$$

where

$$\chi_F^{(l)} = \sum_{l=m+n} \frac{1}{m!n!} \left\langle \frac{\partial^m}{\partial \lambda^m} \Psi_0 \left| P \left| \frac{\partial^n}{\partial \lambda^n} \Psi_0 \right\rangle \right. \right. \quad (166)$$

where  $P$  is defined in Eq. (83). It is easy to check that  $\chi_F^{(1)}$  is zero and  $\chi_F^{(2)}$  the fidelity susceptibility we discussed in previous subsections.

On the other hand, according the perturbation theory, the ground-state wavefunction, up to the second order, is

$$\begin{aligned}
|\Psi_0(\delta\lambda)\rangle &= |\Psi_0\rangle + \delta\lambda \sum_{n \neq 0} \frac{H_I^{n0} |\Psi_n\rangle}{E_0 - E_n} \\
&+ (\delta\lambda)^2 \sum_{m,n \neq 0} \frac{H_I^{nm} H_I^{m0} |\Psi_n\rangle}{(E_0 - E_m)(E_0 - E_n)} \\
&- (\delta\lambda)^2 \sum_{n \neq 0} \frac{H^{00} H_I^{n0} |\Psi_n\rangle}{(E_0 - E_n)^2} \\
&- \frac{(\delta\lambda)^2}{2} \sum_{n \neq 0} \frac{H^{0n} H_I^{n0} |\Psi_n\rangle}{(E_0 - E_n)^2}.
\end{aligned} \quad (167)$$

Therefore,

$$\begin{aligned}
\chi_F^{(3)} &= \sum_{n \neq 0} \frac{(H_I^{00} - \frac{1}{2} H_I^{0n}) H_I^{0n} H_I^{n0}}{(E_0 - E_n)^3} \\
&- \sum_{n \neq 0} \sum_{m \neq 0} \frac{H_I^{0n} H_I^{nm} H_I^{m0}}{(E_0 - E_m)(E_0 - E_n)^2}.
\end{aligned} \quad (168)$$

Eqs. (166) and (168) conclude the main formulism of the higher order expansion of the fidelity. Up to now, the physical meaning of the high order term in the fidelity is still not clear.

## V. FIDELITY PER SITE, MIXED STATE FIDELITY, AND RELATED

Mathematically, the fidelity can be roughly classified into two types, the pure-state fidelity and the mixed-state fidelity. In this section, we introduce various fidelity measure under different physical conditions rather than mathematical view. We will see below, various fidelity expressions can be traced back to the original fidelity definition by Uhlmann.

### A. Fidelity per site

In quantum many-body systems, the fidelity between two ground states increases as the system size increases. It usually scales like  $\mathcal{F}^{L^d}$  in the large  $L$  limit, where  $N = L^d$  is the system size and  $\mathcal{F}$  is called the scaling parameter. Therefore, Zhou, Zhao, and Li [46] proposed the scaling parameter (also called the fidelity per site) might be a good quantity to describe quantum phase transitions. Precisely, the fidelity per site is defined as

$$\mathcal{F}(\lambda, \lambda') = \lim_{N \rightarrow \infty} F^{1/N}(\lambda, \lambda'). \quad (169)$$

The expression can also be written in terms of logarithmic fidelity

$$\ln \mathcal{F}(\lambda, \lambda') = \lim_{N \rightarrow \infty} \frac{1}{N} \ln F(\lambda, \lambda'). \quad (170)$$

Clearly, the fidelity per site has following properties:

- 1) It is symmetric under interchange  $\lambda \longleftrightarrow \lambda'$ ,
- 2)  $\mathcal{F}(\lambda, \lambda) = 1$ ,
- 3)  $0 \leq \mathcal{F}(\lambda, \lambda') \leq 1$ .

Taking the one-dimensional transverse-field Ising model as an example, the fidelity between two ground states at  $h$  and  $h'$  is

$$F(h, h') = |\langle \Psi_0(h') | \Psi_0(h) \rangle| = \prod_{k>0} \cos(\theta_k - \theta'_k), \quad (171)$$

then the logarithmic fidelity becomes

$$\ln \mathcal{F}(h, h') = \lim_{N \rightarrow \infty} \frac{1}{N} \sum_{k>0} \cos(\theta_k - \theta'_k), \quad (172)$$

$$= \frac{1}{2\pi} \int_0^\pi \cos(\theta_k - \theta'_k) dk. \quad (173)$$

Therefore, one can easily discuss the critical behavior of the fidelity per site or the logarithmic fidelity in quantum phase transitions.

The fidelity per site can be mapped onto the partition function of a classical statistical vertex lattice model with the same lattice geometry and dimension [58]. The mapping is due to the recent remarkable finding that any state of a quantum lattice system may be represented in terms of a tensor network [146, 147, 148], such as a matrix product state for one-dimensional systems or

a projected entangled-pair state for systems in  $D \geq 2$  dimensions. Then the fidelity between any two ground states can be calculated in the context of the tensor network algorithms [149]. Clearly, such an approach can be generalized to the fidelity susceptibility.

On the other hand, in case that the adiabatic dimension and system's dimension are not the same  $d_a \neq d$  in a certain phase, the logarithmic fidelity should be redefined [92], in principle,

$$\ln \mathcal{F}(\lambda, \lambda') = \lim_{L \rightarrow \infty} \frac{1}{L d_a} \ln F(\lambda, \lambda') \quad (174)$$

which keeps intensive inside the phase. As a simple example, in the Lipkin-Meshkov-Glick model, if  $\lambda, \lambda' < 1$ , then  $\ln F(\lambda, \lambda') \propto N$ ; while if  $\lambda, \lambda' > 1$ ,  $\ln F(\lambda, \lambda')$  itself is intensive [92].

### B. Reduced fidelity

The reduced fidelity is defined as the fidelity between two reduced-density matrices corresponding to the states of a part of the system separated by a small distance in the parameter space. Precisely, if we divide the system into two parts: A and B, the reduced state of part A can be obtained by tracing out the degree of freedom of part B, i.e.

$$\rho_A(h) = \text{tr}_B (|\Psi_0(\lambda)\rangle\langle\Psi_0(\lambda)|). \quad (175)$$

Then the fidelity between two reduced states  $\rho_A(\lambda)$  and  $\rho_A(\lambda')$  at  $\lambda$  and  $\lambda'$  is simply the mixed-state fidelity

$$F(\lambda, \lambda') = \text{tr} \sqrt{[\rho_A(\lambda)]^{1/2} \rho_A(\lambda') [\rho_A(\lambda)]^{1/2}}. \quad (176)$$

In case that the ground state is  $N$ -fold degenerate, i.e.  $|\Psi_0^i(h)\rangle, i = 1, \dots, N$ , one can either define the thermal ground state as

$$\rho(h) = \frac{1}{N} \sum_i |\Psi_0^i(h)\rangle\langle\Psi_0^i(h)|, \quad (177)$$

or choose either of them as a physical ground state. The reduced-density matrix can be obtained in a similar way.

The reduced fidelity approach to quantum phase transitions was firstly discussed by Zhou [45] in order to study the relation between the fidelity per site and the renormalization group flows. The reduced fidelity was used later to study the quantum phase transitions in a superconducting lattice with a magnetic impurity inserted at its center [55]. Nevertheless, for a pedagogical purpose, here we introduce its application to another class of quantum phase transitions induced by a sequence of ground-state level-crossing, such as the magnetization process. In this case, the fidelity between two ‘‘global’’ ground states is not suitable because it drops to zero at each level-crossing point. For these systems, the Hamiltonian take typically the form

$$H(h) = H_0 - hM, \quad (178)$$

where  $h$  is the external field and  $M$  is the magnetization of the ground state. Unlike the Hamiltonian of Eq. (33) where  $H_0$  and  $H_I$  usually do not commute with each other,  $M$  in Eq. (178) commutes with  $H_0$ . Then  $H_0$  and  $M$  have the same eigenvectors. Suppose the magnetization of the system is zero in the absence of the external field, the system will be magnetized step by step as the external field increases until it is fully magnetized at a certain transition point  $h_c$ . Typically, the ground state has two phases, i.e., a partially magnetized phase and a fully magnetized phase. For the latter, the ground state does not change as the external field changes. Then the fidelity is always one and the fidelity susceptibility is zero. While for the former, the ground state undergoes infinite level-crossings and the fidelity drops to zero at each crossing point. Therefore, it is not convenient to characterize this type of phase transition in terms of global state fidelity. The difficulty can be overcome if one consider only the reduced state of a local part of the system, which is described by a reduced-density matrix. Mathematically, the ‘‘orthogonality’’ of two pure states is very sensitive to the distinguishability between the states, such as good quantum numbers or which-way flag [150]. However, if one consider only the local part of the system, the rate of ‘‘orthogonality’’ is reduced because the reduced state is a mixed state that usually is free of the conserved quantity.

The Lipkin-Meshkov-Glick model still provides a very good example [72, 73]. If  $\gamma = 1$ , the Hamiltonian of Eq. (150) commutes with the  $z$ -component of the total spins. Then  $S^z$  is a conserved quantity. The ground state can be written in  $\{|S, S^z\rangle\}$ . For  $S = N/2$ , the eigenenergies are

$$E(M, h) = \frac{2}{N} \left( M - \frac{hN}{2} \right)^2 - \frac{N}{2} (1 + h^2), \quad (179)$$

and the ground state (with quantum number  $M_0$ ) is then obtained

$$M_0 = \begin{cases} \frac{N}{2}, h \geq 1 \\ I\left(\frac{hN}{2}\right), 0 \leq h < 1 \end{cases}, \quad (180)$$

where  $I(x)$  gives the integer part of  $x$ . We can define the reduced state of a single spin as

$$\rho = \frac{1}{2} \begin{pmatrix} 1 + \langle \sigma^z \rangle & 0 \\ 0 & 1 - \langle \sigma^z \rangle \end{pmatrix}. \quad (181)$$

The fidelity between two reduced states around the each crossing point is

$$F = \frac{1}{2} \sqrt{(1 + \langle \sigma_z \rangle^j) (1 + \langle \sigma_z \rangle^{j+1})} + \frac{1}{2} \sqrt{(1 - \langle \sigma_z \rangle^j) (1 - \langle \sigma_z \rangle^{j+1})}, \quad (182)$$

where  $\langle \sigma_z \rangle^j$  denotes the expectation value of  $\sigma_z$  of  $j$ th state during the level-crossing process. The fidelity sus-

ceptibility can be defined in the similar way, in the thermodynamic limit,

$$\chi_F = \lim_{\delta h \rightarrow 0} \frac{-2 \ln F}{(\delta h)^2}, \quad (183)$$

where  $\delta h = h_{j+1} - h_j$  is the difference of  $h$  between two level-crossing points.

### C. Fidelity between thermal states

At finite temperatures, an equilibrium state of a thermal system is described by a mixed state [151],

$$\rho(\beta) = \frac{1}{Z} \sum_n e^{-\beta E_n} |\Psi_n\rangle \langle \Psi_n|, \quad (184)$$

where  $\beta = 1/T$  is the inverse temperature with Boltzmann constant  $k_B = 1$ ,  $Z$  is the partition function defined as

$$Z = \sum_n e^{-\beta E_n}, \quad (185)$$

and  $|\Psi_n\rangle$  is the eigenstate of the system's Hamiltonian with eigenvalue  $E_n$ . Therefore, if we choose the temperature as a driving parameter, the fidelity between two thermal states at  $\beta - \delta\beta/2$  and  $\beta + \delta\beta/2$  is [42]

$$F(\beta - \delta\beta/2, \beta + \delta\beta/2) = \text{tr} \sqrt{\rho(\beta - \delta\beta/2) \rho(\beta + \delta\beta/2)} \quad (186)$$

$$= \frac{Z(\beta)}{\sqrt{Z(\beta - \delta\beta/2) Z(\beta + \delta\beta/2)}}. \quad (187)$$

This result is very interesting. It establishes a relation between the state overlap and well known thermal quantities. Therefore, one can understand the state evolution at finite temperature from the knowledge of thermodynamics. Since the Helmholtz free energy is

$$G = \langle E \rangle - TS = -\frac{1}{\beta} \ln Z, \quad (188)$$

the thermal fidelity susceptibility then becomes [43, 44]

$$\chi_F = \left. \frac{-2 \ln F}{(\delta\beta)^2} \right|_{\delta\beta \rightarrow 0}, \quad (189)$$

$$= \beta \left. \frac{[2G(\beta) - G(\beta + \delta\beta/2) - G(\beta - \delta\beta/2)]}{(\delta\beta)^2} \right|_{\delta\beta \rightarrow 0} \quad (190)$$

$$= \frac{C_v}{4\beta^2}. \quad (191)$$

To obtain the above result, we have used the following standard relations in the thermodynamics [151]

$$S = -\frac{\partial G}{\partial T}, C_v = -T \frac{\partial S}{\partial T}. \quad (192)$$

Similarly, if the driving term in the Hamiltonian is a Zeemann-like term, say  $-hM$ , which is crucial in Landau-Ginzburg-Wilson symmetry-breaking theory, then the fidelity susceptibility is simply the magnetic susceptibility  $\chi$ [43],

$$\chi_F = \left. \frac{-2 \ln F_i}{\delta h^2} \right|_{\delta h \rightarrow 0} = \frac{\beta \chi}{4}. \quad (193)$$

The thermal fidelity susceptibility is similar to the ground-state fidelity susceptibility. Both of them are a kind of structure factor because of

$$C_v = \beta^2 (\langle E^2 \rangle - \langle E \rangle^2), \quad (194)$$

$$\chi = \beta (\langle M^2 \rangle - \langle M \rangle^2) \quad (195)$$

in thermodynamics. The main difference is that the ground-state fidelity susceptibility involves the dynamic behavior of the system.

As a simple application, we take the two-dimensional Ising model on a square lattice as an example. The Hamiltonian reads,

$$H = - \sum_{\langle ij \rangle} \sigma_i^z \sigma_j^z, \quad (196)$$

where the sum is over all pairs of nearest-neighbor sites  $\mathbf{i}$  and  $\mathbf{j}$ , and the coupling is set to unit for simplicity. The model is certainly the most thoroughly researched model in statistical physics [206, 207]. The results for a  $40 \times 40$ -site system are shown in Fig. 12. Clearly, there is a maximum point in the line of the specific heat, whose scaling behavior to an infinite system defines the critical point. Meanwhile, the middle picture in Fig. 12 shows various fidelity calculated from different temperature interval. This obvious difference in the fidelity disappears if we distill the fidelity susceptibility from them, as shown in the right picture of Fig. 12.

### D. Operator fidelity

The operator fidelity was proposed by Wang, Sun and Wang [64]. For two arbitrary linear operators  $A, B$  defined in a  $d$ -dimensional Hilbert space, the expectation value of their product are  $\text{tr}(AB)$ , which is a kind of inner product in the  $d^2$ -dimensional (or  $d^2 - 1$  for Hermitian operators) space. On the other hand, in a  $d$  dimensional Hilbert space, any state acted after a linear operator becomes another state in the Hilbert space. Then the fidelity between states can be generalized to the operator level. Specifically, for two unitary evolution operators  $U_0$  and  $U_1$ , the fidelity between them can be calculated as

$$F^2 = \frac{1}{d^2} |\text{tr}(U_0^\dagger U_1)|. \quad (197)$$

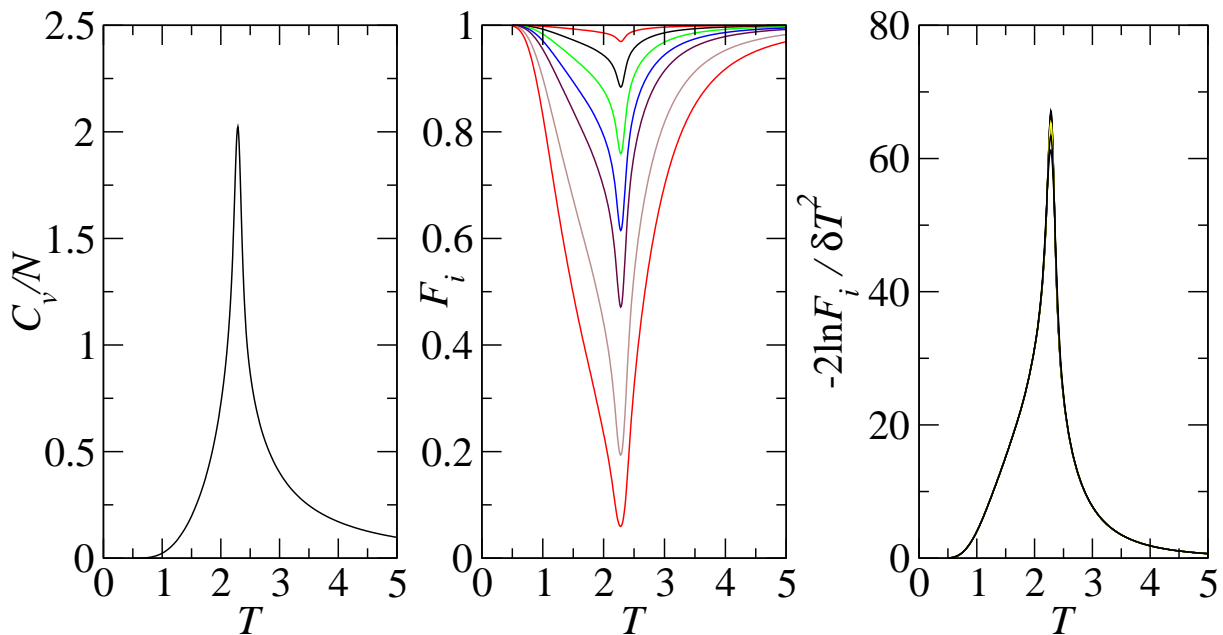


FIG. 12: (Color online) LEFT: The specific heat as a function of the temperature  $T$  for  $40 \times 40$  Ising model. MIDDLE: The fidelity between two states separated by different temperature interval  $\delta T = 0.02, 0.04, 0.06, 0.08, 0.1, 0.15, 0.20$  for lines from up to bottom. RIGHT: the fidelity susceptibility  $\chi_F$  as a function of  $T$ , obtained from the data of the middle picture. All lines in the middle picture collapse onto a single line (From Ref. [43]).

Precisely, for a general Hamiltonian, the evolution operator can be expressed as

$$U(t) = 1 - i\delta\lambda \int_0^t dt_1 V(t_1) - (\delta\lambda)^2 \int_0^t dt_1 \int_0^{t_1} dt_2 V(t_1)V(t_2) + \dots \quad (198)$$

where  $V(t) = \exp(iH_0 t)V \exp(-iH_0 t)$  denotes the perturbation term in the interaction picture. The trace of the evolution operator is,

$$\overline{\text{tr}}[U(t)] = 1 - i\delta\lambda \overline{\text{tr}}[W(t)] - \quad (199)$$

$$- \frac{(\delta\lambda)^2}{2} \overline{\text{tr}}[W(t)^2] + \dots, \quad (200)$$

where

$$\overline{\text{tr}}(A) = \frac{1}{d} \text{tr}(A), \quad (201)$$

and

$$W(t) = \int_0^t dt_1 V(t_1). \quad (202)$$

The left hand side of Eq. (199) denotes the inner product of two states at different time. Then the fidelity becomes

$$F^2 = 1 - (\delta\lambda)^2 [\overline{\text{tr}}[W(t)^2] - (\overline{\text{tr}}W(t))^2] + \dots \quad (203)$$

Similarly, the operator fidelity susceptibility can be extracted

$$\chi_F = \overline{\text{tr}}[W(t)^2] - [\overline{\text{tr}}W(t)]^2. \quad (204)$$

The operator fidelity is remarkable. In its approach to quantum phase transitions, it is a good indicator regardless of the ground-state degeneracy. Moreover, it also reveals that in the state evolution, the driving mechanism is due to the fluctuation of  $W(t)$ .

### E. Density-functional fidelity

The density functional theory (DFT) [208, 209] is based on the Hohenberg-Kohn theorem [208], which asserts that the ground-state properties are uniquely determined by the density distribution  $n_x$  that minimizes the functional for the ground-state energy  $E_0[n_x]$ . To date, the DFT becomes the most successful method for first-principle calculations of the electronic properties of solids. Since the normalized density distribution captures the most relevant information about the ground state, Gu [84] tried to link the fidelity and quantum phase transitions via the DFT.

For a general Hamiltonian system

$$H(\lambda) = H_0 + \lambda H_I + \sum_x \mu_x n_x, \quad (205)$$

where  $H_I$  is the interaction term and  $\lambda$  denotes strength, and  $\mu_x$  is the local (pseudo)potential associated with density distribution  $\{n_x\}$ . The index  $x$  can be discrete or continuous depending on the system under study. Though in the local-density-approximation (LDA) calculation,  $n_x$  usually refers to the density of electrons in real

space, it can also be generalized to the population in configuration space of a reduced-density matrix or the density of state in energy(momentum) space. The density distribution can be obtained by the Hellmann-Feymann theorem

$$n_x = \left\langle \Psi_0(\lambda) \left| \frac{\partial H}{\partial \mu_x} \right| \Psi_0(\lambda) \right\rangle, \quad (206)$$

where  $|\Psi_0(\lambda)\rangle$  is the ground state, and  $\sum_x n_x = 1$ . The density-functional fidelity is defined as the distance between two density distributions at  $\lambda$  and  $\lambda'$  in the parameter space

$$F(\lambda, \lambda') = \text{tr} \sqrt{n(\lambda)n(\lambda')}. \quad (207)$$

Since the density distribution is experimentally measurable, the density-functional fidelity then provides a practicable approach for experimentalist to study quantum phase transitions in perspective of information theory.

Expanding the density-functional fidelity to the leading order, one can find the density-functional fidelity susceptibility has the form

$$\chi_F = \sum_x \frac{1}{4n_x} \left( \frac{\partial n_x}{\partial \lambda} \right)^2. \quad (208)$$

Therefore, if one regards  $\partial n_x / \partial \lambda$  as an independent function besides the density distribution  $n_x$ , the density-functional fidelity susceptibility is a functional of  $n_x$  and  $\partial n_x / \partial \lambda$ , both of which, in principle, maximize the density-functional fidelity susceptibility at the critical point.

Mathematically, the density-functional fidelity and thermal-state fidelity is related to the Fisher-Rao distance. For the probability  $\{n_x\}$  defined in parameter space  $\{\lambda_a\}$ , the Fisher-Rao distance is defined as

$$ds^2 = \frac{1}{4} \sum_x \frac{dn_x dn_x}{n_x}. \quad (209)$$

The Fisher-Rao metric then can be written as

$$g_{ab} = \frac{1}{4} \sum_x \frac{1}{n_x} \frac{dn_x}{d\lambda_a} \frac{dn_x}{d\lambda_b}. \quad (210)$$

## VI. FIDELITY IN STRONGLY CORRELATION SYSTEMS

The fidelity approach to quantum phase transitions has been applied to many strongly correlated systems besides the one-dimensional transverse-field Ising model and the Lipkin-Meshkov-Glick model. This section is devoted to a survey of fidelity in these systems. We mainly focus on those models which are well studied and whose phase diagrams are known.

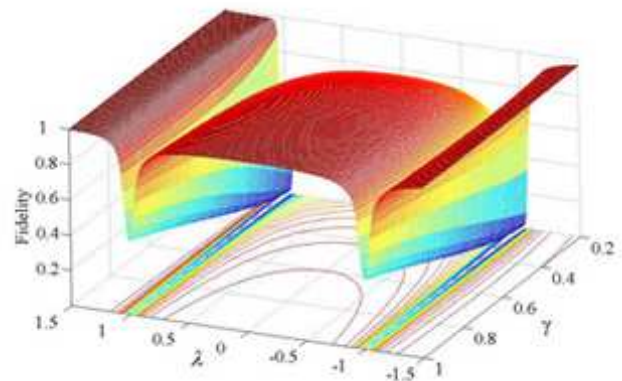


FIG. 13: (Color online) The fidelity of the one-dimensional transverse-field XY model as a function of  $h$  and  $\gamma$ , for a system of  $N = 100$  and  $\delta\lambda = \delta\gamma = 0.1$ . The colored curves on the  $F = 0$  plane constitutes a contour map. The deep grooves in the curved surface of the fidelity separate naturally the whole region into three phases: one order phase in the middle and two polarized phases on both sides (Reproduced from Ref. [36])

### A. Pure-state fidelity

#### 1. One-dimensional spin systems

*The one-dimensional transverse-field XY model:* The model is an extended version of the one-dimensional transverse-field Ising model. The XY model can be exactly solved too [129, 130]. Its Hamiltonian reads

$$H(\gamma, \lambda) = - \sum_{j=1}^L \left( \frac{1+\gamma}{2} \sigma_j^x \sigma_{j+1}^x + \frac{1-\gamma}{2} \sigma_j^y \sigma_{j+1}^y + \lambda \sigma_j^z \right), \quad (211)$$

where  $\gamma$  defines the anisotropy and  $\lambda$  represents the external magnetic field. Obviously, if  $\gamma = 1$ , the XY model becomes the transverse-field Ising model which is presented as an example in section III. The role of quantum entanglement in the quantum phase transitions occurred in the XY model has been widely studied [7, 8, 9, 10, 11]. It was shown that either the pairwise entanglement [7, 8], as measured by the concurrence [152, 153], or the two-site local entanglement [10, 11] shows interesting singular and scaling behavior around the critical point. The fidelity approach to the one-dimensional transverse-field XY model was firstly done by Zanardi and Paunković [36]. They used the XY model as an example to present a new characterization of quantum phase transitions in terms of the fidelity. Their physical intuition behind the fidelity approach is in order: since the fidelity measures the similarity between two states, then the fidelity between two ground states obtained for two different values of external parameters should has a minimum around the critical point(See Fig. 13). The work is one of original works in this promising field.

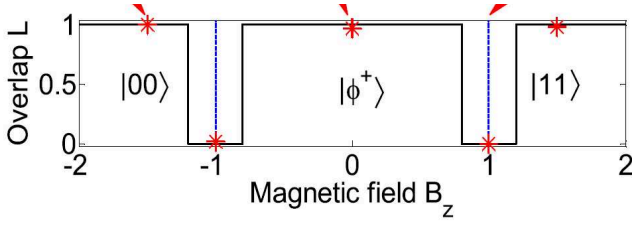


FIG. 14: (Color online) The theoretical (line) and experimental (asterisks) fidelity in the quantum phase transition of the Ising dimer induced by the ground-state level-crossing. (From Ref. [71])

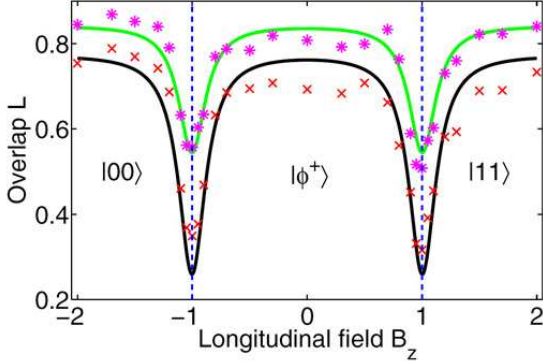


FIG. 15: (Color online) The experimental fidelity of the Ising dimer measured by the nuclear-magnetic-resonance experiments for  $\delta h_x = 0.2$  (\*) and  $\delta h_x = 0.3$  (x). (From Ref. [71])

Meanwhile, Zhou, Zhao, and Li [46] studied the critical phenomena in the XY model in terms of the fidelity per site. They found that the logarithmic function of fidelity per site with respect to the transverse field is logarithmically divergent at the critical point. The scaling and universality hypothesis based on the fidelity per site was also confirmed in the vicinity of the transition point. This work is the first one that proposed the idea of fidelity per site.

A noticeable achievement is the experimental detection of the quantum phase transitions in terms of the fidelity [71]. Using the nuclear-magnetic-resonance technique, Zhang *et al* measured the sensibility of the ground state of the Ising model to perturbations when it comes to the critical point. Their system can be described by the Hamiltonian

$$H^s = \sigma_1^z \sigma_2^z + B_x (\sigma_1^x + \sigma_2^x) + B_z (\sigma_1^z + \sigma_2^z). \quad (212)$$

If  $B_x = 0$ , the system undergoes a first-order phase transition induced by the ground-state level-crossing. They found that the ground-state overlap shows a drop at the crossing point (14). While if  $B_z = 0$ , the model becomes the transverse-field Ising model. Though the second-order quantum phase transition occurs only in the thermodynamic limit, the fidelity in a small sample can

still tell us the significant change in the structure of the ground state around the critical point (See Fig. 15).

*The one-dimensional XXZ model:* The Hamiltonian of the one-dimensional XXZ model reads

$$H(\lambda) = \sum_{j=1}^L (\sigma_j^x \sigma_{j+1}^x + \sigma_j^y \sigma_{j+1}^y + \lambda \sigma_j^z \sigma_{j+1}^z). \quad (213)$$

The XXZ model can be solved by the Bethe-ansatz method [154, 155, 156], through which the energy spectra can be fully determined. The ground-state of the one-dimensional XXZ model consists three phases. If  $\lambda < -1$ , all spins are align to the same direction, the ground-state is in a fully polarized state; when  $-1 < \lambda < 1$ , the quantum fluctuation term dominates, then the ground state is a quantum fluctuation phase; while if  $\lambda > 1$ , the antiferromagnetic coupling dominates, the ground state is in an antiferromagnetic state. So there are two critical points  $\lambda = \pm 1$ . There are various tools to witness the quantum phase transition occurred at  $\lambda = 1$ . They include the vanishing energy gap and divergent correlation length [157] as  $\lambda \rightarrow 1^+$ , abrupt change in the spin stiffness [158, 159], and the maximum value of quantum entanglement [12].

The fidelity approach to the quantum phase transition of the one-dimensional XXZ model is not easy because the ground-state wave function is not known. Yang [52] first used the Luttinger Liquid model to describe the one-dimensional XXZ model in the quantum fluctuation region [160], i.e.

$$H(\lambda) = \frac{u}{2} \int dx \left( K \Pi(x)^2 + \frac{1}{K} (\partial_x \Phi)^2 \right). \quad (214)$$

Here

$$K = \frac{\pi}{2} [\pi - \arccos(\lambda)], \quad (215)$$

$$u = \frac{\pi \sqrt{1 - \lambda^2}}{2 \arccos \lambda}, \quad (216)$$

and  $\Pi, \Phi$  are bosonic phase field operators. They obtained the fidelity as

$$F(K, K') = \prod_{k \neq 0} \frac{2}{\sqrt{K/K'} + \sqrt{K'/K}}, \quad (217)$$

and the fidelity susceptibility

$$\frac{\chi_F(\lambda)}{L} = \frac{1}{4[\pi - \arccos(\lambda)]^2} \frac{1}{1 - \lambda^2}. \quad (218)$$

Therefore the critical exponent  $\alpha = 1$ . So they conclude that the fidelity might be able to signal the Beresinskii-Kosterlitz-Thouless phase transition occurring in the XXZ model. This conclusion is a little surprising. Because in previous studies, some groups claimed that the Beresinskii-Kosterlitz-Thouless transitions cannot be signalled from the singularity of the fidelity susceptibility [43, 61].

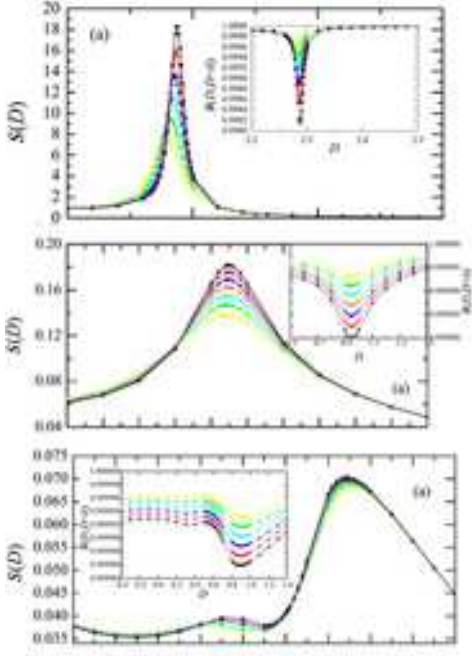


FIG. 16: (Color online) The fidelity and fidelity susceptibility in the spin-one anisotropic model (From Ref. [70]).

*The spin-one anisotropic model:* The Hamiltonian of the spin-one anisotropic model reads

$$H(\lambda) = \sum_{j=1}^L [S_j^x S_{j+1}^x + S_j^y S_{j+1}^y + \lambda S_j^z S_{j+1}^z + D(S_j^z)^2], \quad (219)$$

where  $S_j^\kappa$  ( $\kappa = x, y, z$ ) stands for spin-1 operators, and  $\lambda$  and  $D$  parameterize the Ising-like and the uniaxial interaction. The ground-state phase diagram of the model consists of six phases [161, 162]. Specifically, for three cases of  $\lambda = 2.59, 1$ , and  $0.5$ , the system undergoes second-order, third-order, and fifth-order quantum phase transitions, respectively. For the case of  $\lambda = 2.59$ , the authors found the fidelity susceptibility as a function of  $D$  around  $D = 2.30$ . For the second case of  $\lambda = 1$ , though the second-order derivative of the ground-state energy does not show singular behavior around  $D = 0.95$ , the fidelity susceptibility is still able to signal the transition. For the third case of  $D = 0.5$ , however, both the fidelity susceptibility and the second derivative of the ground-state energy is continuous in the critical region. The authors then conclude that the fidelity susceptibility might not be able to characterize the Gaussian transition. (See Fig. 16).

*The spin-ladder model:* The Hamiltonian of a general

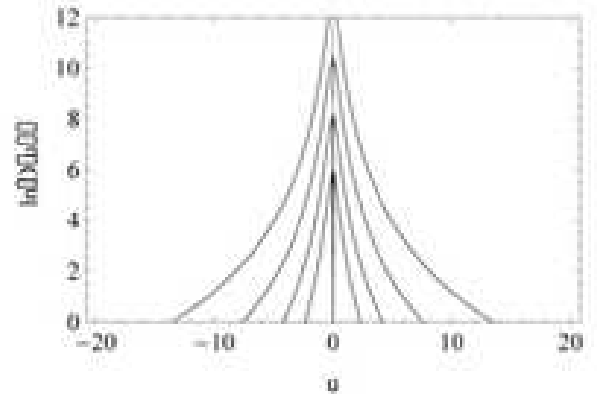


FIG. 17: (Color online) The fidelity (TOP) as a function of  $u$  and  $N$  for  $\delta = 0.001$ , and the fidelity as a function of  $u$  for various system size ( $N = 10^3, 10^4, 10^5$ , and  $10^6$ ) (From Ref. [50]).

spin ladder model reads [163]

$$H = \sum_{j=1} [J(S_{1,j}S_{1,j+1} + S_{2,j}S_{2,j+1}) + J_r S_{1,j}S_{2,j} + V(S_{1,j}S_{1,j+1})(S_{2,j}S_{2,j+1}) + J_d(S_{1,j}S_{2,j+1} + S_{2,j}S_{1,j+1}) + K[(S_{1,j}S_{2,j+1})(S_{2,j}S_{1,j+1}) - (S_{1,j}S_{2,j})(S_{1,j+1}S_{2,j+1})], \quad (220)$$

where the indices 1 and 2 distinguish the lower and upper legs of the ladder and  $i$  labels the rungs. The ground state of the spin ladder is very complicated. However, if we redefine the parameters

$$u = -u, K = J_r = \frac{(u^2 - 1)(u^2 + 3)}{2}, J_d = 0, \quad (221)$$

$$V = \frac{(5u^4 + 2u^2 + 9)}{4}, J = \frac{3(u^4 + 10u^2 + 5)}{16}, \quad (222)$$

$$\epsilon_1 = \frac{(3u^4 + 14u^2 + 15)}{8}, \epsilon_2 = \frac{(5u^4 + 18u^2 + 9)}{8} \quad (223)$$

the Hamiltonian becomes a one-parameter model. The ground state of the system can be explicitly written as a matrix product state

$$|\Psi_0(u, u')\rangle = \frac{1}{\sqrt{N_c}} \text{tr}[g_1(u)g_2(u') \cdots g_{2N-1}(u)g_{2N}(u')],$$

where  $N_c$  is the normalization constant. Such a ground state undergoes two second-order quantum phase transitions at  $u = 0$  and  $u = \infty$ . At  $u = 0$ , the ground state changes from the dimerized phase to the Haldane phase. The latter can be described by an effective Hamiltonian of the  $S = 1$  Affleck-Kennedy-Lieb-Tasaki chain

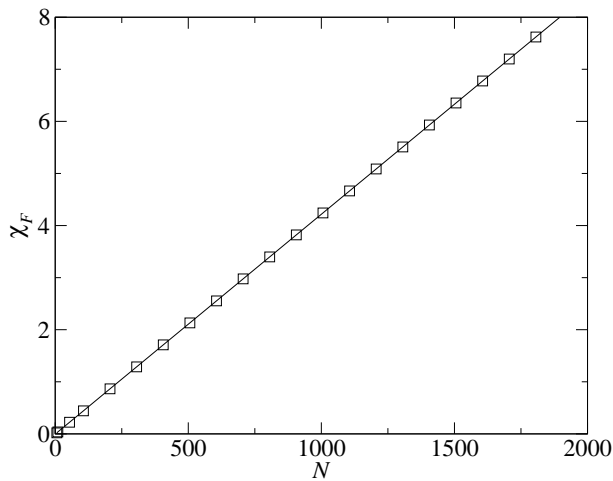


FIG. 18: (Color online) The dependence of the fidelity susceptibility of the Hubbard model on the system size at  $U = 0$  (From Ref. [43]).

[164]. Fig. 17 shows the fidelity approach to the phase transition occurring at  $u = 0$ . Clearly the fidelity shows a minimum and the fidelity susceptibility shows a sharp peak at  $u = 0$ , corresponding to an abrupt change in the ground-state wavefunction.

## 2. One-dimensional fermionic systems

*The one-dimensional Hubbard model:* The Hamiltonian of the one-dimensional Hubbard model [165] reads

$$H_{\text{HM}} = - \sum_{j=1}^L \sum_{\delta=\pm 1} \sum_{\sigma} t c_{j,\sigma}^{\dagger} c_{j+\delta,\sigma} + U \sum_{j=1}^L n_{j,\uparrow} n_{j,\downarrow}, \quad (224)$$

where  $c_{j,\sigma}^{\dagger}$  and  $c_{j,\sigma}$ ,  $\sigma = \uparrow, \downarrow$  are creation and annihilation operators for fermionic atoms with spin  $\sigma$  at site  $j$  respectively,  $n_{\sigma} = c_{\sigma}^{\dagger} c_{\sigma}$ , and  $U$  denotes the strength of on-site interaction. Besides the obvious SU(2) symmetry in the spin sector, the model has charge SU(2) symmetry [166]. The global symmetry [167] of the model is SO(4) since half of the irreducible representations of SU(2)  $\otimes$  SU(2) are excluded. The Hubbard model was solved by the Bethe-ansatz method [168, 169, 170]. For the half-filled case, the system undergoes a Mott-insulator transition at the critical point  $U_c = 0$ . According to the exact solution, the ground-state energy can be differentiated to an arbitrary order, therefore the transition is of infinite order [169, 170] (Berezinskii-Kosterlitz-Thouless like). The role of quantum entanglement in the phase transitions occurred in the Hubbard model was addressed by Gu *et al* [14], Deng *et al*, [16] and Larsson and Johannesson [15]. The fidelity approach to the one-dimensional Hubbard was firstly studied by You *et al* [43]. They found that the fidelity susceptibility is not singular at the transition point and concluded that it might not be able to signal

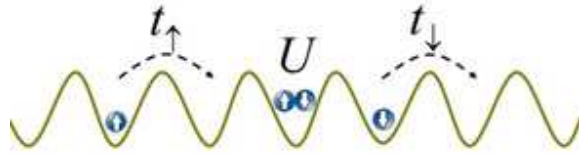


FIG. 19: (Color online) A sketch of the asymmetric Hubbard model which can be realized in an optical lattice. The solid sinusoid denotes the periodic potential formed by two interfering standing laser waves. Two species of fermionic atoms are supposed to be trapped in the potential. In case of  $t_{\uparrow} = t_{\downarrow}$

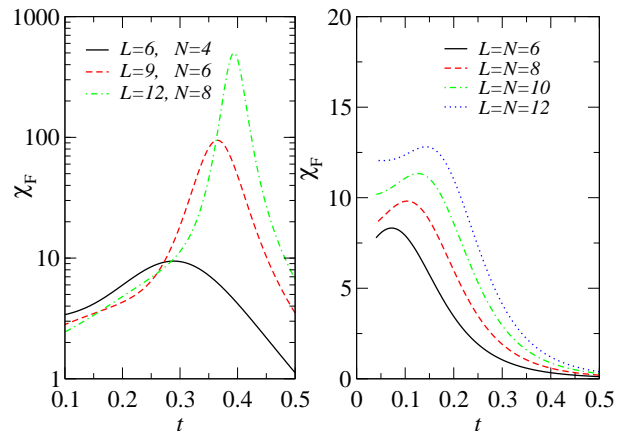


FIG. 20: (Color online) The scaling behavior of the FS as a function of  $t$  for the cases of  $n = 2/3$  (LEFT) and  $n = 1$  (RIGHT). Here  $U = 30$ . (From Ref. [49])

the transition. Especially at the critical point  $U_c = 0$ , the Hamiltonian is diagonal, and the fidelity susceptibility per system length, as an intensive quantity, is a constant (See Fig. 18). The fidelity in the Hubbard model was later revisited by Venuti *et al* [63], with the strategy of bosonization and Bethe-ansatz techniques. They showed that the metal-insulator phase transition can be insightfully analyzed in term of the fidelity. The fidelity susceptibility shows divergences depending on the path approaching to the critical point. Bosonization results shows that the fidelity susceptibility may diverge as

$$\chi_F \propto U^{-4},$$

if the doping rate is proportional to  $\sqrt{U} \exp[-2\pi/U]$ . The authors also performed exact diagonalization for a system up to 14 sites. Based on the scaling analysis, their results indicate that the fidelity might be super-extensive, hence divergent in the thermodynamic limit. However, they also stated that the available sizes of the exact diagonalization are too small to provide a conclusive answer. Therefore, whether the fidelity susceptibility shows singular behavior in the one-dimensional Hubbard model is still not conclusively answered.

*The one-dimensional asymmetric Hubbard model:* The Hamiltonian of the asymmetric Hubbard model [171, 172]

reads

$$H_{\text{AHM}} = - \sum_{j=1}^L \sum_{\delta=\pm 1} \sum_{\sigma} t_{\sigma} c_{j,\sigma}^{\dagger} c_{j+\delta,\sigma} + U \sum_{j=1}^L n_{j,\uparrow} n_{j,\downarrow}, \quad (225)$$

where  $t_{\sigma}$  is  $\sigma$ -dependent hopping integral. Not much attention was paid to the model in the last century because we did not have a realistic system that the model can be applied. However, in describing a mixture of two species of fermionic atoms in optical lattices which has been realized by recent experiments on the cold atoms [173], the model itself becomes a current research interest [174, 175, 176]. The ground-state phase diagram of the asymmetric Hubbard model can be understood from its two limiting cases, i.e. the Falicov-Kimball (FK) model region [177, 178] ( $t_{\uparrow} = 0$ ) and the Hubbard model region (HM) [165] ( $t_{\uparrow} = t_{\downarrow}$ ). The schematic phase diagram of the model was obtained from the renormalization group analysis [174]. Subsequently, a quantitative phase diagram was also obtained by analyzing structure factor with the density-matrix renormalization group [175] and bosonization techniques [176]. The fidelity approach to the model was firstly done by Gu *et al* [49]. The authors found that the fidelity susceptibility can be used to identify the universality class of the quantum phase transitions in this model. That is the quantum phase transitions occurred at different band filling can be characterized by the critical exponents of the fidelity susceptibility. Fig. 20 shows the fidelity susceptibility as a function of  $t_{\downarrow}/t_{\uparrow}$  for the cases of  $n = 2/3$  and  $n = 1$ , and various system sizes. Obviously, the fidelity susceptibility diverges quickly as the system is away from the half-filling, and relatively slow at half-filling. The scaling analysis reveals that the maximum value of the fidelity susceptibility scales like

$$\chi_F \propto L^{5.3}$$

at  $n = 2/3$  case, while

$$\chi_F \propto L$$

at half-filling. Then the intensive fidelity susceptibility shows singularity away from half-filling, while no singularity at half-filling. These observations support their conclusions on the role of fidelity in describing the universality class.

*The one-dimensional Bose-Fermi mixture:* The simplest one-dimensional Bose-Fermi Hubbard model can be modeled by

$$H_{\text{BF}} = - \sum_{i=1}^N (t_{\text{F}} c_i^{\dagger} c_{i+1} + t_{\text{B}} b_i^{\dagger} b_{i+1} + \text{H.c.}) + U_{\text{BF}} \sum_{i=1}^N c_i^{\dagger} c_i b_i^{\dagger} b_i + U_{\text{BB}} \sum_{i=1}^N b_i^{\dagger} b_i (b_i^{\dagger} b_i - 1) \quad (226)$$

Here  $b_i$  ( $b_i^{\dagger}$ ) and  $c_i$  ( $c_i^{\dagger}$ ) are the bosonic and fermionic annihilation (creation) operators at site  $i$ , respectively.

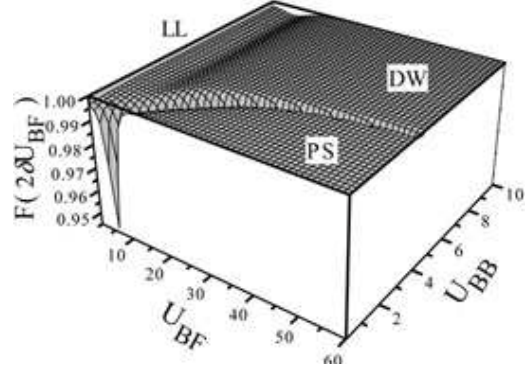


FIG. 21: (Color online) The ground-state phase diagram defined on the  $U_{\text{BB}}-U_{\text{BF}}$  plane of the one-dimensional Bose-Fermi Hubbard model in terms of the fidelity (Reproduced from Ref. [54]).

$t_{\text{F}}$  ( $t_{\text{B}}$ ) is the hopping integral of fermions (bosons).  $U_{\text{BF}}$  denotes the on-site interaction between fermion and bosons, and  $U_{\text{BB}}$  the interaction between bosons. The ground state of the model has been studied by the quantum Monte-Carlo method [179]. Several phases, including Luttinger liquid phase, density wave phase, phase separation state, and Ising phase, are predicted. The fidelity approach to the quantum phase transitions occurring in the ground state was done by Ning *et al* [54]. As shown in Fig. 21, Luttinger liquid phase, density wave phase, phase separation state can be observed from the behaviors of the fidelity. However, it is difficult to find the phase boundary between the Ising phase and density wave phase. The authors interpret that the phase transition between the Ising phase and density wave phase is of the Beresinskii-Kosterlitz-Thouless type since in the large  $U_{\text{BB}}$  and  $U_{\text{BF}}$  limit, the effective Hamiltonian of Eq. (226) becomes the one-dimensional XXZ model. Instead, they found that the concurrence [152, 153], as a measure of entanglement between two  $1/2$  spins, can locate the transition point because the concurrence shows a maximum at the isotropic point of the XXZ model [12]. Nevertheless, as we mentioned before, the role of fidelity in the Beresinskii-Kosterlitz-Thouless phase transitions is still controversial.

*The extended Harper model:* The Harper model [180, 181, 182] was proposed to describe electrons in a two-dimensional periodic potential under a magnetic field, for understanding Hofstadter-butterfly energy spectrum [183]. For a system of electrons moving on a triangle lattice in a magnetic field, the Hamiltonian can be written as [182]

$$H_{\text{Harp}} = - \sum_n \left[ t_a + t_c e^{-2\pi i \phi (n-1/2) + i k_y} \right] c_n^{\dagger} c_{n-1} - \sum_n \left[ t_a + t_c e^{2\pi i \phi (n+1/2) - i k_y} \right] c_n^{\dagger} c_{n+1} - \sum_n t_b \cos(2\pi \phi n + k_y) c_n^{\dagger} c_n, \quad (227)$$

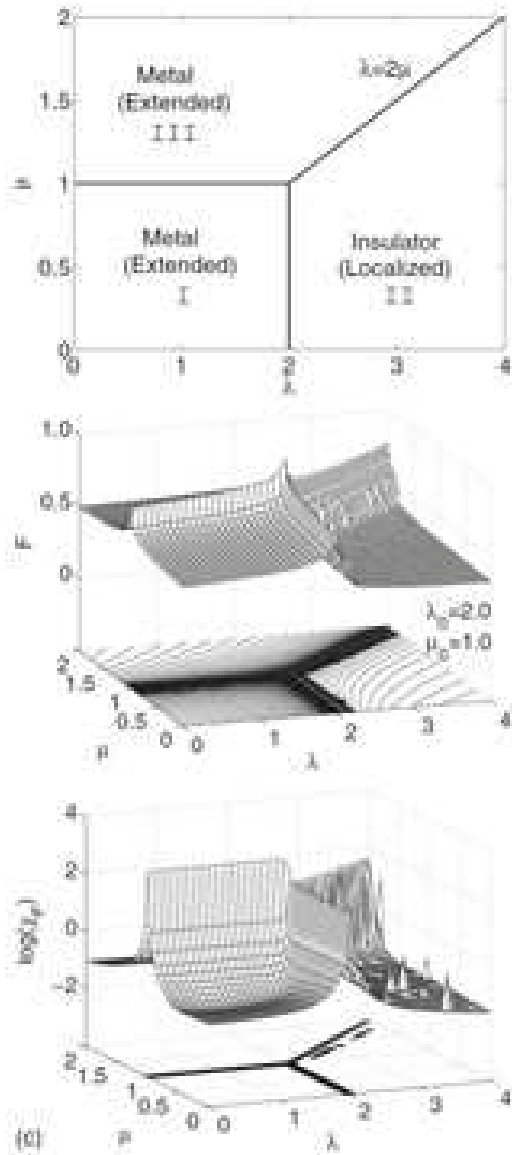


FIG. 22: (Color online) (a) The ground-state phase diagram in the  $\lambda$ - $\mu$  plane. (b) The fidelity  $F(\lambda, \mu; \lambda_0, \mu_0)$  for  $(\lambda_0, \mu_0) = (2.0, 1.0)$ . (c) The fidelity susceptibility and its contour map as a function of  $\lambda$  and  $\mu$  along the direction  $(1/\sqrt{5}, -2/\sqrt{5})$ . (From Ref. [83]).

where  $t_a, t_b, t_c$  are hopping amplitude for each bond on the triangular lattice,  $n$  lattice index,  $\phi/2$  magnetic flux piercing each triangle, and  $k_y$  the momentum in  $y$  direction. Since there is no interaction between electrons, the model can be solved exactly. The ground state of the model consists of three different phase, two conducting phases and one insulating phase. Defining  $\lambda = 2t_b/t_a, \mu = t_c/t_a$ , the ground-state phase diagram

is shown in Fig. 22(a) [182]. Therefore, in addition to metal-insulator transitions, there is also an interesting metal-metal transition.

The fidelity approach to quantum phase transitions between the three phases of the Harper model was done by Gong and Tong [83]. They studied the fidelity between the ground state at  $(\lambda, \mu)$  and various reference states. For example, Fig. 22(b) shows the fidelity of a reference state at  $(\lambda_0, \mu_0) = (2.0, 1.0)$  which is a tricritical point in the phase diagram. At that point, the fidelity is 1, while away from the tricritical point, the ground state changes quickly, then the fidelity show distinct behavior in the parameter space. One can find that the ground-state phase diagram can be sketched out by the contour map of the fidelity. Such a property also is consistent with the primary motivation of the fidelity approach. The authors studied also the fidelity susceptibility along various evolution directions. Fig. 22(c) shows the fidelity susceptibility in the  $\lambda - \mu$  plane along  $(1/\sqrt{5}, -2/\sqrt{5})$  direction. In this case, the fidelity susceptibility are a combination of two elements in the quantum geometric tensor. Since the direction is not parallel to any transition line, the fidelity susceptibility reaches maximum at the boundary between three phases. Interestingly, the authors found the critical exponents of the fidelity susceptibility depend on the different choice of system size. For example, if the system size equal to Fibonacci number  $F_m (F_m = F_{m-1} + F_{m-2})$  with  $m = 3l + 1$ , the adiabatic dimension at the critical point  $d_a^c = 4.9371$  and  $\nu = 2.4718$ ; while form  $m \neq 3l + 1$ ,  $d_a^c = 2$  and  $\nu = 1$ . Therefore, the critical exponent  $\alpha = d_a^c/\nu = 2$  in both cases.

### 3. The fidelity in topological quantum phase transitions

Topological phase transitions are very special in quantum critical phenomena. They do not rely on any local order parameters nor on a symmetry breaking mechanism, hence cannot be described by Landau-Ginzburg-Wilson paradigm. A typical example of these novel phases is the fractional quantum Hall state, in which electrons in two dimension are strongly correlated and their fluctuations are entirely quantum in nature, therefore, the Landau-Ginzburg-Wilson theory, which is based on a classical local order, might fail. The fidelity approach provides an alternative method to study these fascinating phase transitions.

*The deformed Kitaev toric model:* The deformed Kitaev toric model [184] is defined on a square lattice with spin-1/2 degrees of freedom residing on the bonds (Fig.

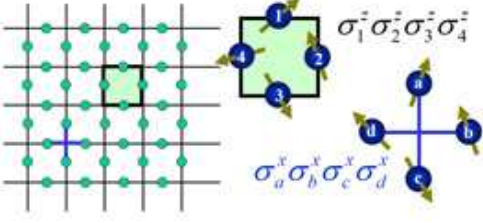


FIG. 23: (Color online) A sketch of the Kitaev toric model: The square lattice (LEFT) is defined on a torus. All 1/2 spins locate at the middle point (solid dot) of bonds. Four neighboring spins interact with other by plaquette or star operators (RIGHT) depending on their locations.

23, left). The Hamiltonian reads

$$\begin{aligned} H_{\text{DKT}} &= -\lambda_0 \sum_p B_p - \lambda_1 \sum_s A_s \\ &+ \lambda_1 \sum_s \exp\left(-\beta \sum_{i \in s} \sigma_i^z\right), \quad (228) \\ &= H_{\text{Kitaev}} + \lambda_1 \sum_s \exp\left(-\beta \sum_{i \in s} \sigma_i^z\right). \quad (229) \end{aligned}$$

Here  $A_s = \prod_{i \in s} \sigma_i^x$  and  $B_p = \prod_{i \in p} \sigma_i^z$  are the star and plaquette operators (Fig. 23, right) of the Kitaev model,  $\lambda_{0,1} > 0$  and  $\beta$  is a parameter tuning the system across a topological phase transition. The ground state of the deformed Kitaev toric model has been obtained exactly [185]

$$|\Psi_0(\beta)\rangle = \sum_{g \in G} \frac{\exp[-\beta \sum_i \sigma_i^z(g)/2]}{\sqrt{Z(\beta)}} g |0\rangle, \quad (230)$$

$$Z(\beta) = \sum_{g \in G} \exp\left[-\beta \sum_i \sigma_i^z(g)/2\right], \quad (231)$$

where  $G$  is the Abelian group of all spin-flip operators obtained as products of star-type operators. The fidelity approach to the topological phase transition occurring in this model has been done [65, 68].

The ground state of the model consists of two distinct phases[185]. If  $\beta = 0$ , the model is pure Kitaev toric model and its ground state is a closed string condensed phase, in which each  $x(z)$  string is a collection of spins that are flipped in the  $\sigma^z(\sigma^x)$  basis. While if  $\beta$  is very large, the ground state favors a fully polarized phase. A quantum phase transition is found to be occurred at the critical point  $\beta_c = (1/2) \ln(\sqrt{2} + 1)$ . The system shows a topological order if  $\beta < \beta_c$ . The fidelity between two states at the points  $\beta \pm \delta\beta$  was obtained by Abasto,

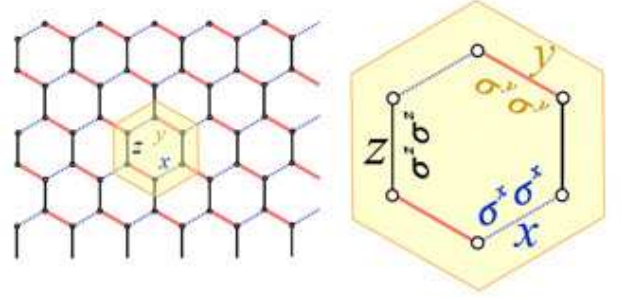


FIG. 24: (Color online) A sketch of the Kitaev honeycomb model: Spins locate at the vertices of a honeycomb lattice (LEFT). Each spin interacts with three neighboring spins through three types of bonds, i.e. “ $x(y, z)$ ” bonds depending on their direction (RIGHT).

Hamma, and Zanardi [68]

$$F(\beta - \delta\beta/2, \beta + \delta\beta/2) = \langle \Psi_0(\beta - \delta\beta/2) | \Psi_0(\beta + \delta\beta/2) \rangle, \quad (232)$$

$$= \sum_{g \in G} \frac{\exp[-\beta \sum_i \sigma_i^z(g)]}{\sqrt{Z(\beta - \delta\beta/2)Z(\beta + \delta\beta/2)}}, \quad (233)$$

and the fidelity susceptibility is

$$\chi_F = \left. \frac{-2 \ln F}{(\delta\beta)^2} \right|_{\delta\beta \rightarrow 0}, \quad (234)$$

$$= \frac{C_v}{4\beta^2}. \quad (235)$$

where  $C_v$  denotes the specific heat of the two-dimensional Ising model. Then the fidelity susceptibility shows a logarithmic divergence at the critical point  $\beta_c$ . These findings are very interesting. The corresponding to the thermal phase transition occurring in the two-dimensional Ising model reveals that the topological phase transition in the deformed Kitaev toric model could be detected by the local magnetization[185].

*The Kitaev honeycomb model:* The Kitaev honeycomb model was also introduced by Kitaev in search of topological order and anyonic statistics. The model is associated with a system of 1/2 spins which are located at the vertices of a honeycomb lattice (Fig. 24: left). Each spin interacts with three nearest neighbored spins through three types of bonds, called “ $x(y, z)$ -bonds” depending on their direction (Fig. 24: right). The model Hamiltonian [184] is as follows:

$$\begin{aligned} H_{\text{KH}} &= -J_x \sum_{x\text{-bonds}} \sigma_j^x \sigma_k^x - J_y \sum_{y\text{-bonds}} \sigma_j^y \sigma_k^y \\ &- J_z \sum_{z\text{-bonds}} \sigma_j^z \sigma_k^z, \quad (236) \end{aligned}$$

$$= -J_x H_x - J_y H_y - J_z H_z, \quad (237)$$

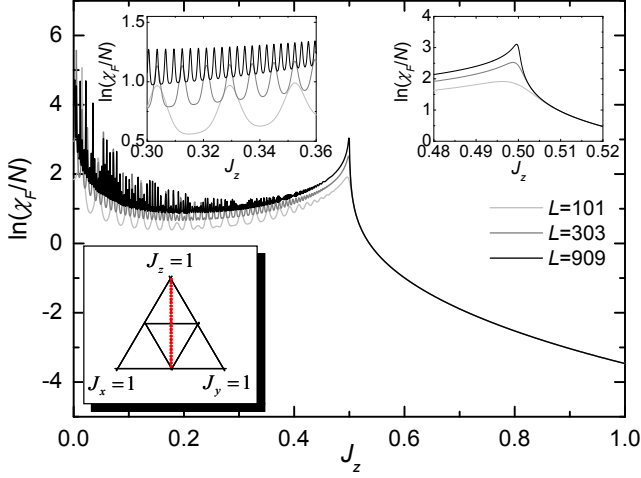


FIG. 25: (Color online) The fidelity susceptibility as a function of  $J_z$  along the dashed line shown in the triangle for various system sizes  $L = 101, 303, 909$ . Both up insets correspond to enlarged picture of two small portions (From Ref. [67]).

where  $j, k$  denote two ends of the corresponding bond, and  $J_a$  ( $a = x, y, z$ ) are coupling constants. The ground state of the Kitaev honeycomb model consists of two phases, i.e., a gapped A phase with Abelian anyon excitations and a gapless B phase with non-Abelian anyon excitations. A quantum phase transition occurred between these two phase is believed to be a topological phase transition because no local operators can be used to describe such a transition.

The Kitaev honeycomb model can be diagonalized exactly in the vortex-free subspace. The ground state can be written as

$$|\Psi_0\rangle = \prod_{\mathbf{q}} \frac{1}{\sqrt{2}} \left( \frac{\sqrt{\epsilon_{\mathbf{q}}^2 + \Delta_{\mathbf{q}}^2}}{\Delta_{\mathbf{q}} + i\epsilon_{\mathbf{q}}} a_{-\mathbf{q},1} + a_{-\mathbf{q},2} \right) |0\rangle, \quad (238)$$

where

$$\epsilon_{\mathbf{q}} = J_x \cos q_x + J_y \cos q_y + J_z, \quad (239)$$

$$\Delta_{\mathbf{q}} = J_x \sin q_x + J_y \sin q_y. \quad (240)$$

$$q_{x(y)} = \frac{2n\pi}{L}, n = -\frac{L-1}{2}, \dots, \frac{L-1}{2}, \quad (241)$$

and  $a_{-\mathbf{q},1(2)}$  are Majorana operators for two sites of a single bound. Then the fidelity between two states is [66, 67]

$$F^2 = \prod_{\mathbf{q}} \cos^2(\theta_{\mathbf{q}} - \theta'_{\mathbf{q}}). \quad (242)$$

with

$$\begin{aligned} \cos(2\theta_{\mathbf{q}}) &= \frac{\epsilon_{\mathbf{q}}}{E_{\mathbf{q}}}, \sin(2\theta_{\mathbf{q}}) = \frac{\Delta_{\mathbf{q}}}{E_{\mathbf{q}}}, \\ \cos(2\theta'_{\mathbf{q}}) &= \frac{\epsilon'_{\mathbf{q}}}{E'_{\mathbf{q}}}, \sin(2\theta'_{\mathbf{q}}) = \frac{\Delta'_{\mathbf{q}}}{E'_{\mathbf{q}}}. \end{aligned} \quad (243)$$

The fidelity depends on the positions of two states in the parameter space. Therefore, in order to extract the fidelity susceptibility, we must know the direction of line connecting the two points. If we define the ground-state phase diagram on the plane  $J_x + J_y + J_z = 1$ , and consider a certain line  $J_x = J_y$  along which the ground state of the system evolves at zero temperature. The fidelity susceptibility becomes [67]

$$\chi_F = \frac{1}{16} \sum_{\mathbf{q}} \left[ \frac{\sin q_x + \sin q_y}{\epsilon_{\mathbf{q}}^2 + \Delta_{\mathbf{q}}^2} \right]^2. \quad (244)$$

Fig. 25 shows the fidelity susceptibility's dependence on the driving parameter (red line in the figure) for various system size. The authors also performed the scaling analysis, and found that the fidelity susceptibility scaling like

$$\frac{\chi_F}{L^2} \sim \frac{1}{(J_z - 1/2)^{1/2}}, \quad (245)$$

around the critical point  $J_z = 0.5^+$ . While in the gapless phase, Gu and Lin [78] found that the fidelity susceptibility is superextensive, i.e.

$$\chi_F \sim L^2 \ln L. \quad (246)$$

Then the critical exponent is quite different at the other side of the critical point, i.e.

$$\frac{\chi_F |J_z - 1/2|^{1/2}}{L^2 \ln L} \sim \ln |J_z - 1/2|, \quad (247)$$

Meanwhile, the topological phase transition was studied in terms of the fidelity per site by Zhao and Zhou [66]. According to the definition of Eq. (170), the fidelity per site in the ground state of the Kitaev honeycomb model has the form

$$\begin{aligned} \ln d(J, J') &= \frac{1}{L^2} \sum_{\mathbf{q}} \ln [\cos(\theta_{\mathbf{q}} - \theta'_{\mathbf{q}})], \quad (248) \\ &= \frac{1}{(2\pi)^2} \int_0^\pi dq_x \int_0^\pi dq_y \ln [\cos(\theta_{\mathbf{q}} - \theta'_{\mathbf{q}})], \quad (249) \end{aligned}$$

where  $\theta_{\mathbf{q}}$  is determined by Eq. (243). The above expression makes it possible to study the scaling and critical behavior of the fidelity per site easily. More precisely, if  $J'$  is fixed, they found that the fidelity per site is logarithmically divergent when  $J$  is varied such that a critical point is crossed. For example, if only  $J_x$  of  $J$  is considered as a driving parameter, they found the fidelity per site

$$\left. \frac{d^2 \ln d(J, J')}{dJ_x^2} \right|_{J_x = J_{x_{\text{cm}}}} \sim \ln L, \quad (250)$$

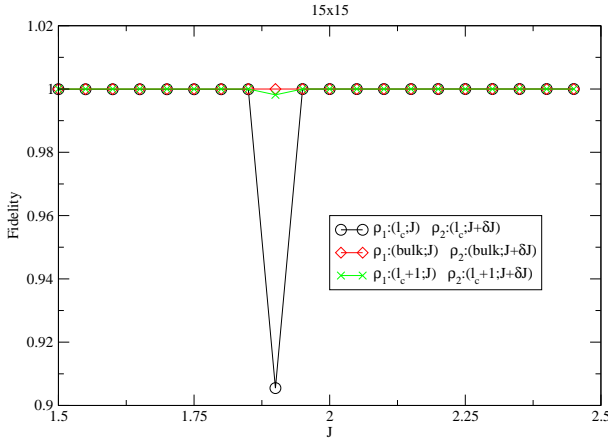


FIG. 26: (Color online) The single-site reduced fidelity in the two-dimensional s-wave conventional superconductor. (From Ref. [55]).

where  $J_{xm}$  denotes the position of extremum point for a finite system, and

$$\frac{d^2 \ln d(J, J')}{dJ_x^2} \sim \ln |J_x - J_{xc}|, \quad (251)$$

in the thermodynamic limit.

Therefore, the fidelity now is believed to be able to characterize the topological phase transition occurring in the Kitaev honeycomb model [66, 67].

## B. Mixed-state fidelity

### 1. Reduced fidelity in quantum phase transitions

There are several works on the role of reduced fidelity in quantum phase transitions.

*The one-dimensional transverse-field XY model:* The reduced fidelity approach to the XY model was firstly touched by Zhou [45] in order to confirm the relation between the fidelity per site and renormalization group flow. He noted that the fidelity per site can capture nontrivial information including stable and unstable fixed points in the renormalization process in which the entanglement cannot.

Ma *et al* [81] and Li [88] studied the two-site reduced fidelity in the ground state of the transverse-field Ising model independently. In the work by Ma *et al*, the fidelity of the reduced state of two neighboring site in the model is

$$F = \text{tr} \sqrt{\rho(\lambda)^{1/2} \rho(\lambda + \delta\lambda) \rho(\lambda)^{1/2}}, \quad (252)$$

where  $\rho(\lambda)$  is the reduced-density matrix of the two spins. Then the reduced fidelity susceptibility is defined by

$$\chi_F = \lim_{\delta h \rightarrow 0} \frac{-2 \ln F}{(\delta\lambda)^2}. \quad (253)$$

For this model,  $\rho(\lambda)$  can be expressed in terms of the two-site correlation functions that can be calculated explicitly. This property enables them to study the scaling and critical behavior of the reduced fidelity easily. They found that, for a finite  $N$ -site system, the function

$$\chi_F(\lambda_m, N)^{1/2} - \chi_F(\lambda_m, N)^{1/2} = Q[N^\nu(\lambda - \lambda_m)] \quad (254)$$

is universal around the critical point. The scaling relation reveals that reduced fidelity susceptibility diverges logarithmically

$$\chi_F(\lambda)^{1/2} \sim \ln |\lambda - \lambda_c|, \quad (255)$$

which is quite different from the global state fidelity in the same model. While Li [88] calculated the reduced fidelity directly. It is reported that the extremum of the reduced fidelity scales like  $F \propto (\ln N)^{2.25}$  around the critical point. Later, You *et al* [90] also make an extension to the one-dimensional XY model. Similar results are obtained.

*The Lipkin-Meshkov-Glick model:* The quantum phase transition occurring in the Lipkin-Meshkov-Glick model was also studied in terms of the reduced fidelity [72, 73].

It is not convenient to use the global-state fidelity to characterize those quantum phase transitions induced the continuous level-crossing, such as the magnetization process, because the global-state fidelity drops to zero at each level crossing point. Kwok *et al* proposed that the reduced fidelity can overcome the difficulty. They used both the Lipkin-Meshkov-Glick model and the one-dimensional XXX model as examples to show that the reduced fidelity and its leading term, i.e. the reduced fidelity susceptibility help to study scaling and critical behavior. Ma *et al* [73] also study the behaviors of the two-site reduced fidelity in the Lipkin-Meshkov-Glick model.

*The one-dimensional extended Hubbard model:* Though the role of the ground-state fidelity in the Hubbard model is still not very clear, it is shown by Li [88] that the two-site reduced fidelity is able to sketch out the ground-state phase diagram of the model. Previously, it is firstly reported by Gu *et al* [14] that the contour map of single-site entanglement can describe the change of symmetry in the ground-state of the system. Due to the competition between various correlation, the entanglement usually reaches a maximum at the critical point; while from fidelity approach, it is shown that fidelity shows a minimum at the critical point due to the abrupt change in the structure of the ground state.

*Two-dimensional s-wave conventional superconductor:* The Hamiltonian reads

$$\begin{aligned} H = & - \sum_{\langle ij \rangle \sigma} t c_{i\sigma}^\dagger c_{j\sigma} - \varepsilon_F \sum_{i\sigma} c_{i\sigma}^\dagger c_{i\sigma} \\ & + \sum_i \left( \Delta_i c_{i\uparrow}^\dagger c_{i\downarrow}^\dagger + h.c. \right) \\ & - \sum_{\sigma\sigma'} J \left( \cos \varphi c_{0\sigma}^\dagger \sigma_{\sigma\sigma'}^x c_{0\sigma'} + \sin \varphi c_{0\sigma}^\dagger \sigma_{\sigma\sigma'}^z c_{0\sigma'} \right). \end{aligned} \quad (256)$$

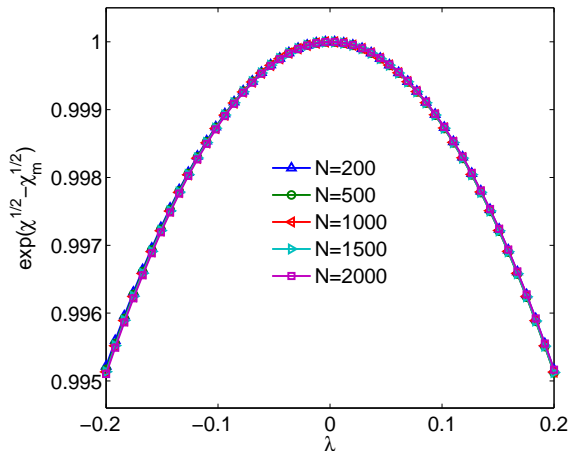


FIG. 27: (Color online) The scaling behavior the reduced fidelity susceptibility of the one-dimensional transverse-field Ising model. (From Ref. [81] ).

The first three terms in Eq. (256) denote the Hamiltonian of s-wave conventional superconductor, and the last term represents the interaction between electrons and an classical spin placed at the origin. Paunković *et al* [55] first studied the reduced fidelity (or the partial-state fidelity) in the ground state of the system. They observed that the one-site reduced fidelity shows a sudden drop in the vicinity of the quantum phase transition. Since the one-site reduced-density matrix depends on a single quantity, i.e. magnetization. They interpret the drop of the reduced fidelity due to that the on-site magnetization plays an order parameter in this model. Such a behavior is very similar to that of entanglement [19] in the same model.

## 2. Thermal state fidelity in strongly correlated systems

The leading term of the fidelity, i.e. the thermal fidelity susceptibility is simply the specific heat if we choose the temperature as the driving parameter, and magnetic susceptibility if we choose the magnetic field as the driving parameter. Despite of this there are still some works on fidelity in thermal phase transitions, especially for those Hamiltonians with non-commuting driving terms.

*The BCS superconductor:* The effective Hamiltonian of the Bardeen-Cooper-Schrieffer (BCS) superconductor [210, 211] can be written as

$$H_{\text{BCS}} = \sum_{k\sigma} \varepsilon_k c_{k\sigma}^\dagger c_{k\sigma} + \sum_{kk'} V_{kk'} c_{k'\uparrow}^\dagger c_{-k'\downarrow}^\dagger c_{-k\downarrow} c_{k,\uparrow}. \quad (257)$$

where  $\varepsilon_k$  is the dispersion and  $V_{kk'}$  are coupling constant. The BCS Hamiltonian provides us with an example of a model with a mutually non-commuting Hamiltonian. The fidelity approach to its thermal phase transition from a normal state to a superconducting state was done by

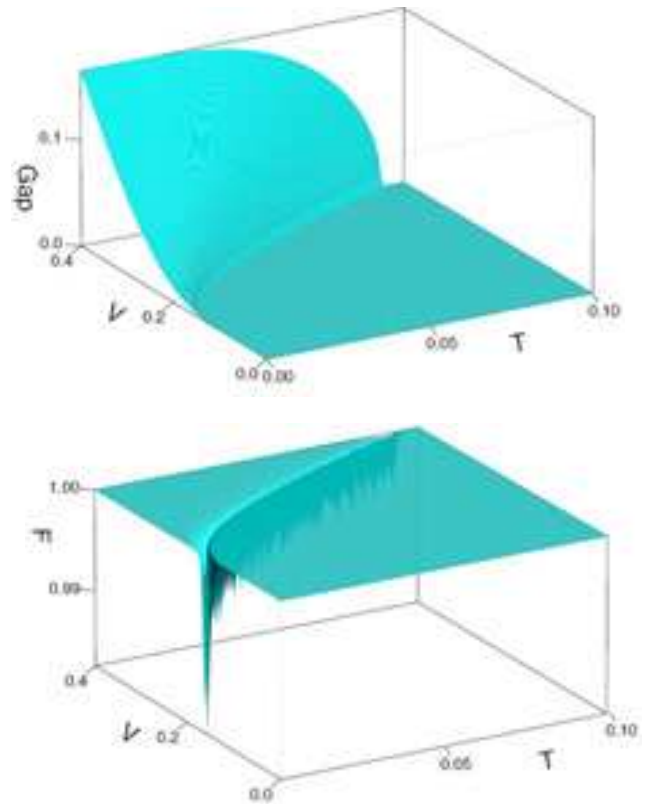


FIG. 28: (Color online) The gap  $\Delta$  (UP) and the fidelity of  $\delta V = 10^{-3}$ ,  $\delta T = 0$  (DOWN) as a function of the temperature  $T$  and the coupling constant  $V$ . The plot is given in rescaled quantities  $T \rightarrow k_B T / (\hbar \omega_D)$ ,  $V \rightarrow D_F V$  and  $\Delta \rightarrow \Delta / (\hbar \omega_D)$  (From Ref. [56]).

Paunković and Vieira [56]. Based on the mean-field approach, the gap function and the thermal-state fidelity was obtained analytically. Fig. 28 shows both the gap and the fidelity as a function of the coupling and temperature. Clearly, when the gap appears, the system becomes a superconducting state. A thermal phase transition occurs at the critical point. On the  $V - T$  plane, both  $V$  and  $T$  can be regarded as the driving parameter, therefore, the fidelity between two thermal state separated by a small distance on the plane shows a sharp peak around the critical point. On the other hand, since the two terms at the right hand side of Eq. (257) do not commute, the fidelity is not easy to be calculated. However, the authors found that distance obtained from Eq. (187) and the fidelity have the same qualitative behavior (constant value 1 everywhere, except for the sudden drop along the line of phase transition).

Paunković and Vieira studied also the thermal phase transitions in the Stoner-Hubbard model whose Hamiltonian reads

$$H_{\text{SH}} = \sum_{k\sigma} \varepsilon_k c_{k\sigma}^\dagger c_{k\sigma} + U \sum_l n_{l\uparrow} n_{l\downarrow}. \quad (258)$$

where  $\varepsilon_k = k^2/2m$  is the dispersion, and  $U$  the on-site

interaction. Unlike the BCS superconductor, the phase transition they addressed in the Stoner-Hubbard model is due to the existence of Zeemann-like term for conserved quantities. In this case, the fidelity susceptibility is simply the susceptibility of the conserved quantity[43]. The fidelity shows a sharp peak around the transition point from an order phase at low temperature to a disorder phase at high temperature.

## VII. NUMERICAL METHODS FOR THE GROUND-STATE FIDELITY

This section is for students who are not familiar with the numerical diagonalization and the density matrix renormalization group technique.

### A. Exact diagonalization

*Direct diagonalization:* One of the main goals of quantum mechanics is to diagonalize Hamiltonian matrices. Except for a few cases, however, the Hamiltonian of most quantum many-body systems cannot be diagonalized explicitly. Fortunately, advance in digital computers make it possible to diagonalize the Hamiltonian numerically. Up to now, many numerical methods rooting in computer science have been extensively developed, among which the most straightforward method is the exact diagonalization. Though the system size that can be diagonalized numerically is still not large, the numerical results actually are very instructive for studies of the quantum many-body systems.

In the exact diagonalization, we need to express the Hamiltonian in a set of basis, and then diagonalize it numerically. As a warm-up example, let's consider a spin dimer system. The Hamiltonian of a spin dimer with the Heisenberg interaction reads

$$H = \sigma_1 \cdot \sigma_2, \quad (259)$$

$$= \sigma_1^x \sigma_2^x + \sigma_1^y \sigma_2^y + \sigma_1^z \sigma_2^z. \quad (260)$$

To see its matrix form, we use the eigenstates of  $\sigma^z$  operators as basis, i.e.,  $\{|\uparrow\uparrow\rangle, |\uparrow\downarrow\rangle, |\downarrow\uparrow\rangle, |\downarrow\downarrow\rangle\}$ . In this set of basis, the Hamiltonian can be written as

$$H = \begin{pmatrix} 1 & 0 & 0 & 0 \\ 0 & -1 & 2 & 0 \\ 0 & 2 & -1 & 0 \\ 0 & 0 & 0 & 1 \end{pmatrix} \begin{pmatrix} |\uparrow\uparrow\rangle \\ |\uparrow\downarrow\rangle \\ |\downarrow\uparrow\rangle \\ |\downarrow\downarrow\rangle \end{pmatrix}. \quad (261)$$

With some standard technique in Linear algebra, we can find that its ground state is a spin singlet state

$$\Psi_0 = \frac{1}{\sqrt{2}} [|\uparrow\downarrow\rangle - |\downarrow\uparrow\rangle], \quad (262)$$

with eigenvalue  $E_0 = -3$ , while three degenerate excited states are

$$\begin{aligned} \Psi_1 &= \frac{1}{\sqrt{2}} [|\uparrow\downarrow\rangle + |\downarrow\uparrow\rangle], \\ \Psi_2 &= |\uparrow\uparrow\rangle, \quad \Psi_3 = |\downarrow\downarrow\rangle. \end{aligned} \quad (263)$$

with higher eigenvalue  $E_{1(2,3)} = 1$ .

Numerically, we can construct the basis by a set of integer which is usually a binary digit. For the above example, we can use 0, 1, 2, 3 (that are 00, 01, 10, 11 in binary system) to denote the basis  $|\uparrow\uparrow\rangle, |\uparrow\downarrow\rangle, |\downarrow\uparrow\rangle, |\downarrow\downarrow\rangle$ , respectively. Then, we can define an array to save the Hamiltonian. There are some standard methods [212] to diagonalize a matrix, such as Householder method and QR algorithm, or standard libraries, such as Linear Algebra Package(LAPACK) [213] and Intel's Math Kernel Library (MKL) [214].

*Lanczos method:* For a small size sample, such as a 10 1/2-spin chain, the dimension of the Hamiltonian matrix is not very large. We are able to diagonalize the whole matrix. All eigenstates and eigenvalues can be obtained. While if the dimension of the matrix size is very large, say 100000, it is almost impossible to implement the traditional diagonalization methods. However, if we are only interested in the ground state of the Hamiltonian, it is still possible for us to find the wavefunction via the famous Lanczos method.

Here we would like to introduce the Lanczos method to diagonalize a large sparse matrix and how to calculate the fidelity and its susceptibility via the Lanczos method. We are not going to address the principle of the Lanczos method, instead we show that the perturbation nature of the method facilitates calculation of the fidelity susceptibility numerically. Now we briefly introduce the basic steps of the Lanczos method.

The first step in the Lanczos method is to transform a large sparse matrix  $H$  to a tri-diagonal matrix  $T$  as

$$T_m = \begin{pmatrix} \alpha_1 & \beta_1 & \cdots & \cdots & 0 \\ \beta_1 & \alpha_2 & & & \vdots \\ \vdots & & \ddots & & \vdots \\ \vdots & & & \alpha_{m-1} & \beta_{m-1} \\ 0 & \cdots & \cdots & \beta_{m-1} & \alpha_m \end{pmatrix}, \quad (264)$$

where  $m$  is the cut-off number. The cut-off number is determined by the precession. For a real symmetric matrix  $H$ , we need an orthogonal matrix to do such a transformation, i.e.

$$V = (\mathbf{v}_1, \mathbf{v}_2, \cdots, \mathbf{v}_m), \quad (265)$$

which satisfy

$$\langle \mathbf{v}_i | \mathbf{v}_j \rangle = \delta_{ij}, \quad (266)$$

and

$$HV = VT_m. \quad (267)$$

Therefore, starting from an initial (random) vector  $\mathbf{v}$ , we have the following relations

$$\begin{aligned}
\mathbf{v}_1 &= \mathbf{v}, \\
\beta_1 \mathbf{v}_2 &= H\mathbf{v}_1 - \langle \mathbf{v}_1 | H | \mathbf{v}_1 \rangle \mathbf{v}_1, \\
\beta_2 \mathbf{v}_3 &= H\mathbf{v}_2 - \langle \mathbf{v}_2 | H | \mathbf{v}_2 \rangle \mathbf{v}_2 - \langle \mathbf{v}_1 | H | \mathbf{v}_2 \rangle \mathbf{v}_1, \\
\beta_3 \mathbf{v}_4 &= H\mathbf{v}_3 - \langle \mathbf{v}_3 | H | \mathbf{v}_3 \rangle \mathbf{v}_3 - \langle \mathbf{v}_2 | H | \mathbf{v}_3 \rangle \mathbf{v}_2, \\
&\dots \\
\beta_m \mathbf{v}_{m+1} &= H\mathbf{v}_m - \langle \mathbf{v}_m | H | \mathbf{v}_m \rangle \mathbf{v}_m, \\
&\quad - \langle \mathbf{v}_{m-1} | H | \mathbf{v}_m \rangle \mathbf{v}_{m-1}.
\end{aligned} \tag{268}$$

From these relations, we can find that, using the orthogonal condition (266),

$$\begin{aligned}
\alpha_1 &= \langle \mathbf{v}_1 | H | \mathbf{v}_1 \rangle, \\
|\mathbf{r}_i\rangle &= (H - \alpha_i) |\mathbf{v}_i\rangle - \beta_{i-1} |\mathbf{v}_{i-1}\rangle, \\
\beta_i &= \sqrt{\langle \mathbf{r}_i | \mathbf{r}_i \rangle}, \\
|\mathbf{v}_{i+1}\rangle &= |\mathbf{r}_i\rangle / \beta_i, \\
\alpha_{i+1} &= \langle \mathbf{v}_{i+1} | H | \mathbf{v}_{i+1} \rangle, \\
i &= 1, 2, \dots, m-1.
\end{aligned} \tag{269}$$

The above steps are the famous Lanczos iteration, which was proposed by Cornelius Lanczos in 1950.

After the matrix  $T$  is obtained, one can easily calculate its eigenvalues  $E_i$  and their corresponding eigenvectors  $|\mathbf{u}_i\rangle$ . This procedure is simple because  $T$  is already tri-diagonal. It can be proved that the lowest eigenvalue of  $T$  is the ground-state energy of  $H$ . Then the ground-state wavefunction (Ritz eigenvector) can be calculated as

$$|\Psi_0\rangle = V|\mathbf{u}_0\rangle, \tag{270}$$

where  $|\mathbf{u}_0\rangle$  is the ground state of  $T$ .

To calculate the fidelity between two ground states in parameter space, the Lanczos method is very promising because it is actually a numerically perturbative method. To be concrete, if  $H(\lambda)|\Psi_0(\lambda)\rangle = E_0|\Psi_0(\lambda)\rangle$ , then for the Hamiltonian

$$H(\lambda + \delta\lambda) = H(\lambda) + \delta\lambda H_I, \tag{271}$$

we can use  $|\Psi_0(\lambda)\rangle$  as an initial state, then

$$\alpha_1 = E_0 + \delta\lambda \langle \Psi_0(\lambda) | H_I | \Psi_0(\lambda) \rangle,$$

which is simply the ground-state energy up to the first-order perturbation. To the second order, one can find that

$$\begin{aligned}
\alpha_1 &= E_0 + \delta\lambda \langle \Psi_0(\lambda) | H_I | \Psi_0(\lambda) \rangle, \\
\beta_1 &= \delta\lambda \sqrt{\langle \Psi_0(\lambda) | H_I^2 | \Psi_0(\lambda) \rangle - \langle \Psi_0(\lambda) | H_I | \Psi_0(\lambda) \rangle^2}, \\
\alpha_2 &= \frac{\delta\lambda^2}{\beta_1^2} \langle \Psi_0(\lambda) | \Delta H_I H(\lambda + \delta\lambda) \Delta H_I | \Psi_0(\lambda) \rangle,
\end{aligned} \tag{272}$$

TABLE II: The fidelity susceptibility of the one-dimensional transverse-field Ising model obtained by the exact diagonalization (middle) and exact analytical results(right). Small difference might be caused by numerical derivation. Here  $N = 20$ .

$h$	FS(ED with $\delta h = 0.005$ )	FS of Eq. (141)
0.2	1.30206	1.30208
0.3	1.37360	1.37362
0.4	1.48807	1.48809
0.5	1.66672	1.66675
0.6	1.95535	1.95539
0.7	2.48564	2.48568
0.8	3.81093	3.81096
0.9	7.96763	7.96833
1.0	11.87198	11.87500
1.1	5.83999	5.84015
1.2	2.28066	2.28060
1.3	1.13390	1.13388
1.4	0.67720	0.67719
1.5	0.44735	0.44735
1.6	0.31372	0.31372
1.7	0.22904	0.22904

where  $\Delta H_I = H_I - \langle \Psi_0(\lambda) | H_I | \Psi_0(\lambda) \rangle$ . Then the  $T$  matrix, to the second order, becomes

$$T_2 = \begin{pmatrix} \alpha_1 & \beta_1 \\ \beta_1 & \alpha_2 \end{pmatrix}. \tag{273}$$

The eigenvalue of  $T_2$  is

$$\frac{1}{2} \left[ \alpha_1 + \alpha_2 - \sqrt{(\alpha_1 - \alpha_2)^2 + 4\beta_1^2} \right]. \tag{274}$$

Therefore, the Lanczos method is not only a perturbative method, but also a variational method. The advantage is that we can use  $|\Psi_0(\lambda)\rangle$  as the initial state to calculate  $|\Psi_0(\lambda + \delta\lambda)\rangle$ . Once the latter is obtained, the fidelity  $\langle \Psi_0(\lambda) | \Psi_0(\lambda + \delta\lambda) \rangle$  can be easily calculated.

Here, we take the one-dimensional transverse-field Ising model as an example. In section III, we can find the fidelity susceptibility at the point takes the form

$$\chi_F = \sum_{k>0} \left( \frac{d\theta_k}{d\lambda} \right)^2, \tag{275}$$

where

$$\frac{d\theta_k}{d\lambda} = \frac{1}{2} \frac{\sin k}{1 + h^2 - 2h \cos k}. \tag{276}$$

From Eq. 275, we can calculate the fidelity susceptibility up to a very large systems. For a comparison, we simply show both the analytical results and numerical results for a 20-site system in Table. II.

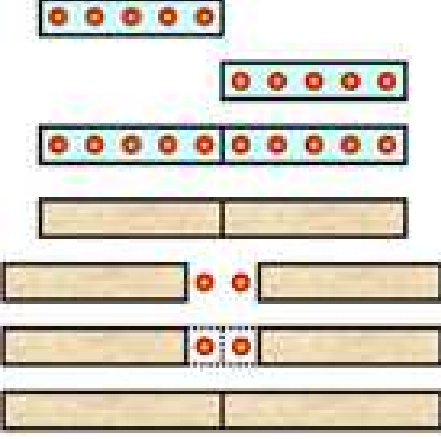


FIG. 29: (Color online) The infinite-system algorithm of the DMRG technique: The system size grows under the renormalization group transformation.

## B. Density matrix renormalization group

The density matrix renormalization group (DMRG) technique is a very successful numerical method for one-dimensional strongly correlated systems. The algorithm was invented by S. R. White [215] in 1992. Tzeng and Yang [53] firstly applied the DMRG technique to calculate the ground-state fidelity. In this section, we briefly explain the basic ideas of the DMRG algorithm and its application to the fidelity.

The main idea of the DMRG algorithm is a smart reduction of the number of effective degrees of freedom and a variational and perturbative search of the ground state within the reduced space. This idea is very important in computational physics. For a quantum many-body system, the dimension of the Hilbert space grows exponentially with the system size. For example, a  $L$ -site spin-1/2 system, the dimension of its Hilbert space is  $2^L$ . The growth in the Hilbert-space dimension quickly exhausts computing resources. This fact discourage us from doing exact diagonalization for larger systems. Fortunately, the DMRG algorithm is able to capture the most relevant degrees of freedom, hence allows us to reduce the effective dimension of the Hilbert space significantly.

The DMRG algorithm consists of two fundamental sections: infinite-system algorithm and finite-system algorithm. In both algorithms, a system of  $L$  sites usually is divided into four blocks, i.e,  $L^S$ -site system block S, two intermediate sites, and the rest environmental block E of  $L^E = L - L^S - 2$  sites. The infinite-system algorithm aims to grow the system to the size we want to study, and the finite-system algorithm to reduce the numerical error based on the variational principle. The DMRG al-

gorithm is more efficient for a system with open boundary conditions. So we limit our discussion to this case here. Readers interested in other details of the DMRG algorithm are recommended to refer to the review paper by U. Schollwöck [217] and the book by Peschel *et al* [216]. There are also some new development in the time-dependent DMRG method[218], and DMRG algorithm from the perspective of quantum information theory [219].

*The infinite-system algorithm* (Fig. 29):

Step 1: Start with a small system block of  $l$  sites. Construct a set of real-space basis (for instance,  $\{|\uparrow\rangle, |\downarrow\rangle\}$  for a single spin or  $\{|\uparrow\uparrow\rangle, |\uparrow\downarrow\rangle, |\downarrow\uparrow\rangle, |\downarrow\downarrow\rangle\}$  for two spins). Then under the basis, construct the Hamiltonian matrix  $H^S$  and matrices of operators responsible for interactions, say  $O_r^S$ , at the rightmost site.

Step 2: Construct the environment block of the same size (range from  $l + 1$  to  $2l$ ), including the Hamiltonian matrix  $H^E$  and interaction-operator matrices, say  $O_l^E$ , at the leftmost site, say  $O_l$ , in a similar way.

Step 3: Build the superblock by connecting the system and environment blocks. The superblock Hamiltonian can be constructed from

$$H = H_l^S \otimes I^E + I^S \otimes H_l^E + O_r^S \otimes O_l^E \quad (277)$$

where  $H^I = O_r^S \otimes O_l^E$  is the interaction Hamiltonian between the  $l$ th site of the system block and  $(l + 1)$ th of the environment block. If there are more interaction terms, they should be included in  $H^I$  too. Diagonalize the superblock Hamiltonian  $H$  to obtain the ground state  $|\Psi_0\rangle$  by the Lanczos method or Davidson method [220]. Calculate the reduced-density matrices of the system block and the environment block by

$$\rho^S = \text{tr}_E |\Psi_0\rangle\langle\Psi_0|, \rho^E = \text{tr}_S |\Psi_0\rangle\langle\Psi_0|, \quad (278)$$

then diagonalize  $\rho^S$  by the traditional diagonalization method for dense matrix, such as Householder-QR method,

$$\rho^S |\mathbf{v}_j\rangle = w_j |\mathbf{v}_j\rangle, \quad (279)$$

where  $w_j$  is in a decreasing order. Form a new set of basis for the system block by  $M$  eigenstates of  $\rho^S$  with the largest eigenvalues, and construct the transformation matrix

$$\Omega = \{\mathbf{v}_1, \mathbf{v}_2, \dots, \mathbf{v}_M\}. \quad (280)$$

Here  $M$  is chosen based on the desired precision. Transform the Hamiltonian of the system block and the interaction operators at the rightmost site into the new basis

$$\tilde{H}^S = \Omega^\dagger H^S \Omega, \quad (281)$$

$$\tilde{O}_r^S = \Omega^\dagger O_r^S \Omega. \quad (282)$$

The environment block Hamiltonian and  $O_l$  are transformed in a similar way.

Step 4: Connect a new site to the rightmost site of the system block, and a new site to the leftmost site of the environment block. The new Hamiltonian is

$$H^S = \tilde{H}^S \otimes I + \tilde{I}^S \otimes H^N + H^I, \quad (283)$$

$$H^E = I \otimes \tilde{H}^E + H^N \otimes \tilde{I}^E + H^I, \quad (284)$$

where  $H^N$  is the single-site Hamiltonian. If the total size of the system block, environment block, and two sites is small than the target size, then goto the step 3, otherwise, jump to the following finite-system algorithm.

*The finite-system algorithm* (Fig. 30):

Once the size of the superblock in the infinite-system algorithm reaches the target size we want to study, one can calculate the ground-state properties. However, the results usually are not satisfactory because the error is still very large. We need to use the finite-system algorithm to reduce the error. The finite-system algorithm is similar to the infinite-system algorithm. Instead of growing both blocks in the infinite-system algorithm, the growth of one block is accompanied by shrinkage of the other block in the finite-system algorithm. The information of the block shrunk should be retrieved. For this purpose, one need to store the block information, including matrices of the Hamiltonian and interaction operators in the reduced space, obtained in the infinite-system algorithm.

Step 1: Followed from the infinite-system algorithm, now we have a system block of  $L/2 - 1$  sites, two independent sites, and an environment block of  $L/2 - 1$  sites. Construct the superblock Hamiltonian, and compute the ground state by the Lanczos method or Davidson method. Differ from the infinite-system algorithm, here we do the reduced basis transformations for the system block only. Then the new system block has  $L/2$  sites.

Step 2: Continue to grow the system block in a similar way, while using the stored information of the environment block, until the system block reaches the maximum size.

Step 3: Once the environment block is minimized, then grow the environment block at the expense of the system block in the same way, until the environment is maximized.

Step 4: Grow the system block, and shrink the environment block to  $L/2 - 1$ .

A complete shrinkage and growth sequence for both blocks (From step 1-4) is called a sweep (Fig. 30). Usually more sweeps, higher precision the final results have. Once the desired precision is reached, the ground state can be expressed in reduced space.

In the DMRG algorithm, the reduced basis obtained by the numerical renormalization group strongly depend on the parameter of the Hamiltonian. So we cannot compare two ground states at distinct points in the parameter space directly. In order to calculate the fidelity between the two ground states, one has to find a transformation between the two sets of reduced basis. Such a transfor-

mation, as proposed in Ref. [70], can be established in the final sweep of the finite-system algorithm.

The ground-state wavefunctions of the Hamiltonian  $H_0 + \lambda H_I$  at two points  $\lambda_1$  and  $\lambda_2$ , in their own reduced space, can be expressed as

$$|\Psi_0(\lambda_1)\rangle = \sum_{i,m,n,j} \Phi_{imnj}(\lambda) |\varphi_i^S\rangle |m\rangle |n\rangle |\varphi_j^E\rangle, \quad (285)$$

$$|\Psi_0(\lambda_2)\rangle = \sum_{i,m,n,j} \bar{\Phi}_{imnj}(\lambda) |\bar{\varphi}_i^S\rangle |\bar{m}\rangle |\bar{n}\rangle |\bar{\varphi}_j^E\rangle, \quad (286)$$

where  $|\varphi_i^S\rangle (|\varphi_j^E\rangle)$  is the reduced basis of the system(environment) block, and  $|m\rangle, |n\rangle$  are the basis of the middle two sites. Since  $|m\rangle, |n\rangle$  are the basis of local sites, we have

$$\langle m|\bar{m}\rangle = \delta_{m\bar{m}}, \langle n|\bar{n}\rangle = \delta_{n\bar{n}}. \quad (287)$$

Then the fidelity between two ground states becomes

$$\begin{aligned} & \langle \Psi_0(\lambda_1) | \Psi_0(\lambda_2) \rangle \quad (288) \\ &= \sum_{i,j,i',j',m,n} \Phi_{imnj}(\lambda) \bar{\Phi}_{i'mnj'}(\lambda) \langle \varphi_i^S | \bar{\varphi}_{i'}^S \rangle \langle \varphi_j^E | \bar{\varphi}_{j'}^E \rangle, \end{aligned}$$

where  $T_{ii'}^S \equiv \langle \varphi_i^S | \bar{\varphi}_{i'}^S \rangle$  ( $T_{jj'}^E \equiv \langle \varphi_j^E | \bar{\varphi}_{j'}^E \rangle$ ) defines the transformation matrix between the two sets of reduced basis of the system (environment) block at  $\lambda_1$  and  $\lambda_2$ .

Now we focus on how to obtain the  $T^S$  of a  $L^S$ -site system block, the  $T^E$  of the environment block can be obtained in a similar way.

Step 1: During the final sweep of the finite-system algorithm of the two Hamiltonians  $H(\lambda_1)$  and  $H(\lambda_2)$ , if both system blocks are minimized (to a single site), their basis are defined in the real space and not reduced, then the transformation matrix between the two system blocks is simply the unity matrix, i.e.,

$$T^S(l=1) = I. \quad (289)$$

Step 2: Suppose the transformation matrix of the two system blocks up to  $l$  sites (including  $l=1$ ) is obtained, i.e.

$$T^S(l) = |\bar{\varphi}_{j'}^E(l)\rangle \langle \varphi_j^E(l)|, \quad (290)$$

the basis of the system blocks together and the new site before the renormalization group transformation are

$$|\varphi_j^E(l)\rangle \otimes |m(l+1)\rangle, \quad (291)$$

$$|\bar{\varphi}_{j'}^E(l)\rangle \otimes |m(l+1)\rangle, \quad (292)$$

respectively. The transformation matrix between the two sets of basis becomes

$$T^S(l) \otimes I(l+1). \quad (293)$$

After the RG transformation, one can find the transformation matrix  $T^S$  becomes

$$T^S(l+1) = \Omega^\dagger [T^S(l) \otimes I(l+1)] \Omega, \quad (294)$$

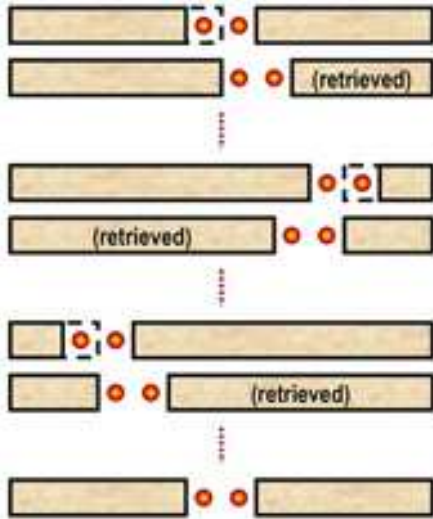


FIG. 30: (Color online) The finite-system algorithm of the DMRG technique: The system block grows under the renormalization group transformation, under the environment block shrinks with the retrieved representation; and vice versa.

which gives a recursion relation of the transformation matrix  $T^S$  in the RG transformation.

Step 3: repeat the step 2 until both the two system block grow upto  $L^E$  sites.

Clearly, the transformation matrix  $T^E$  can be obtained if we start from the minimized environment block. Finally, the fidelity of Eq. (288) can be calculated. The fidelity susceptibility can be also computed by the numerical differentiation.

## VIII. SUMMARY AND OUTLOOK

As mentioned in the introductory section, quantum information theory provides us opportunities to investigate quantum phenomena from new angles. It is fair to say, besides huges of works on the role quantum entangle-

ment in the ground state of quantum many-body systems, the fidelity approach to quantum phase transitions have shed new light on the critical phenomena. Moreover, unlike the entanglement, which is somehow still mysterious in quantum many-body system, the fidelity has, from our point of view, a clearer physical picture. Especially, its leading term manifests scaling and critical behaviors around the phase transition point. Therefore, the fidelity is really a new optional method to investigate quantum phase transitions, especially for those cases that we know nothing about order parameters.

However, there are still some remaining problems. Firstly, the validity of the fidelity in the Beresinskii-Kosterlitz-Thouless phase transitions is still controversial. Secondly, the deep reason that the fidelity can signal the topological phase transitions remains unknown. Thirdly, one of most difficulties of the fidelity in quantum many-body systems is that it is really difficult to find the exact ground state, except for a few cases. Finally, it is a challenging problem to measure the fidelity in experiment on scalable systems.

Finally, since the field is still quickly developing, we hope again that this introductory review can offer some rough essays first, then to arouse other people's better or more mature ideas.

## Acknowledgments

We acknowledge our indebtedness to many people. We received genuine interest and words of encouragement from Hai-Qing Lin and Chang-Pu Sun. We would also like to thank Libin Fu, Ho-Man Kwok, Hai-Qing Lin, Li-Gang Wang, Xiaoguang Wang, Shuo Yang, Yi-Zhuang You, Yi Zhou for many helpful discussions. We thank N. Paunković for nice feedbacks.

We thank Ho-Man Kwok for his final critical reading and efforts on textual improvement.

We apologize if we omit acknowledging your relevant works.

This work is supported by the Direct grant of CUHK (A/C 2060344).

- 
- [1] S. Sachdev, *Quantum Phase Transitions*, (Cambridge University Press, Cambridge, UK, 2000).
  - [2] G. S. Tian and H. Q. Lin, Phys. Rev. B **67**, 245105 (2003).
  - [3] X. G. Wen, *Quantum Field Theory of Many-Body Systems* (Oxford University, New York, 2004).
  - [4] V. L. Beresinskii, Sov. Phys. JETP **32**, 493 (1971).
  - [5] J. M. Kosterlitz and D. J. Thouless, J. Phys. C **6**, 1181(1973); J. M. Kosterlitz, *ibid.* **7**, 1046 (1974).
  - [6] M. A. Nielsen and I. L. Chuang, *Quantum Computation and Quantum Information* (Cambridge University Press, Cambridge, England, 2000)
  - [7] A. Osterloh, Luigi Amico, G. Falci and Rosario Fazio, Nature **416**, 608 (2002).
  - [8] T. J. Osborne and M. A. Nielsen, Phys. Rev. A **66**, 032110(2002).
  - [9] G. Vidal, J. I. Latorre, E. Rico, and A. Kitaev, Phys. Rev. Lett. **90**, 227902 (2003).
  - [10] S. Q. Su, J. L. Song, and S. J. Gu, Phys. Rev. A **74**, 032308 (2006).
  - [11] H. D. Chen, J. Phys. A: Math. Theor. **40**, 10215 (2007).
  - [12] S. J. Gu, H. Q. Lin, and Y. Q. Li, Phys. Rev. A **68**, 042330 (2003).
  - [13] S. J. Gu, G. S. Tian, and H. Q. Lin, Phys. Rev. A **71**,

- 052322 (2005).
- [14] S. J. Gu, S. S. Deng, Y. Q. Li, and H. Q. Lin, Phys. Rev. Lett. **93**, 086402 (2004).
- [15] D. Larsson and H. Johansson, Phys. Rev. Lett. **95**, 196406 (2005).
- [16] S. S. Deng, S. J. Gu, and H. Q. Lin, Phys. Rev. B **74**, 045103 (2006).
- [17] Y. Chen, Z. D. Wang, Y. Q. Li, and F. C. Zhang, Phys. Rev. B **75**, 195113 (2007).
- [18] S. J. Gu, G. S. Tian, H. Q. Lin, Chin. Phys. Lett. **24**, 2737 (2007).
- [19] P. D. Sacramento, P. Nogueira, V. R. Vieira, and V. K. Dugaev, Phys. Rev. B **76**, 184517 (2007).
- [20] L. Amico, R. Fazio, A. Osterloh and V. Vedral, Rev. Mod. Phys. **80**, 517 (2008).
- [21] A. Uhlmann, Rep. Math. Phys. **9**, 273 (1976).
- [22] P. Alberti and A. Uhlmann, in *Proceedings of the Second International Conference on Operator Algebras, Ideals, and their Applications in Theoretical Physics*, edited by H. Baumgartel, G. Laßner, A. Pietsch, and A. Uhlmann (1983).
- [23] P. M. Alberti, Lett. Math. Phys. **7**, 25 (1983).
- [24] P. M. Alberti and A. Uhlmann, Lett. Math. Phys. **7**, 107 (1983).
- [25] W. K. Wootters, Phys. Rev. D **23**, 357 (1981).
- [26] R. Jozsa, J. Mod. Opt. **41**, 2315 (1994).
- [27] B. Schumacher, Phys. Rev. A **51**, 2738 (1995).
- [28] C. A. Fuchs, *Distinguishability and Accessible Information in Quantum Theory*, Ph.D. Thesis, eprint: quant-ph/9601020.
- [29] D. Bures, Trans. Amer. Math. Soc. **135**, 199 (1969), ISSN 0002-9947.
- [30] A. Rastegin, *Sine distance for quantum states*, arXiv:quant-ph/0602112v1.
- [31] J. L. Chen, L. Fu, A. A. Ungar, and X. G. Zhao, Phys. Rev. A **65**, 054304 (2002).
- [32] T. Gorin, T. Prosen, T. H. Seligman, and M. Znidaric, Phys. Rep., **435**, 33-156 (2006).
- [33] P. E. M. F. Mendonca, R. d. J. Napolitano, M. A. Marchioli, C. J. Foster, Y. C. Liang, arXiv:0806.1150.
- [34] X. Wang, C. S. Yu, X. X. Yi, arXiv:0807.1781.
- [35] H. T. Quan, Z. Song, X. F. Liu, P. Zanardi, and C. P. Sun, Phys. Rev. Lett. **96**, 140604 (2006).
- [36] P. Zanardi and N. Paunković, Phys. Rev. E **74**, 031123 (2006).
- [37] H. Q. Zhou and J. P. Barjaktarevic, J. Phys. A: Math. Theor. **41** 412001 (2008).
- [38] P. Zanardi, M. Cozzini, and P. Giorda, J. Stat. Mech. **2**, L02002 (2007).
- [39] M. Cozzini, P. Giorda, and P. Zanardi, Phys. Rev. B, **75**, 014439 (2007).
- [40] M. Cozzini, R. Ionicioiu, and P. Zanardi, Phys. Rev. B, **76**, 104420 (2007).
- [41] P. Buonsante and A. Vezzani, Phys. Rev. Lett. **98**, 110601 (2007).
- [42] P. Zanardi, H. T. Quan, X. Wang, and C. P. Sun, Phys. Rev. A **75**, 032109 (2007).
- [43] W. L. You, Y. W. Li, and S. J. Gu, Phys. Rev. E **76**, 022101 (2007).
- [44] P. Zanardi, P. Giorda, and M. Cozzini, Phys. Rev. Lett. **99**, 100603 (2007).
- [45] H. Q. Zhou, arXiv:0704.2945.
- [46] H. Q. Zhou, J. H. Zhao, and B. Li, arXiv:0704.2940;
- [47] L. C. Venuti and P. Zanardi, Phys. Rev. Lett. **99** , 095701 (2007).
- [48] S. Chen, L. Wang, S. J. Gu, and Y. Wang, Phys. Rev. E **76** 061108 (2007)
- [49] S. J. Gu, H. M. Kwok, W. Q. Ning, and H. Q. Lin, Phys. Rev. B **77**, 245109 (2008).
- [50] A. Tribedi and I. Bose, Phys. Rev. A **77**, 032307 (2008).
- [51] P. Zanardi, L. C. Venuti, and P. Giorda, Phys. Rev. A **76**, 062318 (2007).
- [52] M. F. Yang, Phys. Rev. B **76**, 180403 (R) (2007).
- [53] Y. C. Tzeng and M. F. Yang, Phys. Rev. A **77**, 012311 (2008).
- [54] W. Q. Ning, S. J. Gu, Y. G. Chen, C. Q. Wu, and H. Q. Lin, J. Phys.: Condens. Matter **20**, 235236 (2008).
- [55] N. Paunković, P. D. Sacramento, P. Nogueira, V. R. Vieira, and V. K. Dugaev, Phys. Rev. A **77**, 052302 (2008).
- [56] N. Paunković and V. R. Vieira, Phys. Rev. E **77**, 011129 (2008).
- [57] H. M. Kwok, W. Q. Ning, S. J. Gu, and H. Q. Lin, Phys. Rev. E **78**, 032103 (2008).
- [58] H. Q. Zhou, R. Orus, and G. Vidal, Phys. Rev. Lett. **100** 080601 (2008).
- [59] H. Q. Zhou, J. H. Zhao, H. L. Wang, and B. Li, arXiv:0711.4651.
- [60] J. O. Fjærestad, J. Stat. Mech. P07011 (2008).
- [61] S. Chen, L. Wang, Y. Hao, and Y. Wang, Phys. Rev. A **77**, 032111 (2008).
- [62] D. F. Abasto, N. T. Jacobson, and P. Zanardi, Phys. Rev. A **77**, 022327 (2008).
- [63] L. C. Venuti, M. Cozzini, P. Buonsante, F. Massel, N. Bray-Ali, and P. Zanardi, Phys. Rev. B **78**, 115410 (2008).
- [64] X. Wang, Z. Sun, and Z. D. Wang, arXiv:0803.2940
- [65] A. Hamma, W. Zhang, S. Haas, and D. A. Lidar, Phys. Rev. B **77**, 155111 (2008).
- [66] J. H. Zhao and H. Q. Zhou, arXiv:0803.0814.
- [67] S. Yang, S. J. Gu, C. P. Sun, and H. Q. Lin, Phys. Rev. A **78**, 012304 (2008).
- [68] D. F. Abasto, A. Hamma, and P. Zanardi, Phys. Rev. A **78**, 010301(R) (2008).
- [69] H. Q. Zhou, arXiv:0803.0585
- [70] T. C. Tzeng, H. H. Hung, Y. C. Chen, and M. F. Yang, Phys. Rev. A **77**, 062321 (2008).
- [71] J. Zhang, X. Peng, N. Rajendran, and D. Suter, Phys. Rev. Lett. **100**, 100501 (2008).
- [72] H. M. Kwok, C. S. Ho, and S. J. Gu, arXiv:0805.3885.
- [73] J. Ma, L. Xu, H. Xiong, and X. Wang, arXiv:0805.4062.
- [74] H. M. Kwok, *Quantum criticality and fidelity in many-body systems*, MPhil Thesis.
- [75] H. T. Quan and F. M. Cucchietti, arXiv:0806.4633.
- [76] L. C. Venuti, H. Saleur, P. Zanardi, arXiv:0807.0104.
- [77] X. M. Lu, Z. Sun, X. Wang, P. Zanardi, Phys. Rev. A **78**, 032309 (2008).
- [78] S. J. Gu and H. Q. Lin, arXiv:0807.3491.
- [79] Z. Ma, F. L. Zhangg, and J. L. Chen, arXiv:0808.0984.
- [80] J. Zhang, F. M. Cucchietti, C. M. Chandrashekar, M. Laforest, C. A. Ryan, M. Ditty, A. Hubbard, J. K. Gamble, and R. Laflamme, arXiv:0808.1536.
- [81] J. Ma, L. Xu, and X. Wang, arXiv:0808.1816.
- [82] H. N. Xiong, J. Ma, Z. Sun, and X. Wang, arXiv:0808.1817.
- [83] L. Gong and P. Tong, Phys. Rev. B **78**, 115114 (2008).
- [84] S. J. Gu, arXiv:0809.3856.
- [85] Y. Y. Zhang, T. Liu, Q. H. Chen, X. Wang, K. Wang,

- arXiv:0809.4426
- [86] D. F. Abasto and P. Zanardi, arXiv:0809.4740.
- [87] X. Wang and S. J. Gu, arXiv:0809.4898.
- [88] Y. C. Li, Phys. Lett. A **372**, 6207 (2008).
- [89] Y. C. Li and S. S. Li, Phys. Rev. B, to appear.
- [90] W. L. You and W. L. Lu, preprint.
- [91] Y. Z. You, C. D. Gong, and H. Q. Lin, preprint.
- [92] C. Y. Yeung, H. M. Kwok, and S. J. Gu, preprint.
- [93] F. M. Cucchietti, S. Fernandez-Vidal, and J. Pablo Paz, Phys. Rev. A **75**, 032337 (2007).
- [94] Y. C. Ou and H. Fan, J. Phys. A: Math. Theor. **40**, 2455(2007).
- [95] Z. G. Yuan, P. Zhang, and S. S. Li, Phys. Rev. A **75**, 012102 (2007).
- [96] D. Rossini, T. Calarco, V. Giovannetti, S. Montangero, and R. Fazio, Phys. Rev. A **75**, 032333 (2007).
- [97] H. T. Quan, Z. D. Wang, and C. P. Sun, Phys. Rev. A **76**, 012104 (2007).
- [98] L. C. Wang, X. L. Huang, X. X. Yi, Phys. Lett. A **368**, 362 (2007).
- [99] Y. C. Li and S. S. Li, Phys. Rev. A **76**, 032117 (2007).
- [100] X. X. Yi, H. Wang, and W. Wang, Euro. Phys. J. D **45**, 355 (2007).
- [101] Z. G. Yuan, P. Zhang, and S. S. Li, Phys. Rev. A **76**, 042118 (2007).
- [102] C. Cormick and J. Pablo Paz, Phys. Rev. A **77**, 022317 (2008).
- [103] D. Rossini, P. Facchi, R. Fazio, G. Florio, D. A. Lidar, S. Pascazio, F. Plastina, and P. Zanardi, Phys. Rev. A **77**, 052112 (2008).
- [104] W. G. Wang, J. Liu, and B. Li, Phys. Rev. E **77**, 056218(2008).
- [105] C. Y. Lai, J. T. Hung, C. Y. Mou, and P. Chen, Phys. Rev. B **77**, 205419 (2008).
- [106] S. Bose, Phys. Rev. Lett. **91**, 207901 (2003).
- [107] A. Dantan, N. Treps, A. Bramati, and M. Pinard, Phys. Rev. Lett. **94**, 050502 (2005).
- [108] J. Zhang, C. Xie, and K. Peng, Phys. Rev. Lett. **95**, 170501 (2005).
- [109] M. V. Berry, *The quantum phase, five years after in Geometric Phases in Physics*, eds: A. Shapere, F. Wilczek, 7-28 (World Scientific, 1989).
- [110] J. P. Provost and G. Vallee, Comm. Math. Phys. **76**, 289 (1980).
- [111] V. Vedral, M. B. Plenio, M. A. Rippin, and P. L. Knight, Phys. Rev. Lett. **78**, 2275 (1997).
- [112] V. Vedral and M. B. Plenio, Phys. Rev. A **57**, 1619 (1998).
- [113] R. Horodecki, P. Horodecki, M. Horodecki, and K. Horodecki, arXiv:quant-ph/0702225
- [114] S. Y. Meng, L. B. Fu, and J. Liu, arXiv:0709.0359
- [115] L. H. Lu and Y. Q. Li, Phys. Rev. A **77**, 053611 (2008).
- [116] J. Liu, W. Wang, C. Zhang, Q. Niu, and B. Li, Phys. Rev. A **72**, 063623 (2005).
- [117] K. J. Hughes, B. Deissler, J. H. T. Burke, and C. A. Sackett, Phys. Rev. A **76**, 035601 (2007).
- [118] G. Manfredi and P.-A. Hervieux, Phys. Rev. Lett. **100**, 050405 (2008).
- [119] A. Peres, *Quantum Theory: Concepts and Methods* (Kluwer Academic, Dordrecht, 1995).
- [120] G. Casati, B. V. Chirikov, I. Guarneri, and D. L. Shepelyansky, Phys. Rev. Lett. **56**, 2437 (1986).
- [121] G. Benenti, G. Casati, and G. Veble, Phys. Rev. E **68**, 036212 (2003)
- [122] S. Pancharatnam, Proc. Ind. Acad. Sci. A **44** 247 (1956).
- [123] M. V. Berry, Proc. Roy. Soc. London, Ser. A **392**, 45 (1984).
- [124] P. W. Anderson, Phys. Rev. Lett. **18**, 1049 (1967).
- [125] P. Pfeuty, Ann. Phys. **57**, 79 (1970).
- [126] R. J. Elliott, P. Pfeuty, and C. Wood, Phys. Rev. Lett. **25**, 443 (1970).
- [127] R. Jullien, P. Pfeuty, J. N. Fields, and S. Doniach, Phys. Rev. B **18**, 3568 (1978).
- [128] E. Barouch and B. M. McCoy, Phys. Rev. A **2**, 1075 (1970).
- [129] E. Barouch and B. M. McCoy, Phys. Rev. A **3**, 786 (1971).
- [130] P. Jordan and E. Wigner, Z. Phys. **47**, 631 (1928).
- [131] M. N. Barber, *Phase Transition and Critical Phenomena*, Vol. 8 (Academic, London, 1983).
- [132] M. A. Continentino, *Quantum Scaling in Many-Body Systems* (World Scientific Publishing, Singapore, 2001).
- [133] H. J. Lipkin, N. Meshkov, and A. J. Glick, Nucl. Phys. **62**, 188 (1965).
- [134] N. Meshkov, A. J. Glick, and H. J. Lipkin, Nucl. Phys. **62**, 199 (1965).
- [135] N. Meshkov, H. J. Lipkin, and A. J. Glick, Nucl. Phys. **62**, 211 (1965).
- [136] R. Botet and R. Jullien, Phys. Rev. Lett. **49**, 478 (1982).
- [137] R. Botet and R. Jullien, Phys. Rev. B **28**, 3955 (1983).
- [138] T. Holstein and H. Primakoff, Phys. Rev. **58**, 1098 (1940).
- [139] S. Dusuel, and J. Vidal, Phys. Rev. Lett. **93**, 237204 (2004).
- [140] S. Dusuel, and J. Vidal, Phys. Rev. B **71**, 224420 (2005).
- [141] P. Ribeiro, J. Vidal, and R. Mosseri, Phys. Rev. Lett. **99**, 050402 (2007).
- [142] J. Vidal, R. Mosseri and J. Dukelsky, Phys. Rev. A **69**, 054101 (2004).
- [143] J. Vidal, G. Palacios, and R. Mosseri, Phys. Rev. A **69**, 022107 (2004).
- [144] J. I. Latorre, R. Orús, E. Rico, and J. Vidal, Phys. Rev. A **71**, 064101 (2005).
- [145] T. Barthel, S. Dusuel, and J. Vidal, Phys. Rev. Lett. **97**, 220402 (2006).
- [146] G. Vidal, Phys. Rev. Lett. **91**, 147902 (2003).
- [147] G. Vidal, Phys. Rev. Lett. **93**, 040502 (2004).
- [148] V. Murg, F. Verstraete, and J. I. Cirac, Phys. Rev. A **75**, 033605 (2007).
- [149] G. Vidal, Phys. Rev. Lett. **98**, 070201 (2007).
- [150] S. Dürr, T. Nonn, and G. Rempe, Nature **395**, 33 (1998).
- [151] K. Huang, *Statistical Mechanics* (Wiley, New York, 1987).
- [152] S. Hill and W. K. Wootters Phys. Rev. Lett. **78**, 5022-5025 (1997).
- [153] W. K. Wootters, Phys. Rev. Lett. **80**, 2245 (1998).
- [154] H. A. Bethe, Z. Physik **71**, 205 (1931).
- [155] C. N. Yang and C. P. Yang, Phys. Rev. **150**, 321 (1966); **150**, 327 (1966).
- [156] M. Takahashi, *Thermodynamics of one-dimensional Solvable Models* (Cambridge University Press, Cambridge, 1999).
- [157] R. J. Baxter, *Exactly Solved Models in Statistical Mechanics* (Academic Press, New York, 1982), p. 155.
- [158] B. S. Shastry and B. Sutherland, Phys. Rev. Lett. **65**, 1833 (1990).
- [159] S. J. Gu, V. M. Pereira, and N. M. R. Peres, Phys. Rev. B **66**, 235108 (2002).

- [160] T. Giamarchi, *Quantum Physics in One Dimension* (Oxford University Press, New York, 2004).
- [161] H. J. Schulz, Phys. Rev. B **34**, 6372 (1986).
- [162] M. den Nijs and K. Rommelse, Phys. Rev. B **40**, 4709 (1989).
- [163] A. K. Kolezhuk and H. J. Mikeska, Phys. Rev. Lett. **80**, 2709 (1998).
- [164] I. Affleck, T. Kennedy, E. H. Lieb, and H. Tasaki, Phys. Rev. Lett. **59**, 799 (1987).
- [165] J. Hubbard, Proc. R. Soc. London A **276**, 238 (1963).
- [166] C. N. Yang, Phys. Rev. Lett. **63**, 2144 (1989).
- [167] C. N. Yang and S. C. Zhang, Mod. Phys. Lett. B **4**, 40 (1990).
- [168] E. H. Lieb and F.Y.Wu, Phys. Rev. Lett. **20**, 1445 (1968).
- [169] T. Deguchi, F. H. L. Essler, F. Göhmann, A. Klümper, V. E. Korepin, and K. Kusakabe, Phys. Rep. **331** 197 (2000).
- [170] F. H. L. Essler, H. Frahm, F. Göhmann, A. Klümper, and V. E. Korepin, *The One-Dimensional Hubbard Model* (Cambridge University Press, Cambridge, 2005).
- [171] G. Fáth, Z. Domański, and R. Lemański, Phys. Rev. B **52**, 13910 (1995).
- [172] Z. Domański, R. Lemański, and G. Fáth, J. Phys. Condens. Matter **8**, L261 (1996).
- [173] For example: C. Chin, M. Bartenstein, A. Altmeyer, S. Riedl, S. Jochim, J. Hecker Denschlag, and R. Grimm, Science **305**, 1128 (2004).
- [174] M. A. Cazalilla, A. F. Ho, and T. Giamarchi, Phys. Rev. Lett. **95**, 226402 (2005).
- [175] S. J. Gu, R. Fan, and H. Q. Lin, Phys. Rev. B **76**, 125107 (2007).
- [176] Z. G. Wang, Y. G. Chen, and S. J. Gu, Phys. Rev. B **75**, 165111 (2007).
- [177] L. M. Falicov and J. C. Kimball, Phys. Rev. Lett. **19**, 997 (1969).
- [178] T. Kennedy and E. Lieb, Physica A **138**, 320 (1986).
- [179] L. Pollet, M. Troyer, K. V. Houcke, and S. M. A. Rollets, Phys. Rev. Lett. **96**, 190402 (2006).
- [180] J. H. Han, D. J. Thouless, H. Hiramoto, and M. Kohmoto, Phys. Rev. B **50**, 11365 (1994).
- [181] Y. Takada, K. Ino, and M. Yamanaka, Phys. Rev. E **70**, 066203 (2004).
- [182] K. Ino and M. Kohmoto, Phys. Rev. B **73**, 205111 (2006).
- [183] D. R. Hofstadter, Phys. Rev. B **14**, 2239 (1976).
- [184] A. Kitaev, Ann. Phys. **303**, 2 (2003).
- [185] C. Castelnovo and C. Chamon, Phys. Rev. B **77**, 054433 (2008).
- [186] A. Kitaev, Ann. Phys. **321**, 2 (2006).
- [187] X. G. Wen, Phys. Rev. Lett. **90**, 016803 (2003).
- [188] M. A. Levin and X. G. Wen, Phys. Rev. B **71**, 045110 (2005).
- [189] J. Preskill, *Topological quantum computation*, <http://www.theory.caltech.edu/people/preskill/ph229/> (2004).
- [190] J. K. Pachos, IJQI **4**, 947 (2006); Ann. Phys. **322**, 1254 (2007).
- [191] S. D. Sarma, M. Freedman, C. Nayak, S. H. Simon, A. Stern, arXiv: 0707.1889.
- [192] X. Y. Feng, G. M. Zhang, and T. Xiang, Phys. Rev. Lett. **98**, 087204 (2007).
- [193] D. H. Lee, G. M. Zhang, and T. Xiang, Phys. Rev. Lett. **99**, 196805 (2007).
- [194] H. D. Chen and J. P. Hu, arXiv: cond-mat/0702366.
- [195] H. D. Chen and Z. Nussinov, arXiv: cond-mat/0703633;
- [196] Z. Nussinov, G. Ortiz, arXiv: cond-mat/0702377.
- [197] Y. Yu, arXiv: 0704.3829;
- [198] Y. Yu, Z. Q. Wang, arXiv: 0708.0631;
- [199] T. Y. Si and Y. Yu, arXiv:0709.1302;
- [200] T. Y. Si and Y. Yu, arXiv: 0712.4231 .
- [201] S. Yang, D. L. Zhou, and C. P. Sun, Phys. Rev. B **76**, 180404(R) (2007).
- [202] S. P. Kou and X. G. Wen, arXiv: 0711.0571.
- [203] S. Mandal and N. Surendran, arXiv: 0801.0229.
- [204] K. P. Schmidt, S. Dusuel, and J. Vidal, Phys. Rev. Lett. **100**, 057208 (2008).
- [205] S. Dusuel, K. P. Schmidt, and J. Vidal, arXiv:0802.0379.
- [206] L. Onsager, Phys. Rev. **65**, 117 (1944).
- [207] B. M. McCoy, and T. T. Wu, *The Two-dimensional Ising Model*, (Harvard University Press, Cambridge, Massachusetts, 1973).
- [208] P. Hohenberg and W. Kohn, Phys. Rev. **136**, B864 (1964).
- [209] W. Kohn and L. J. Sham, Phys. Rev. **140**, A1133 (1965).
- [210] J. Bardeen, L. N. Cooper, and J. R. Schrieffer, Phys. Rev. **106**, 162 (1957).
- [211] J. Bardeen, L. N. Cooper, and J. R. Schrieffer, Phys. Rev. **108**, 1175 (1957).
- [212] W. H. Press, S. A. Teukolsky, W. T. Vetterling, and B. P. Flannery, *Numerical Recipes in C*, (Cambridge University Press, Cambridge, 2002).
- [213] <http://www.netlib.org/lapack/>.
- [214] [http://www.intel.com/software/products/Flash/clustermkl/SPD\\_nav.swf](http://www.intel.com/software/products/Flash/clustermkl/SPD_nav.swf)
- [215] S. R. White, Phys. Rev. Lett. **69**, 2863 (1992).
- [216] I. Peschel, X. Wang, M. Kaulke, and K. Hallberg (Eds.), *Density-Matrix Renormalization, A New Numerical Method in Physics, in the Serie Lecture Notes in Physics*, (Springer, Berlin, 1999).
- [217] U. Schollwöck Rev. Mod. Phys. **77**, 259 (2005).
- [218] U. Schollwöck and S. R. White, in G. G. Batrouni and D. Poilblanc (eds.): *Effective models for low-dimensional strongly correlated systems*, p. 155, (AIP, Melville, New York, 2006).
- [219] F. Verstraete, D. Porras, and J. I. Cirac, Phys. Rev. Lett. **93**, 227205 (2004).
- [220] E. R. Davidson, J. Comput. Phys. **17**, 87 (1975).